ADDIS ABABA UNIVERSITY

ADDIS ABABA INSTITUTE OF TECHNOLOGY

SCHOOL OF CIVIL AND ENVIRONMENTAL ENGINEERING

MAPPING LANDSLIDE AND MODELLING SLOPE INSTABILITY USING OPTICAL AND PS-InSAR TECHNIQUES

(A case study in Birbir-Mariam Area of the Southern Regional State, Ethiopia)

A Thesis in Geomatics and Geodesy (specialization in Geodesy)

By Endashaw Debru

September 2020

Addis Ababa

A Thesis

Submitted in Partial Fulfillment of the Requirements for the Degree of Master Science

The undersigned have examined the thesis entitled ‘Mapping Landslide Hazard Zone and Modelling Slope Insatiability using Optical and PS-InSAR Technique ’ presented by Endashaw Debru, a candidate for the degree of Master of Science and hereby certify that it is worthy of acceptance.

Dr. Ing. Elias Lewi		
Advisor	Signature	Date
Filagot Mengistu		
Co-Advisor	Signature	Date
Internal Examiner	Signature	Date
External Examiner	Signature	Date
Chair person	Signature	Date

UNDERTAKING

I certify that this research work, with the title "Mapping Landslide Hazard Zone and Modelling Slope Insatiability using Optical and PS-InSAR Technique" is my own work. The work has not been presented elsewhere for assessment. Where material has been used from other sources, it has been properly acknowledged / referred.

Signature of Student

Endashaw Debru
Name of Student

ABSTRACT

Landslides are geo-hazard that mostly occur in mountainous terrain and affect human lives and damage infrastructures. They can be triggered by natural phenomena such as earthquakes, heavy rains and volcanic eruptions. Construction works, legal and illegal mining, as well as the unregulated cutting of hills (carving out land on a slope) caused most of the human-induced landslides. In order to manage and mitigate their negative impact, landslide hazard zonation mapping and slope instability assessment is crucial. In this study, landslide hazard zonation mapping and deformation time series map for slope instability assessment were implemented in Birbir Mariam area. The study area is in Southern region, around 47km northeast of Arbaminch town. The main objective of the study was to carry out the mapping and zonation of landslide hazards using analytical hierarchical process of remotely sensed data and assess slope instability. In order to map landslide hazard zones, eight possible causative factors were studied. These are slope, lineament density, drainage density, land-use and land-cover, elevation, lithology, normalized difference vegetation index and aspect. These factors were compared using analytical hierarchical process method to understand, which factors contribute a significant role for the landslide occurrences and hence analyze the zones that are vulnerable to landslide. The result of the analysis showed that, 15% (16.466km^2) of the study area falls on very low hazard zone, 21.45 %(23.547km^2) under low hazard zone, 23 %(25.25km^2) within moderate hazard zone, 25.7 %(28.221km^2) within high hazard zone and 14.85 %(16.306km^2) within very high hazard zones. For the slope instability assessment in the area, a time series map was generated from Interferometric Synthetic Aperture Radar by making use of sentinel-1A data from 2014 to 2019. The result from this persistent scatterer InSAR analysis showed that the average displacement ranging from +5 mm/yr. to -5.4 mm/yr. with Positive values of the displacement shows that the area is moving towards to line of sight while the negative values of the displacement shows the area is moving away from line of sight. At last by integrating information obtained from optical remote sensing, PS-InSAR and a landslide inventory map a conclusion is drawn that selected areas in the north west, west, central and southern part of the survey area are prone to landslide hazards.

Keywords: Landslide, Persistent Scatterer, Interferometric Synthetic Aperture Radar (InSAR)

ACKNOWLEDGMENT

First, I would like to thanks my almighty God, who helped me in all stages of this work so that it is accomplished successfully.

My special gratitude goes to my Advisor, **Dr.-Ing. Elias Lewi** for his valuable scientific discussions and guidance during the work of this thesis. He has played a major role in creating an enthusiastic discussion and continual guidance. I appreciate his contributions to the research and compilations of the thesis. I am grateful for my Co-advisor **Filagot Mengistu** for her support to end this work. I am very grateful for my wife **Tizita Asefa** for her support and encouragement during this work.

Finally, I would like to thanks my sister **Abeba Debru**, and My Friends **Hailu Regassa, Epheson Kastro**, **Seifu W/Michael, Mekuanint Eresho and Yonas Oyda** for their valuable comments and suggestions for the completion of this work.

Table of Contents

LIST OF FIGURES

LIST OF TABLES

ABRREVIATION AND ACRONYMS

AHP - Analytic Hierarchical Process

ANN - Artificial Neural Network

DEM - Digital Elevation Map

ESA - European space agency

GNSS - Global Navigation Satellite Systems

InSAR - Interferometric Synthetic Aperture Radar

LHZ - Landslide Hazard zone

LOS - Line of Sight

LULC - Land-use Land-cover

MTI - Multi-Temporal InSAR

NDVI - Normalized Difference Vegetation Index

PS - Persistent Scatterer

SAR - Synthetic Aperture Radar

SLC - Single Look Complex

SNAP - Sentinel Application Platform

SSEP - Slope Susceptibility Evaluation Parameter

StaMPS - Stanford Method for Persistent Scatterers

USGS - United States of Geological Survey

CHAPTER ONE

INTRODUCTION

1.1 Background

The earth surface is in a continuous change that can notably be observed in mountainous terrains, because of processes that trigger large mass movement. One of these processes is landslide. Landslides hazards are considered as the major factor for mass wasting and landscape building in the mountainous terrains (www.usgs.gov).

The hilly and mountainous terrains of the Ethiopian highlands that are characterized by rugged topography, steep slope geometry with weak geologic formation (lithological units and soil material), seasonal hydrological variations (surface and groundwater manifestation) where poor land-use land-cover conditions prevails are commonly affected by rainfall-triggered slope failures.

The term "land slide" has a slightly contrasting meaning in professions such as Earth science, and engineering. Such dissimilarity in definitions implies the complicated characteristics of the situation and area of interest of the different disciplines in relation to landslide occurrences (Highland and Bobrowsky, 2008).

Varne (1984) and cruden (1991) defines landslide as it is downslope movement of soil, rock, and organic materials which consists of rock topples, rock falls, earth or debris flows that involve shear displacement along one or several slip surfaces, which are either visible or may be reasonably inferred under the effects of gravity.

The term landslide can in general be defined as the downward movement of rock or soil, or both, occurring on the surface of rupture—either curved (rotational slide) or planar (translational slide)—in which much of the material often moves as a coherent or semi coherent mass with little internal deformation. In some cases, landslides may also involve other types of movement, either at the beginning of the failure or later, if a change in properties occur as the displaced material moves downslope (Highland and Bobrowsky, 2008).

In this research work, landslide is a general term used to describe the downslope movement of soil, rock, and organic materials under the effects of gravity triggered by factors such as rainfall, earthquakes or manmade activities.

Landslide is a major natural and geological hazard occurring in the world every year. In recent past years, various landslides events have been occurred in many places of the world. Landslide accounted for about 9% of all the natural hazards worldwide (Seyedeh, 2011)

In general peoples living in highlands have a large probability of being exposed to landslides compared to those in lowland areas. These natural hazards are mostly triggered during the rainy season or occurrences of earthquakes and many public infrastructures, human live and properties re seriously affected. In countries such as Ethiopia, where the topography is rugged, heavy seasonal rainfall are rampant and earthquakes of different magnitudes are registered, landslides are naturally expected, especially in those areas where the lithological formation is weak and there is a poor practice of land-use.

Landslide hazard is a serious environmental challenge for the developmental endeavor in the highlands of Ethiopia. The magnitude and frequency of land slide occurrences, that might be triggered by human interference is naturally expected to increase with the increase in urbanization and infrastructure development. The management of natural and manmade disasters can benefit from a timely and high-quality information that might be derived from space-borne observations, especially in response to emergencies (N. Casagali et al., 2016).

Information derived from space born observations plays a pivotal role in reducing the response time, particularly through the provision of mapping capacities, and for the delivery of services before and after crisis operations.

Geodetic satellite observations that are considered to be useful for geo-hazard monitoring are categorized as follows (Peidou and Fotopoulos, 2015).

- ✓ A) Global Navigation Satellite Systems (GNSS)
- ✓ B) optical remote sensing images (Optical RS)
- ✓ C) radar-based remote sensing images (such as InSAR)
- ✓ D) satellite altimetry observations (SA) and
- ✓ E) low-Earth-orbit (LEO) gravity observations.

From the listed categories, here the Interferometric Synthetic Aperture Radar (InSAR) and optical remote sensing images will be primarily employed in order to detect the rate of movement and landslide hazard zones in the study area.

1.2 Statements of the Problems

Natural geo-hazards, including landslides, earthquakes, ground fissuring, and, volcanic eruptions are crucial problems in Ethiopia, causing many causalities, economic and social problems to societies especially those that are living in the mountainous regions. As several studies revealed (Lulseged Ayalew and Yamagishi, 2004; Tenalem Ayenew and Barrberie, 2005; Bekele Abebe et al., 2010; Raghuvanshi 2014a; 2014b; Fisseha S., Mewa G., 2016; Tk Mebrehatu, M Alber, S Wohnlich. 2020;) the Ethiopian highlands in general and the rift margins in particular are highly susceptible to landslide activity. In comparison, the rift margins are most susceptible to landslide hazards, than any other regions in the country. Settlements and infrastructures, located at the base or at the edge of fault escarpments in seismic prone areas are exposed to risk (Abebe et al., 2010).

In Ethiopia, landslide generated hazard is becoming a serious concern to the public, development projects planners and decision makers at various levels of the Federal and Regional government structures. Regardless of the reality, all efforts made so far had little impact in reducing losses from such hazards. Considering, the current infrastructural development, urbanization, rural development and land management system, it is foreseeable that the frequency and magnitude of landslide and losses due to such geo-hazard would continue unless appropriate action is taken (Weldearegay, 2013). In mountainous terrain, developmental activity especially, road construction covers large area of slope. Therefore, it needs detailed slope Instability assessment (Raghuvanshi et al., 2014).

There are different fields or office-based hazard zonation techniques and slope instability modeling employed in the past few years to the problem of landslide classification in Ethiopia. These includes Information value methods, Analytical Hierarchy Process (AHP), and Regression Analysis and Statistical Analysis approach for LHZ mapping and PS InSAR techniques for slope instability modeling.

Because of this, LHZ mapping, forecasting, monitoring of landslide is necessary to inform government and the public about the spatial probability of landslide for safer land use planning and developmental activities and to minimize impacts.

1.3 Objectives

The present study aims at mapping the landslide and modeling slope instability in the the Birbir-Mariam area employing different optical and radar remote sensing techniques that may help to improve the current geo-spatial plan and to guide the local government in managing the current and future vulnerability of the area to landslide.

1.3.1 General Objectives

The main objectives of this study is to map the deformation caused by landslide and model slope instability using InSAR and optical remote sensing techniques in the Birbir-Mariam area.

1.3.2 Specific Objectives

The specific objectives of the research were

I) To analyze the deformation patterns due to landslide in the Birbir-Mariam area of the SNNP Regional State
II) To identify the main contributing factor for slope instability
III) To indicate methods that can be used to monitor landslides in the area
IV) To evaluate the capabilities of the InSAR and optical remote sensing methods, to be employed, in monitor deformation that are caused by landslides in the Birbir-Mariam area.

1.4 Significance of the study

The significances of this study is mainly in contributing toward the monitoring and reduction of landslide hazard facing humanity the lives of human beings and the loss of infrastructure like roads, dams, settlements, Electric and telephone facilities in the area.

The study is aiming at identifying which area is highly hazardous and which will be less affected, thus it will be possible to understand the risk associated with the hazard. The study will also test and demonstrate the capabilities of geodetic technique in understanding landslide hazards so that it will be possible to reduce associated risks. It also helps to demonstrate the capability of the methods in assisting institutions that are engaged in risk management endeavor, to plan their work before, during and after events.

In general

- Helps in identifying the most vulnerable place in the area
- Provides relevant information to monitor the landslide
- Contribute towards improving the scientific approaches that used to study landslide hazards
- Serves as an input for further studies that will be carried out in the area.

1.5 Scopes of the Study

It is well known that Ethiopian highlands are mostly vulnerable to natural hazards like landslide and volcanic eruption (Bekele Abebe et al., 2010) and the associated damages to infrastructures and loss of human life (Woldearegay, 2013). Hence, in order to eradicate or reduce such geo-hazard susceptibility problems the hazards should be well studied so that planning and risk management techniques can be designed.

Radar and Optical remote sensing enable to get an up-to-date information to assess changes related to natural hazards with in appropriate cost. This study focuses only in mapping landslide and modelling slope instability in Birbir-Mariam area in SNNP region using InSAR and optical remote sensing techniques and field inspection (Hailu Regassa, personal communication). Thus, this study may give some insight about landslide hazard prone zones in the area and the capabilities of the methods employed in monitoring landslide hazards for future investigators.

1.6 Limitation of the study

The present study strived with all possible efforts in gathering the necessaries input within the kinds of primary and additional data collection, analysis and interpretation. However, the study experience certain limitations.one of the foremost challenging limitation of this study was lack of

adequate resource, and limitation on downloading Sentinel1A (S-1A) data from Copernicus website. Additionally, freshness of PS InSAR analysis methodology was another challenge to become trained. Nevertheless, this study provides valuable information and insight that can be of great importance for the relevant information regarding to landslide hazard assessment.

1.7 Structure of the Thesis

The thesis is structured around six chapters: the first chapter introduces about basic concept of landslide and their effect to the society and infrastructure, state the objectives of the study, describe statement of the problem, scope of the study and limitation of the study as well as the overview of the study area. Chapter two discusses about Literature reviews related to this study, types of landslide and the various approaches of landslide hazard zone assessment and radar remote sensing such as InSAR and persistent scatterer presented in general. The third chapter focuses on Methodological approaches of landslide zonation mapping, description of the causative factors and methodological work flows of Ps InSAR and used software to achieve the objectives of the study described as much as possible. Additionally, the data and materials that have been used in this study explained very well.

Chapter four explain the data analysis and processing of the causative factors and the data processing of S-1A datasets stated in detail and investigating the first outputs. Chapter five present the result and discussion of the thesis. Lastly chapter six cover the topics of conclusion and recommendation.

1.8 Overview of the Study area

1.8.1 Description of the Study area

The study area is in the South Nations Nationalities Peoples Regional State (SNNPRS), Gamo Zone in between Chencha wereda and Mirab Abaya Woreda, in Birbir Mariam area. It is about 450 km south of the capital city, Addis Ababa and about 47km away from the zonal capital, Arba Minch town. It covers a total surface area of 110 $Km^{2.}$. Geographically it is bounded by latitudes 692000m N and 704000m N and longitudes 342000m E and 360000m E using the UTM zone 37N. This area can be accessed from Arba Minch town through the Chenecha to Ezo and Birbir Mariam, using an all-weather gravel road.

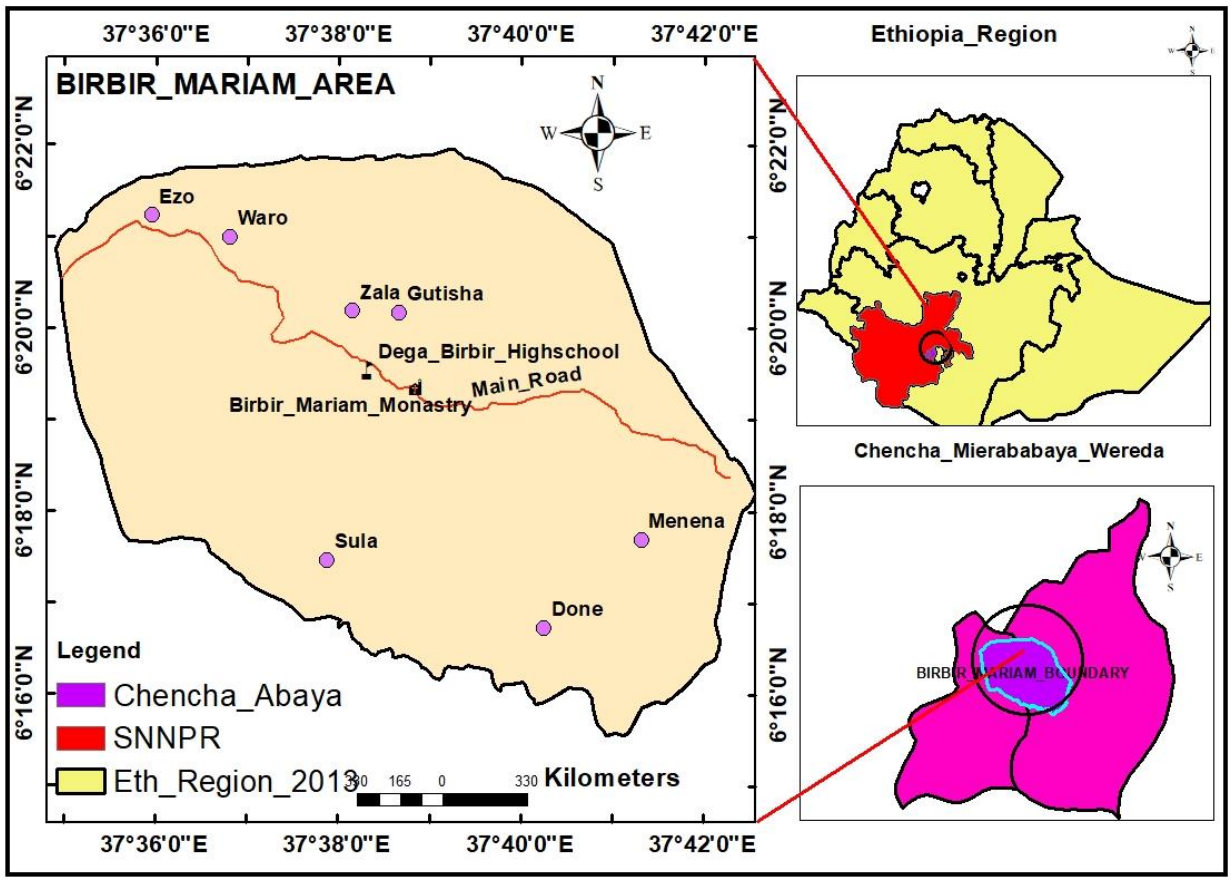

Figure 1. 1: Location map of Study area

1.8.2 Drainage pattern of the study area

The study area is located at the western margin of southern part of the Main Ethiopia Rift system, with elevation between 1582m and 3028m. The study area extends from the highlands in the northern part to Meze river catchment, which finally joins to Derke River. The topography of study area is a result of volcanism and erosion. The area is modified by high degree of erosion at the face and toe of ridges and slopes, which resulted in highly cut topography with steep gullies after volcanism, which has formed ridge in the area.

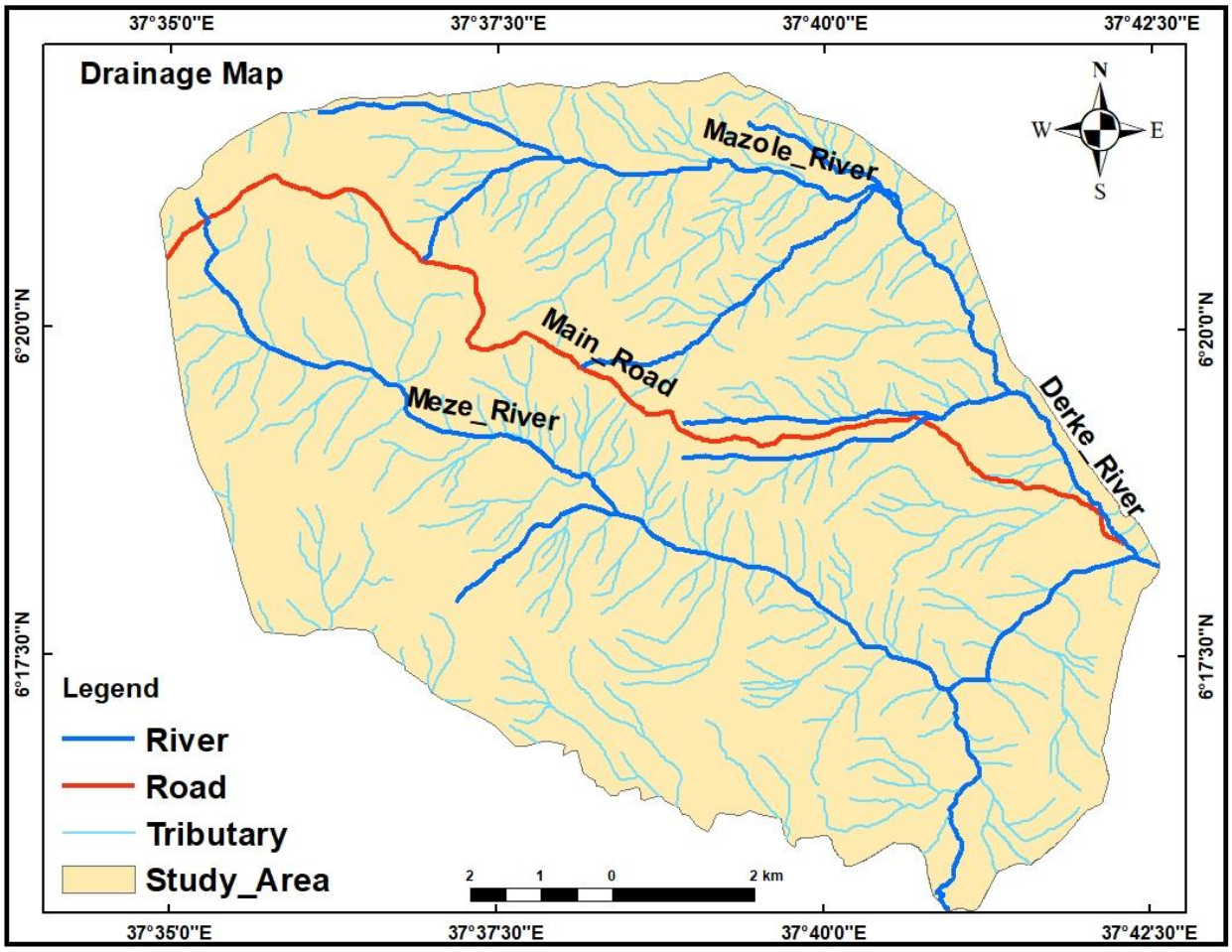

Figure 1. 2: Drainage map of study area

1.8.3 Physiographic situation of study area

The study area has variable altitude, ranging from hills (1582m), to mountains (1900 m), and the highest elevation reaches up to (3028m) above mean sea level.

1.8.4 Climate

The area can be categorized under dry climatic, which can be seen in the lowlands of the study area and wet zone (which can be seen in the highlands of the study area) in which the rain fall pattern is bimodal i.e. the area gets rain fall twice a year; the first one in March, April and May and the other in July, August and September (Table 1.1.). The other seasons are mostly considered as dry season. Highest temperature record are at the main rift margin around Menena and Done that are relatively in lowland part of the survey area

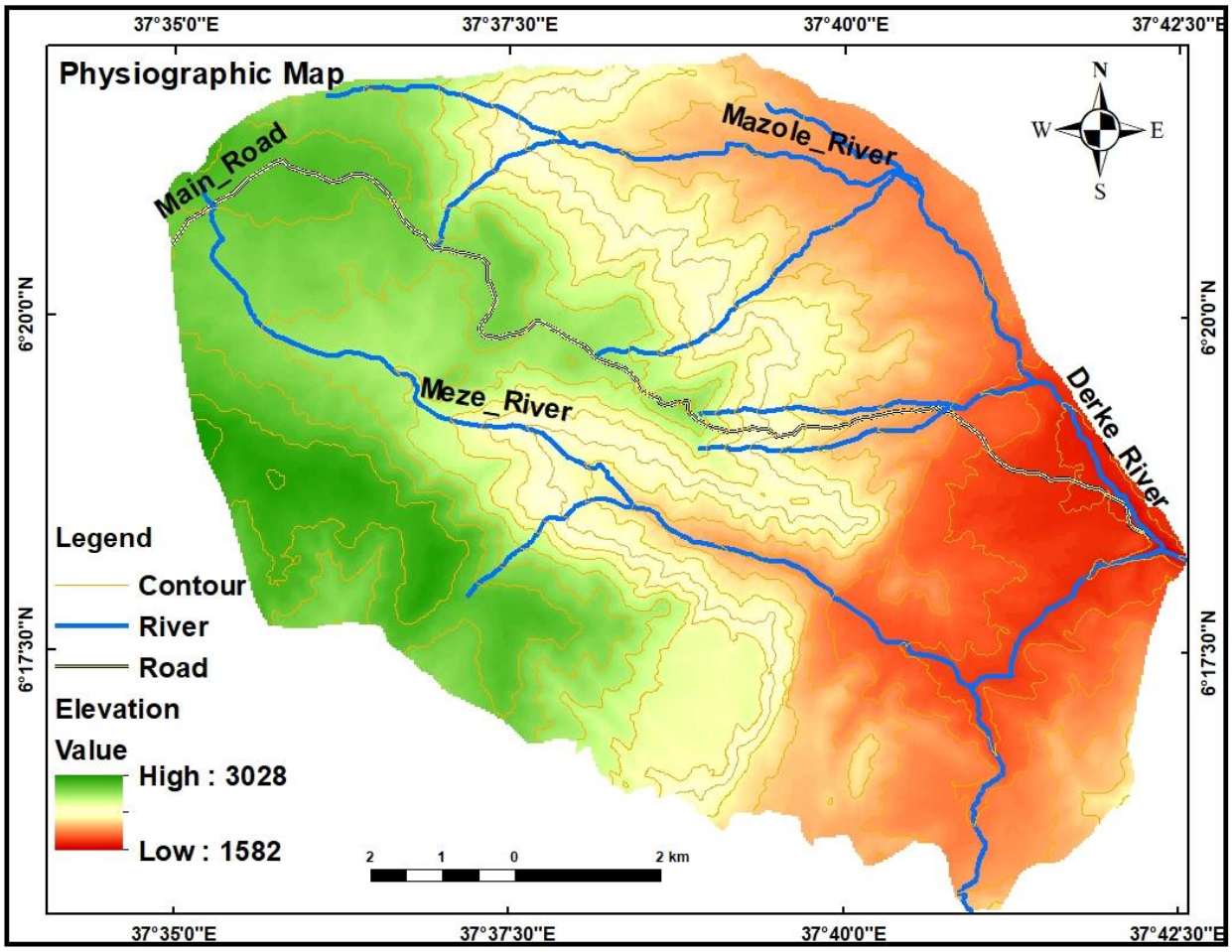

Figure 1. 3: Physiographic map of the study area

Table 1. 1: Mean monthly average rainfall for 20 years

Month of the year	**20 Yrs. Mean monthly Rain fall (Average)**
Jan	17.86
Feb	23.49
Mar	51.49
Apr	123.73
May	132.46
Jun	76.58
July	68.62
Aug	58.89

Sept	65.30
Nov	87.90
Oct	69.13
Dec	32.40

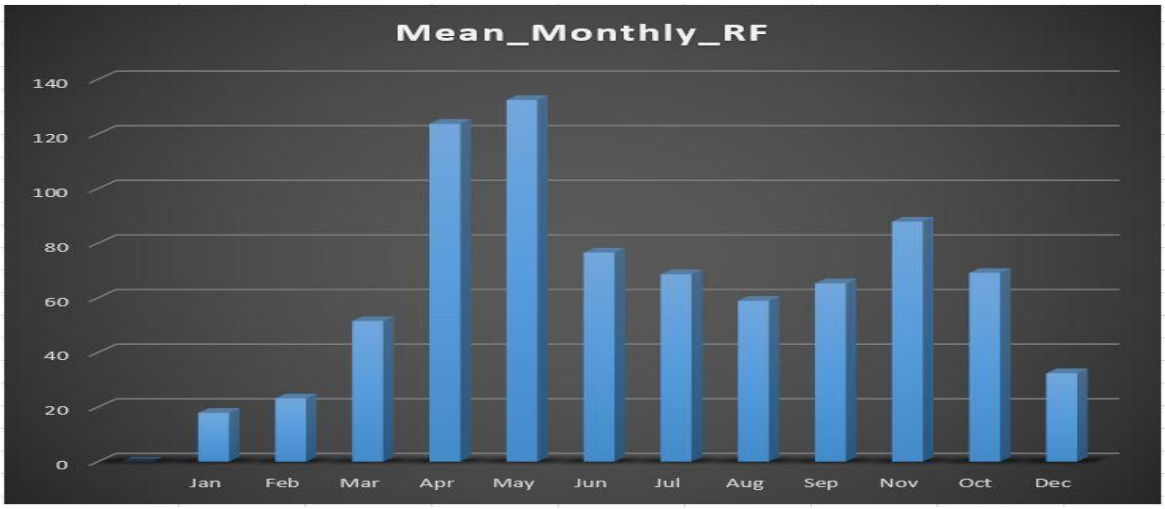

Figure 1. 4 Mean monthly rainfall data of study area (source: Ethiopia metrological agency)

1.8.5 Seismicity

Seismic Risk Map produced by Laike Mariam (Asfaw L. M., 1986), that is based on the likelihood of peak ground acceleration (PGA) with a hundred year return period and 0.99 probabilities shows that the study area falls within eight (8) M.M scale (Fig.). Based on the Modified Mercalli intensity scale the estimated horizontal earthquake acceleration comes out to be 0.04 g, as determined from the MM intensity graph (Johnson R., 1988).

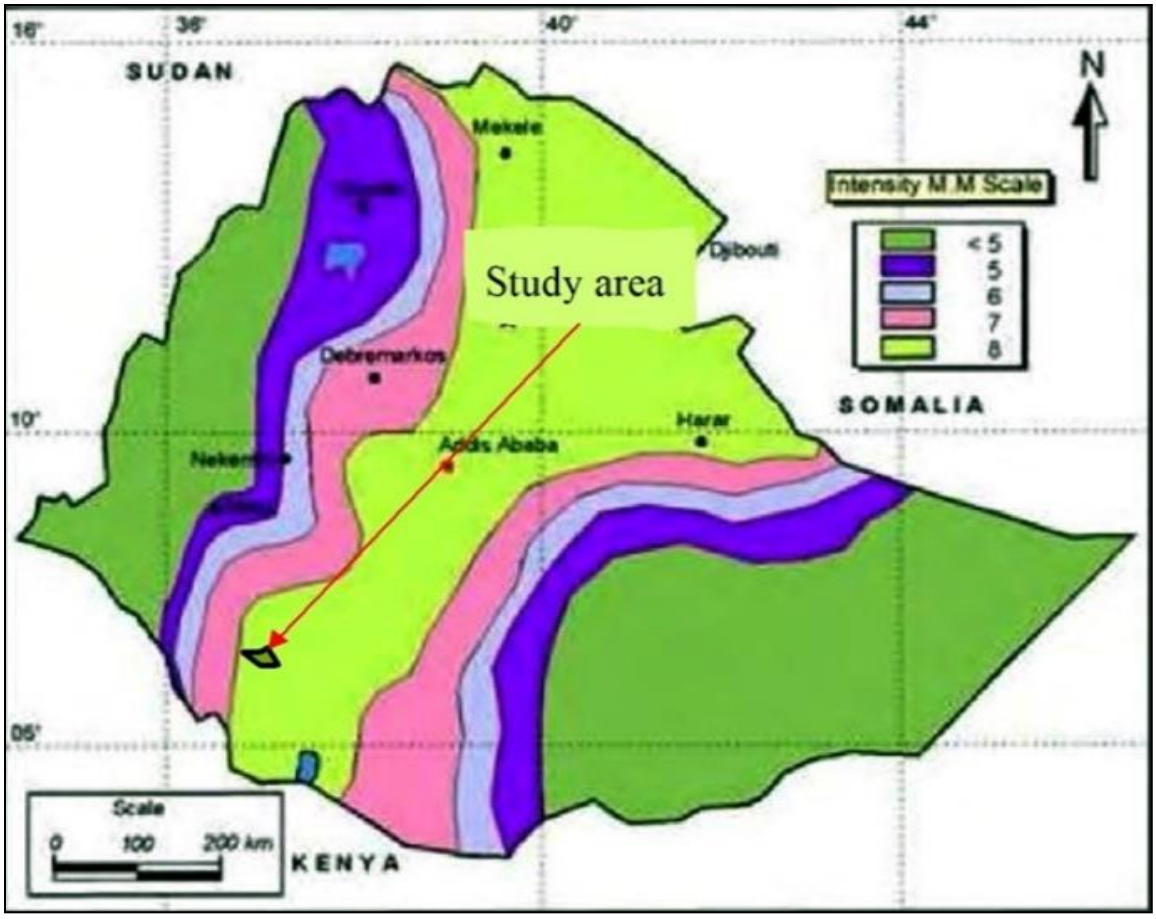

Figure 1. 5: Seismic risk map of Ethiopia 100-year return period, 0.99 probabilities (Asfaw L. M., 1986).

1.9 Regional Geology

Geology plays a fundamental role in controlling the occurrences of landslide in an area. Geologically the area is underlined by Tertiary volcanic rocks, Quaternary alluvial sediments and other volcanic flows (Davidson, 1983) .This MER segment shows a progressive southward narrowing accompanied by a more complex topography, as in the Lake Abaya region where the main depression is bifurcated by the Amaro Horst separating the Ganjuli basin to the west from the Galana basin to the east

The southwestern Ethiopia Cenozoic rocks sub divide into Pre-rift, and post-rift succession. (Davidson, 1983). The geology of the study area is dominated by pre-rift and post rift deposits. The pre-rift deposits include: Early Flood Basalts, Salic, Basaltic, and Intermediate Flows and

Pyroclastic Rocks and Pyroclastic Rocks) but post rift include Holocene Sediment Deposits (Davidson, 1983).

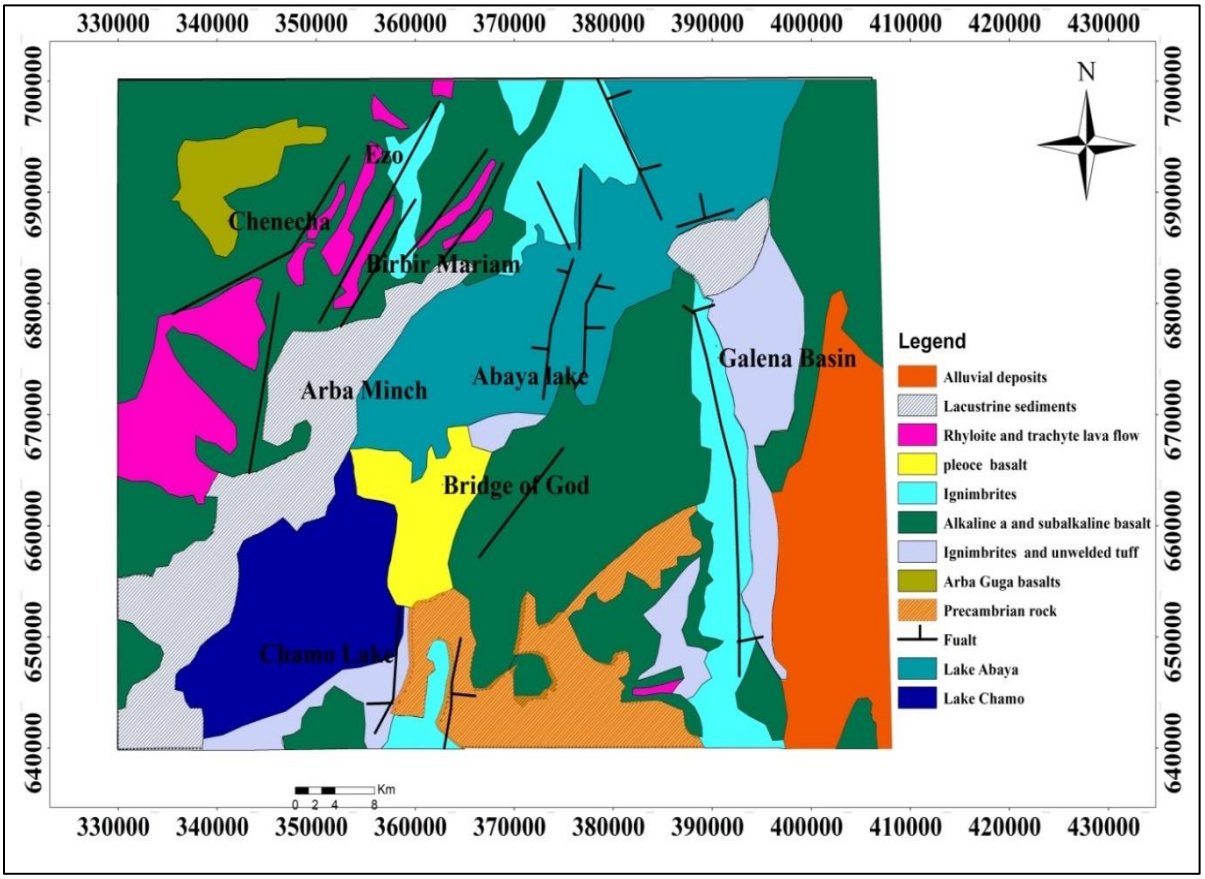

Figure 1. 6: Regional Geological Map (Modified from Davidson, 1983)

An extensive area of Quaternary sedimentation occurs at the northwestern end of the basin along the upper part of Abaya Lake and some are on the side of Chenecha escarpments and they are covered by recent unconsolidated alluvial sediments. Alluvial sediments, which at places attain a thickness of 10 m, has developed on the bed rock on both sides of the sediment deposits. (Davidson et al., 1976)

1.9.1 Local geology of the study area

The geology of the present study area was mapped from secondary source. It consists of porphyritic basalt, Rhyolite, welded tuff, ignimbrite, tuff, unconsolidated deposits such as fluvial and Colluvial deposits. The lithologies are exposed along the road cuts and on the natural hillsides. Among the

exposed rock units the Rhyolites and Tuff are not appropriate to map because it covers very small area. The detailed descriptions of each unit are presented in the following sub-sections;

A. Porphyritic basalt

This rock unit is exposed along the road cuts and on hill slopes, which forms a chain of cliffs. It is highly fractured and weathered, dark-to-dark grey in color with porphyritic texture. This rock unit in the study area is highly weathered, altered and fractured. (Figure 1.7). It covers most of part of the study area (Hailu Regassa personal communication).

Figure 1. 7: highly weathered porphyritic basalt in the study area.

B. Rhyolites

Rhyolite is exposed along hillside and at the bank of streams. It is an extrusive igneous volcanic rock which is characterized by its aphanitic texture and has primary structure like “flow bands” that is unique structure for this rock unit. It has light grey and brownish to dark color respectively. It is exposed at the southeastern part of the study area and un-mapable rock unit. (Hailu Regassa personal communication)

Figure 1. 8: highly weathered banded rhyolite rock unit in study area

C. Tuff:

This lithologic unit contains pyroclastic materials and thin layers of volcanic ash. They are exposed well along the road cut and it covers small parts of the present study area. It is categorized as gray to light gray in color, very weak and it can easily be crashed by hand or powdered into soils with a single knock using geological hammer. (Hailu Regassa personal communication)

Figure 1. 9: Highly weathered gray to light gray color Unwelded tuff in the study area

D. Ignimbrite

This lithologic unit which is composed of felsic minerals, is exposed on hillsides and river banks. This rock unit in the study area is slightly weathered, welded and dissected by secondary geological structure like joints.(Hailu Regassa personal communication)

Figure 1. 10: Highly weathered and jointed ignimbrite rock unit in the study area

E. Unconsolidated deposits

These lithologic units are deposited on the low altitude gentle and flat-lying area close to the river course in the alluvial planes and on the gullies. It consists of gravel, sand, silt, and clay and often contains organic matter that makes it a fertile soil (Hailu Regassa personal communication).

CHAPTER TWO

LITERATURE REVIEW

2.1 General overview

As per Varnes (1984) definition a “natural hazard is the probabilities of the occurrence of potentially damaging phenomenon within a specified period of time within a given area”. The world is facing different types of natural hazards such as volcanic eruption, earthquake, landslide, pandemics and others. Because of these phenomena humanity is threatened with loss of lives, livelihoods and property damage. As a consequence events that might even threaten humanity can be triggered.

Human primary needs such as food, water and shelter as well as other needs, such as electricity, communication, transportation and etc. are comparatively compromised by the impacts of extreme geo-hazards relative to earlier times. This is because of fast urbanization, technological progresses and the usage dangerous resources, such as radioactive materials.

2.2 Geo-hazard in Ethiopia

Ethiopia as a country is exposed to various geo-hazards including flooding, volcanic eruption, landslides and earthquakes. There are multiple factors that triggers the country to different types of geo-hazard including dependency rain-fed agriculture, deforestation, land-degradation, different constructions, denser human settlement and extreme rainfall variabilities due to climate change.

2.2.1 Landslides

The word landslide as defined by Cruden (1991) the movement of mass of rock, debris, or earth down a slope. Varne (1984) defined a landslide as 'a downward and outward movement of slope forming materials under the influence of gravity. Geologists describe landslides as mass wasting (www.usgs.gov). A mass wasting is any downward movement of mass, within which the surface is worn away. Mass wasting include rock-falls and the flow of shore deposits called alluvium.

According to Meng (1998) Landslides, occur when gravitational and other types of shear stresses within a slope exceed the shear strength (resistance to shearing) of the materials that form the slope. Shear stress can be fortified within a slope due to a numbers of processes including

excessively steepening of the base of the slope, such as by natural erosion or excavation, and loading of the slope, such as by an inflow of water, a rise in the groundwater table, or the accumulation of debris on the slope's surface. Short-term stresses, such as those imposed by earthquakes and rainstorms, can likewise contribute to the activation of landslides. Processes that weaken the shear strength of a slope's material also can activate landslides. Shear strength is dependent mainly on two factors: frictional strength, which is the resistance to movement between the slope material's interacting constituent particles, and cohesive strength, which is the bonding between the particles. Coarse particles like sand grains have high frictional strength but low cohesive strength, whereas the opposite is true for clays, which are composed of fine particles. Another factor that affects the shear strength of a slope-forming material is the spatial disposition of its constituent particles, referred to as the sediment fabric. Some materials with a loose, open sediment fabric will weaken if they are mechanically disturbed or flooded with water. An increase in water content, resulting from either natural causes or human activity, typically weakens sandy materials through the reduction of inter-particle friction and weakens clays through the dissolution of inter-particle cements, the hydration of clay minerals, and the elimination of inter-particle (capillary) tension (Meng, 1998).

As it is the case worldwide, landslide is the most crucial environmental problem in Ethiopia, as it is causing lose to human life and damages property. It is especially a common incidence in the tectonically fragile and sensitive mountainous terrains of Ethiopia. Bekele Abebe et al. (2010) stated that the spread of landslide distribution in Ethiopian highland is mostly related to the occurrence of several factors such as, high relief, rugged topography and the nature of the soil and rocks.

2.2.2 Causative factors for Landslides

A. Intrinsic Factors

Intrinsic parameters are the inherent or static causative parameters which define the encouraging or unfavorable stability conditions and it includes slope geometry, slope material (lithological units), structural discontinuities, land use and land cover (Raghuvanshi et al., 2014).

.

B. Slope Geometry

This intrinsic parameter includes the relative relief and slope morphometry of the slope (Tarun Kumar Raghuvanshi, 2014). Morphometry is the process of measuring the external shape and dimensions of landforms and slope morphometry express the steepness of the slope (Hoek and Bray, 1981). According to Hoek and Bray (1981) the slope will be prone to instability when the slope morphometry is steep.

Varnes (1984) explained that the chance of occurrence of landslide increases with an increase in slope steepness though landslide occurs in all slope. The relative relief tells the difference between maximum and minimum elevation of individual facet. As the relative relief is higher the slope is prone to instability (Bekele Abebe a, 2010).

C. Slope Material

Slope material can be soil, rock or both soil and rock (Varne, 1984). The composition, fabric, texture and other properties of slope material influence shear strength, permeability and susceptibility to chemical and physical weathering of slope material. The grain size, shape, sorting, the amount and type of cement also determine the strength and stability of slope material. The unconsolidated slope materials are more susceptible to instability than consolidated one because they have less cohesion and friction, have higher infiltration rates than consolidated slope materials (Varne, 1984).

D. Structural Discontinuities

According to Bell (2007) a discontinuity represents a plane of weakness within a rock mass across which the rock material is structurally discontinuous. Both primary and secondary discontinuities such as bedding, joints, foliation, cleavage, schistocyte, folds and faults are potentially weak planes in a slope that intense influence up on the stability of the slope especially if their inclination facilitates downhill movement of the slope in which they occur (Blyth, 2005).As Blyth and de Freitas (Blyth, 2005) described the strength of joints and other geological surfaces is usually less than that of the intact rock they bound; often they are the weakest component of slope geology. It is therefore vital to know their orientation, spacing, continuity, roughness, separation, and nature of filling material in relation to slope angle, direction, and strength along such potential weak planes. Fault zones increase landslide potential by creating steep slopes and sheared and weak

zones (Wachal, 2000). The rock mass may fail along one or more discontinuity plane (Raghuvanshi et al., 2014).

E. Land Use and Land Cover

Land use/land cover affects slope stability. Vegetation tends to increase the stability of slope by increasing shear strength, and the action of climatic agents on natural mass. By intercepting and protecting the mass from action of sunshine, wind and rain it reduces soil erosion. Vegetation cover also prevents the excesses seepage of water into the slope though it depends on soil depth, slope and type of vegetation. The roots of plants also increase the shear strength of the slope by binding the soil mass. Regions with dense vegetation are found to be less prone to slope instability than sparse vegetation, agriculture and urbanization. The areas that are barren and sparse vegetation cover are more prone to erosion and weathering because the type of ground cover affects the stability (Wachal, 2000; Bekele Abebe a, 2010; Raghuvanshi et al., 2014).

F. Groundwater condition

Saturation of groundwater in slope reduces the shear strength of the material and also creates pore water pressure which plays important role in slope instability condition (Waltham, 2009); (Bobrowsky, 2008). Waltham explained that groundwater within jointed rock mass, and in soil mass reduces the shear strength of slope material by developing of joint water and pore water pressure.

G. External triggering factors

According to Varnes (1984) and (Raghuvanshi et al., 2014) the external causative factors are relatively variable or dynamic, temporary and imposed by new events which include rainfall, volcanic activity, seismic vibration and manmade activities.

a. Rainfall

Rainfall is a primary cause of landslides and worse slope stability problems. According to Varnes (1984) the rainfall intensity and duration play an important role in triggering landslide like debris flows, mudflows, and medium to large-scale rockslides though it depends on climatic conditions, topography, the geological structure of slopes, and permeability of material. It plays vital role in decreasing the shear strength of material by saturating the slope material. It also causes the sliding of rock along discontinuities plane by lubricating discontinuities surface and developing pore

water pressure in rock slope (Bobrowsky, 2008). Rainwater can also cause slope instability by increasing the weight on slope especially in areas where the slope material is soil mass (Hoek, 1981).

b. Seismicity

Earthquakes are a major cause of landslide in many parts of the world and have caused tens of thousands of deaths and billions of dollars in economic losses. Earthquake shaking is one of the agents that can cause landslide due to ground shaking, liquefaction of susceptible sediments, or shaking-caused dilation of soil materials (Highland and Bobrowsky, 2008). Ground shaking decreases the shear resistance of slope material and generates the high excess pore water pressure, which adds slope instability condition (Highland and Bobrowsky, 2008).

c. Man-made Factors

Bekele Abebe et al. (2010) and Kifle Weldearegay (2013) explained that the demand for new land for settlement, infrastructure and agriculture are primary causes that contribute to slope instability conditions caused by human interferences. Human activities like changing or disturbing drainage pattern, destabilizing the slopes, removing vegetation, overstepping of slopes by undercutting the bottom slope, loading the top of slope and irrigation may result directly or indirectly initiate the slope instability condition (Highland and Bobrowsky, 2008).

2.3 Occurrence and characteristics of various types of landslides

2.3.1 Occurrence of landslides

As Highland and Bobrowsky (2008) explained landslides can occur anywhere in the world. It occurs both on land and under water, they can occur in bedrock or soils, cultivated land, barren slopes and natural forests, extremely dry areas or wet areas, gentle slope or steep slope.

2.3.2 Characteristics of various types of landslide

Slope movements (slope instability) can be classified in several ways, with each method having some usefulness to the recognition, avoidance, control, or correlation of the hazard. The classification of a landslide based on its activity is mainly significant in the evaluation of future events. The most widely used classification system developed by Varnes (1978) divides landslides into different types according to the material and the type of movement. This

classification distinguishes five types of mass movement (fall, topples, slides, spreads, and flows) in addition to that combinations of these principal types along with types of material (bedrock, coarse soils, and predominant fine soils) (Table 2.1).

There are various types of slope movements; however, there is no simple way to classify such movements. Classification of landslides depends on the composition and the texture of the material, the amount of water or air presence, and the steepness of the slope, type and velocity of the movement.

Table 2. 1: Landslide classification (Varnes, 1978)

<table>
<tr><td colspan="3" rowspan="3">Type of movement</td><td colspan="3">Type of material</td></tr>
<tr><td rowspan="2">Bed rock</td><td colspan="2">Engineering soils</td></tr>
<tr><td>Predominantly fine</td><td>Predominantly coarse</td></tr>
<tr><td colspan="3">Fall</td><td>Rock fall</td><td>Earth fall</td><td>Debris fall</td></tr>
<tr><td colspan="3">Topple</td><td>Rock topple</td><td>Earth topple</td><td>Debris topple</td></tr>
<tr><td rowspan="3">Slide</td><td colspan="2">Rotational</td><td>Rock slump</td><td>Earth slump</td><td>Debris slump</td></tr>
<tr><td rowspan="2">Translational</td><td>Few units</td><td>Rock block slide</td><td>Earth block slide</td><td>Debris block slide</td></tr>
<tr><td>Many units</td><td>Rock slide</td><td>Earth slide</td><td>Debris Earth slide</td></tr>
<tr><td colspan="3">Lateral spreads</td><td>Rock spread</td><td>Earth spread</td><td>Debris spread</td></tr>
<tr><td colspan="3" rowspan="2">Flow</td><td>Rock flow</td><td>Earth flow</td><td>Debris flow</td></tr>
<tr><td>Rock avalanche</td><td></td><td>Debris avalanche</td></tr>
<tr><td colspan="3">Complex and compound</td><td colspan="3">Combination in time and space of two or more principal type of movement</td></tr>
</table>

2.3.3 Types of landslides

a) Fall

Falls are most often characterized as abrupt free fall of bedrock or soil. A fall starts with the detachment of soil or rock from a steep slope along a surface on which little or no shear

displacement takes place. The material then descends mainly through the air by falling, bouncing, or rolling (Wachal, 2000). The triggering mechanism of fall are undercutting of slopes by streams and rivers or differential weathering, excavation during road building and earthquake shaking. It is common in on steep slopes, or vertical slopes also in coastal area, along rocky bank of river and streams, road cuts, and jointed, fractured and weathered bedrock (Wachal, 2000). The material in fall can vary from individual rocks or masses of soil and massive blocks. The rate of movement depends on steepness of slope and usually ranges from very rapid to extremely rapid. It can damage on life and property particularly beneath the fall line of large blocks (Wachal, 2000; Bobrowsky, 2008).

b) Topples

Topples is the forward rotation out of the slope of mass of soil or rock about a point or axis below the center of gravity of the displaced mass. The triggering mechanism of topples are gravity, water or ice occurring in cracks within the mass, vibration, undercutting, differential weathering, excavation or stream erosion. It occurs in columnar jointed volcanic terrain, as well as along streams and river courses where the banks are steep. It can consist of rock, coarse and fine materials. The rate of movement ranges from extremely slow to extremely rapid. It can be extremely destructive especially when failure is sudden or velocity is rapid (Highland and Bobrowsky, 2008).

c) Slides

A slide is a down slope movement of soil or rock mass occurring predominantly on the surface of rupture or on relatively thin zones of intense shear strain (Wachal, 2000); (Highland and Bobrowsky, 2008). It is categorized into rotation slide and translational slide.

In rotational slide surface of rupture is curved or spoon-shaped and it is triggered by intense rainfall or snowmelt. They are common in loose unconsolidated soils and their rate of movement ranges from extremely slow to moderately fast. It can extremely damage structures but not life if the movement is slow (Highland and Bobrowsky, 2008).

In translational slide the surface of rupture is planar surface and it is triggered by intense rainfall, snow melt, and human induced disturbances. Translational slides commonly fail along geologic discontinuities such as faults, joints, bedding surfaces or the contact between rock and soil

(Bobrowsky, 2008). The material ranges from loose, unconsolidated soil to extensive slab of rock or both. The movement may initially slow but many are moderate to extremely rapid. Highland and Bobrowsky (2008) added that slow moving landslides can occur on relatively gentle slopes and can cause significant property damage, but are far less likely to result in serious injuries than rapidly moving landslides.

d) Spread

Spread is defined as an extension of a cohesive soil or rock mass combined with a general subsidence of the fractured mass of cohesive material into softer underlying material. The dominant mode of movement is lateral accommodated by shear or tensile fractures. They often occur on gentle slopes. They are more common in fine grained soils, such as clay, especially if the soil has been remodeled or disturbed by construction, grading or similar activities. Lateral spreads typically damage pipelines, utilities, bridges, and other structures having shallow foundations (Highland and Bobrowsky, 2008).

e) Flow

Wachal and Haduk (2000) described flows as rapid but viscous movement of soil, bedrock, or debris. The component velocities in the displacing mass of a flow resemble those in a viscous liquid. Often, there is a gradation of change from slides to flows, depending on the water content, mobility, and evolution of the movement (Highland and Bobrowsky, 2008).

Flows can be classified into debris flow or earth flows. Debris flows is a form of rapid mass movement in which loose soil, rock and sometimes organic matter combine with water to form that flows downslope. It occurs around in steep gullies and canyons and, nearly saturated, and consists of a large proportion of silt and sand-sized material. They are commonly caused by intense surface water flow, due to heavy precipitation or rapid snowmelt, which erodes and mobilizes loose soil or rock on steep slopes. They can move objects as large as houses in their downslope flow or can fill structures with a rapid accumulation of sediment and organic matter (Highland and Bobrowsky, 2008).

Earthflows can occur on gentle to moderate slopes, generally in fine-grained soil, commonly clay or silt, but also in very weathered, clay-bearing bedrock. It is triggered by prolonged or intense rainfall or snowmelt, sudden lowering of adjacent water surfaces causing rapid drawdown of the

ground-water table, stream erosion at the bottom of a slope, excavation and construction activities, excessive loading on a slope, earthquakes, or human-induced vibration. It possibly results in human fatalities, destruction of buildings and linear infrastructure, and blocking of rivers with resultant flooding upstream and water siltation problems downstream (Highland and Bobrowsky, 2008).

f) Complex movements

Complex movement is a combination of falls, topples slides, spreads and flows (Highland and Bobrowsky, 2008).

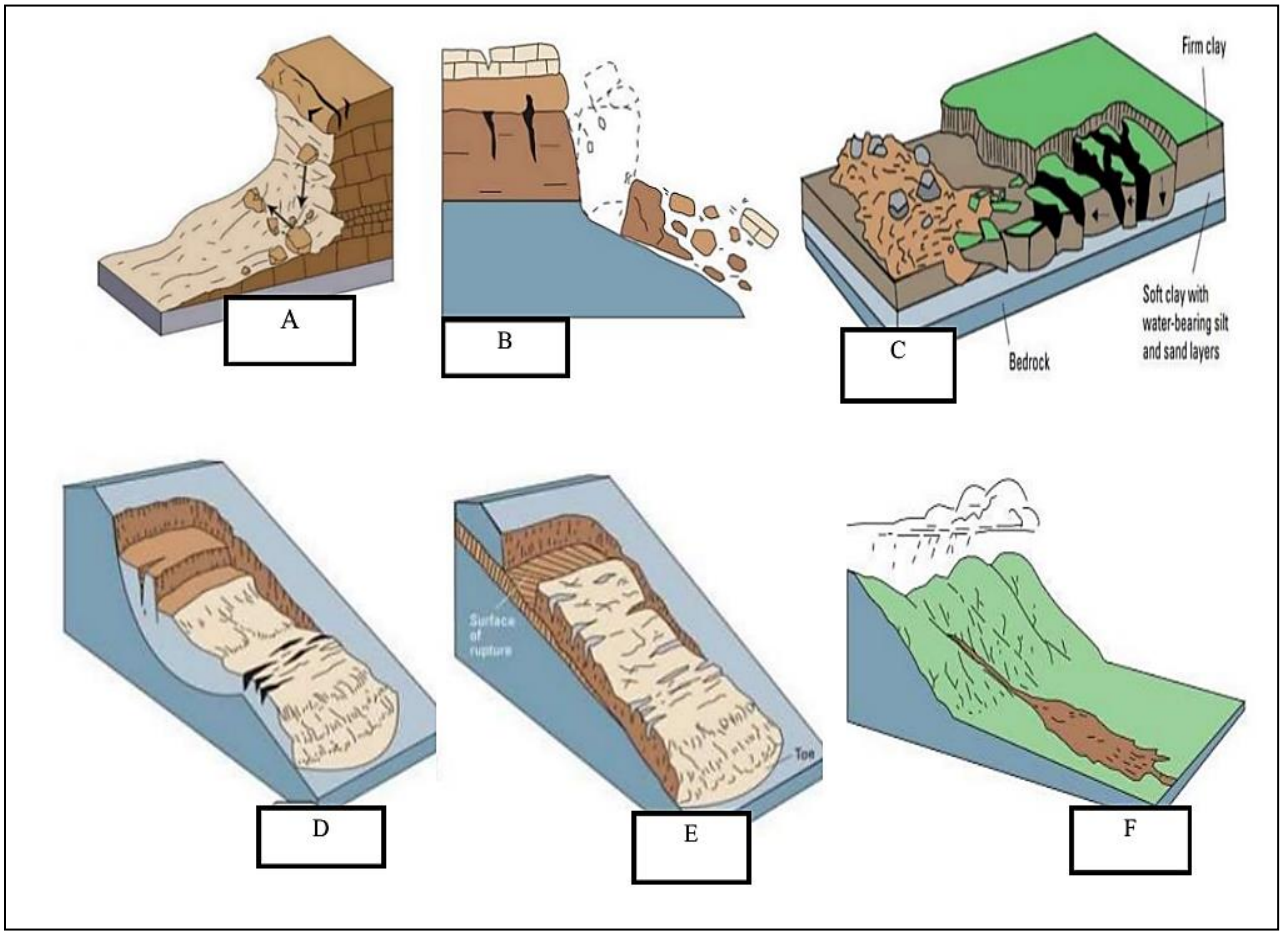

Figure 2. 1: Schematics of diagram rock fall (A), rock topple (B), Spread (C), Rotational slid (D), Translational slide (E), and Debris flow (F) (Highland and Bobrowsky, 2008)

2.4 Various Approaches of Landslide Hazard Zonation Mapping

Landslide hazard zonation is crucial step in landslide studies, landslide risk management and assist in development of sustainable land use planning.

In addition, LHZ zonation has significant role in identifying potential landslide areas or other mass movements establish a relationship between landslide and triggering factors, ranking according to the degrees of actual or potential landslide susceptibility, and in predicting the landslide hazard in the future (Tenalem , 2005; Hamza and Raguvanshi, 2016). The different approaches of landslide hazard zonation discussed as follows:

2.4.1 Landslide Inventory Mapping

Landslide inventory maps show locations and characteristics of landslides that have moved in the past but generally do not indicate the mechanism(s) that triggered them. The geologic, topographic and climatic conditions that led to past slope failures often provide hints to the locations and conditions of future slope failures. Therefore, inventory maps provide useful information about the potential for future land sliding. Generally, widely used methods for making a landslide inventory map are field investigations and remote sensing techniques. By fieldwork surveys, evidence of current and past land sliding can be determined from slope morphology.

2.4.2 Analytic Hierarchy Process

AHP, developed by Thomas L. Saaty in 1975 (Saaty,1977), is useful mechanism for decision-making processes. It enables the choice makers in placing priorities and implementing leading decision on complex decisive problems. It distributes the problems in hierarchy of criteria and options (alternatives), i.e. it reduces complex decisions to pairwise comparisons so synthesizes the result. The AHP considers both the rational and thus the intuitive to choose the foremost effective from type of alternatives evaluated with relevance several criteria. It checks for consistencies in decision maker's evaluation and allows limited inconsistencies in judgements.

The AHP uses a gaggle of evaluation criteria and a bunch of various options among which the foremost effective decision is to be made. It generates a weight for each evaluation criteria according to pairwise comparisons of criteria. The factors with higher weight are selected since

it's most important of all the standards. Further, for fixed criteria, it assigns a score to each alternative option according to pairwise comparisons of options supported those criteria. Higher the score for an option, better the performance of that option with regard to considered criteria. Information is then arranged during a hierarchical tree. Finally, the AHP generates global score for each option using the combinations of the standards weights and options scores and determines relative ranking of alternatives. AHP is implemented in three simple steps. These are:-

I. Computation of weight vector for all criteria

ii. Computation of score matrix for all options

iii. Ranking of options supported final score

The AHP could be a general theory of measurement and is employed to derive relative priorities of various criteria on absolute scales. Pairwise comparisons of criteria and/or options are performed based on the scale given in Table (2.2.).

Table 2. 2: The fundamental scale by Saaty (1977)

Intensity of importance	Definition	Explanation
1	Equal importance	Two activities contribute equally to the objective
2	Week	
3	Moderate importance	Experience and judgment slightly favor one activity over the other
4	Moderate plus	
5	Strong importance	Experience and judgment strongly favors one activity over the other
6	Strong plus	
7	Very strong	An activity is favored very strongly over another ;its dominance is demonstrated in practice
8	Very, very strong	
9	Extreme importance	The evidence favoring one activity over the another is of the highest possible order of affirmation

Various authors have applied this decision-making technique for assigning weights to various factors of landslide occurrence. The effect of each factor and factor classes, on landslide

occurrence, is determined using pairwise comparison, and an equation is modelled for landside susceptible index (LSI), as given below in equation below

$$LSI_{AHP} = \sum_{i=1}^{n} Factor\_i * W_{AHP\_i} \ldots\ldots\ldots (1)$$

Where Factor-i = landslide conditioning factor such as slope, aspect, lithology, etc.

WAHPi=Weightage for each causative factor. Pixel (LSI) values derived from above equations are classified into various susceptibility classes (low, moderate, high, and very high) based on natural break.

2.4.4 Artificial Neural Network

ANN has been used widely in the preparation of LHZ maps. People have used variations of ANN with one input layer, two hidden layers, and one output layer for various factors controlling landslide occurrence. ANN connection weights are used to provide weights or rankings to the input data source (landslide-causative factors). Weights of factors and rankings of categories are integrated to provide LSZ map.

2.4.5 Statistical Approach

Methods, which depends on statistical analysis of geo-environmental factors related to landslide occurrence, are preferred. The statistical methods for LHZ classified into two *viz*. bi-variate statistical analysis and multi-variate statistical analysis and aims minimizing of subjectivity in weightage assignment for causative factors.

The statistical methods is usually employed to evaluate spatial landslide instability based on relationship between the landslide activities and their causative factors (Hamza and Raguvanshi, 2016).

2.5 Records of Landslide in Ethiopia

Landslide activity is very common in Ethiopia, mostly in the Highlands and rifts margins due to factors such as high relief and rugged topography, geology (the nature of the out-cropping rocks), hydrology (surface and groundwater), rainfall, land-use conditions, manmade activity and seismicity. The most important landslide types are soil slips or mudflows, rockslides, toppling and falls in hilly and mountainous terrains of the highlands of north, south and western regions of Ethiopia and parts of rift valley escarpments.

Bekele (2010) studied landslides in the Ethiopian highlands and the rift margins. Findings show that the high relief and rugged topography, the occurrence of clayey horizons within the sedimentary sequences, the dense network of tectonic fractures and faults, the thick eluvial materials on volcanic out-crops, and the thick colluvial–alluvial deposits at the foot of steep slopes are the predisposing factors for a large variety of mass movements. Heavy summer rainfall is the main triggering factor of most landslides, some of which undergo a step-like evolution with long-lasting quiescence intervals. In last decade notable landslides have occurred in areas such as the northern Omo River basin, the lower Wabe-Shebele River valley, the Wendo Genet slope, the Blue Nile Gorge, the town of Dessie, the Wudmen area in Weldiya, the Gilgel Gibe River, the Uba Dema village in Sawla and the Gidole area in the south.

Woldearegay (2013) reviewed the occurrences and influencing factors of landslides in the highlands of Ethiopia, with implications for infrastructural development. Findings of this study showed that rainfall is a major triggering factor for debris/earth slides, debris/earth flows and medium to large-scale rockslides.

Raghuvanshi (2014) made a study on landslide hazard zonation using Slope stability susceptibility evaluation parameter (SSEP) expert approach in the area around Wurgessa Kebelle of North Wollo Zonal Administration, Amhara National Regional State in northern Ethiopia. The results obtained indicates that 8.33% of the area fall under Moderately hazard and 83.33% fall within High hazard whereas 8.34% of the area fall under Very high hazard.

Hamza and Raghuvanshi (2016) made a study about landslide hazard evaluation and zonation (LHZ) in Jeldu District in Central Ethiopia. The considered governing factors in this study are: aspect, slope and elevation, lithology, soil and land use/land cover. The results revealed that 12% of the study area falls under no hazard, 27% as low hazard, 32% as moderate hazard, 21% as high hazard and the rest 8% as very high hazard.

Filagot Mengistu et al. (2018) made a study about landslide hazard zonation mapping and slope instability assessment using optical and InSAR remote sensing techniques on Arbaminch-Gidole road, in the southern part of Ethiopia, making use of the Information value Method for LSH mapping and InSAR for time serious analysis.. The result states that 36.3% of the study area falls under very low hazard zone, 34.2% of the study area falls under Low hazard zone, 7.5% of under moderate hazard zone, 15.4% under High hazard zone and 6.6% under very high hazard zone.

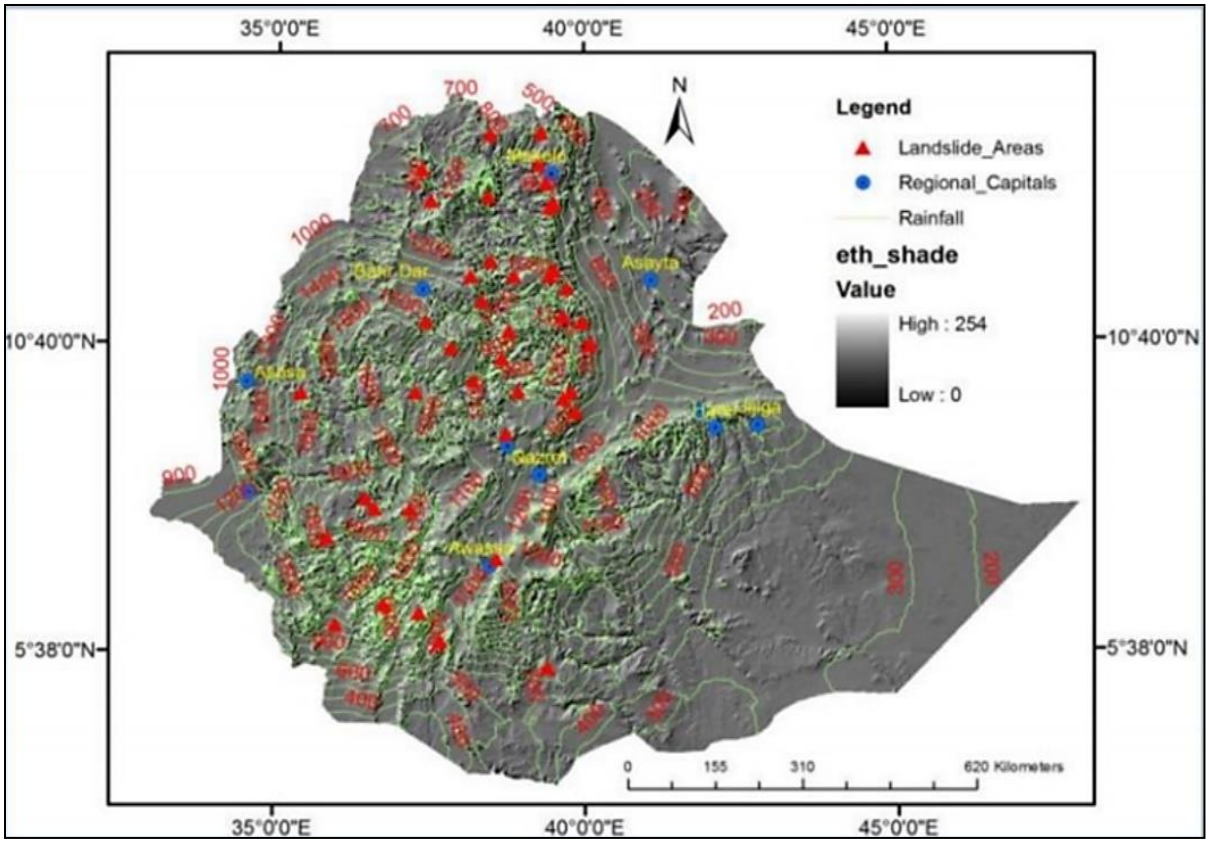

Figure 2. 2: Locations of landslide affected areas in the highlands of Ethiopia (Weldearegay, 2013)

2.6 PS-Interferometric Synthetic Aperture Radar

Persistent Scatter Radar Interferometry (PSRI) is an extension of conventional InSAR. Here the fundamental principles of InSAR will first be discussed, its limitations and persistent scatters will be reviewed later.

2.5.1 Space borne radar remote sensing

Sentinel-1 (S-1), a C-band SAR system, unlike an optical system such as Sentinel-2 (S-2), is an active and therefore independent of solar radiation. The sensor transmits electromagnetic microwave pulses with a wavelength of 5.6 cm to illuminate a swath on the earth's surface and receives the backscattered signals from the scatterers within the illuminated swath (ESA, 2018a; Höser, 2018). The differences of SAR imaging geometry as opposed to optical sensors are important for understanding system capability as well as limitations due to technical specifications.

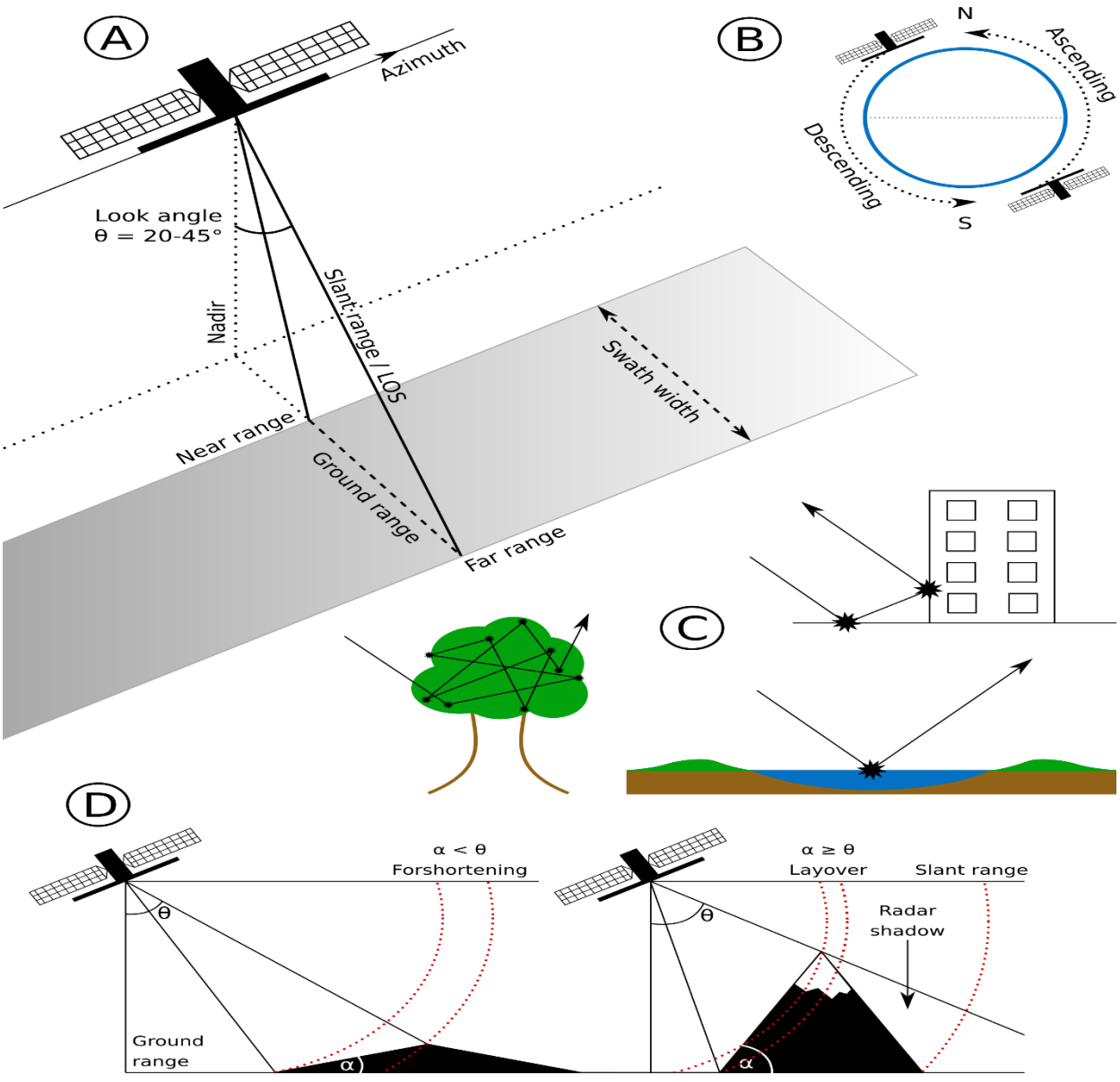

Figure 2. 3: Fundamental sensing geometry, geometric effect and scattering of radar sensors

(A) The side looking sensing geometry, which ends up within the geometric effects pictured in (D). Where the angle α is that the slope angle. If $\alpha < \theta$, the globe appears shortened in slant range, called foreshortening and if $\alpha \leq \theta$, the very best of the slope appears to dwell front of the foot of the slope in slant range, called Layover. (B) Explains the orbit directions and (C) shows typical scattering behaviors of three principle surface classes, where the arrow describes the EM radiation coming from the

sensor and its direction towards or far from the sensor after its reflection on these surfaces. Sources: (Höser, 2018).

2.5.2 Synthetic Aperture Radar

Skolink (2001) defines radar as an electromagnetic system for location and detection of reflecting objects such as aircrafts, ships, spacecraft's, vehicles, peoples, and thus the natural environment. It functions by radiating energy into space and detect the echo signal reflected from an object or simply a target. Synthetic Aperture Radar (SAR) delivers upgraded image resolution over radar without sophisticated post processing by employing the movement of the antenna with reference to the target. Airborne and space borne SAR systems typically have a specified side-looking antenna that illuminates a strip or swath parallel to the sensor's ground track with a series of monochromatic microwave pulses. The platform's flight direction is termed the azimuth direction and thus the direction of the foremost lobe of the transmitting antenna is known as the range direction. The antenna, when inactive between transmissions of pulses, is meant to receive the scattered echoes from the illuminated surface of earlier transmitted pulses. From antenna theory, the place illuminated on the bottom has inverse reference to the physical shape and dimensions of the antenna (Skolnik, 2001). Therefore, to urge fine azimuth resolution in real-aperture radar systems we'd need a very long antenna. SAR is an alternate option to employ an extended physical antenna. The SAR concept separates two targets at an equivalent range but different azimuth positions by their different relative velocities regarding the moving platform. The reflected monochromatic waves from two different scatterers within an equivalent illuminated beam have different Doppler shifts or phases associated with them. Using the concept of the path of the imaging platform, we'll evaluate the precise phase history for every point target on the bottom. Resolution depends on the whole amount of phase information available for each target. The extended a target is illuminated the higher is our ability to resolve it. Thus, SAR enables us to extract high-resolution images using small physical antennas. There are numerous published algorithms (Höser, 2018) which can be applied to process the recorded echoes to make high resolution images using the SAR concept.

2.5.3 SAR imaging Geometry

The imaging geometry shown in Figure (2.3) is termed as the strip-map mode and is the most well-known. Recent phased-array antennas implement complicated data acquisition strategies, e.g.,

Scan-SAR and spotlight SAR, to increase the area of the place imaged by the radar platform. The output from SAR processing algorithm could also be a single look complex (SLC) image, a two-dimensional array of complex numbers, representing the brightness and phase of the scatterers on the ground. The indices of pixels within the matrix are directly related with the azimuth and range position of the scatterers with respect to a point of reference on the platform's path.

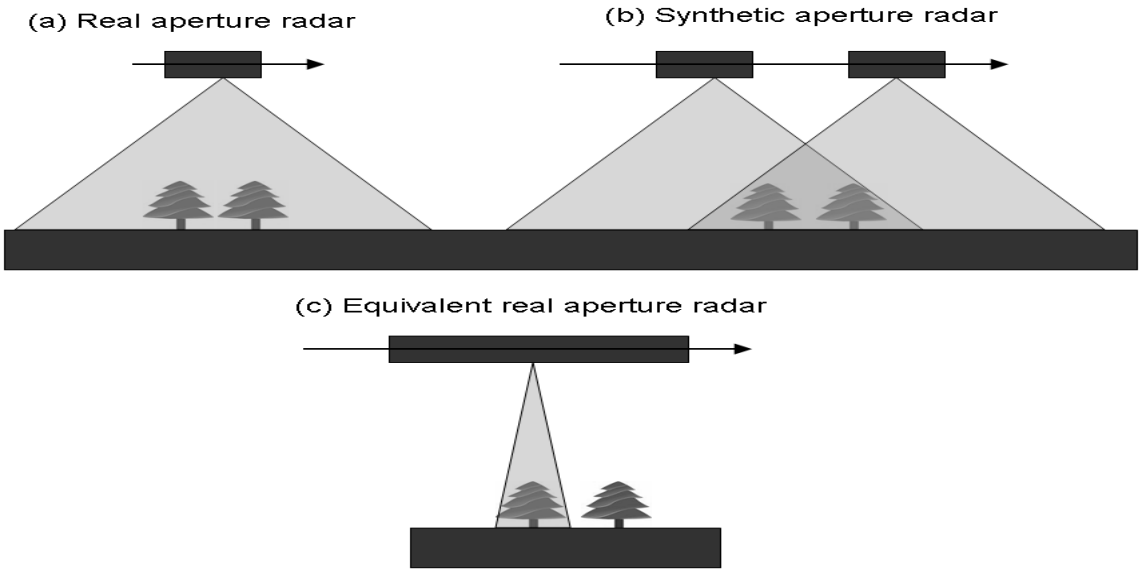

Figure 2. 4: (a) Real aperture antenna, (b) Synthetic aperture antenna created by combining information from many pulses and (c) a real aperture antenna that is equivalent to the synthetic aperture antenna Source: (Agram, 2010).

SAR is one among many other microwave imaging systems. Its cloud-penetrating capabilities resulted from application of microwaves. It has day and night operational capabilities because it is an active system that doesn't depend on natural light emanating from the Sun. Finally, its 'interferometric configuration', InSAR, assist the accurate measurements of the radiation travel path because it's coherent. The computation of travel distance difference as a function of the satellite position and time differences between transmission and acquisition enables us to generate Digital Elevation Models (DEM) and computation of centimeter level surface deformations of the place (Alessandro Ferretti, 2007).

2.5.4 Interferometric Synthetic Aperture Radar

InSAR is one type of an active satellite based remote sensing tool that enables us measuring mm-scale ground displacements at a spatial resolution of < 5–10 m^2 over large (100Km scales) regions.

The detailed understanding of the working principles of SAR imaging are fundamental to fully understand InSAR. In SAR the reflected signal, which is detected by the sensor is referenced to the original signal to depict how different types of scatterers and topography are imaged in a SAR scene (Höser, 2018). In fact, the signal detected is not just a real number describing amplitude, but a complex consisting of amplitude and phase, whereby the latter is of major interest when doing interferometry. The recorded signal can be described by

$$\boldsymbol{g = Ae^{-j\varphi} = Ae^{-j\frac{4\pi}{\lambda}\rho}} \ldots\ldots\ldots (2)$$

Where g = is the measured complex signal

A = is amplitude

$\boldsymbol{j\varphi}$ = is the recorded phase

ρ = is the distance in slant range between the sensor and certain scatterer (Lauknes, 2004; Rosen et al., 2000; Simons and Rosen, 2007)

The term phase refers to a measure from -1π to 1π of the sensor specific wavelength. To understand how the phase signal ϕ is detected, the understanding of the Line of Sight (LOS) geometry is mandatory. It helps to explain the path the electromagnetic signal must travel, from the SAR antenna to a certain scatterer and back to the SAR system, from where it was emitted. This means that the position of a scatterer in slant range can be recognized by the SAR system due to the value of the phase signal. Equation below describes how the phase depends on the range position

$$\boldsymbol{\varphi = -\frac{2\pi}{\lambda}2\rho = -\frac{4\pi}{\lambda}\rho} \ldots\ldots\ldots (3)$$

Where φ is that the phase under the belief that the initial phase of the emitted signal is zero, the equation is negative, because the measured signal represents phase delay and λ is the wavelength of the electromagnetic pulse, which amounts to 5.6 cm for S-1. Because the signal must travel two ways, i.e. from the satellite to the target and back to the satellite, the distance from the satellite to

the target (ρ) is doubled. Differences of this path's length determine changes within the phase and the range position of the scatterer (Simons and Rosen, 2007; Ferretti et al., 2007; Hooper et al., 2007; Rosen et al., 2000). Negative displacement values, derived from the phase value, are interpreted as movements away from the sensor in slant range direction and positive values towards the sensor. In InSAR the disparity between two phase signals is exploited with two complex SAR images used to build a fancy interferogram Φ. During interferogram formation to check the coherency between the two signals, the 2 SAR images are combined by multiplying the primary image, later called master, with the secondary, later called slave. The complex conjugate of the phase of the second image is usually used during multiplication, to form an interferometric phase φ that represents the phase difference between the 2 SAR images. Using two images recorded from nearly the identical sensor position and two different points in time by a repeat pass system like S-1 to make the complex interferogram (Eq. 4) is employed (Höser, 2018).

$$\boldsymbol{\Phi} = \boldsymbol{A_{mst}A_{slv}e^{-j\frac{4\pi}{\lambda}\Delta\rho}} = \boldsymbol{A_{mst}A_{slv}e^{-j\Delta\varphi}} \ldots\ldots\ldots (4)$$

Therefore, the interferometric phase φ can be rewritten as (Eq. 5) (Rosen et al., 2000)

$$\boldsymbol{\phi = \varphi_{mst} - \varphi_{slv} = \frac{4\pi}{\lambda}(\rho_{mst} - \rho_{slv})} \ldots\ldots\ldots (5)$$

2.5.5 Persistent scatterer InSAR

Permanent Scatterer Interferometry is a sophisticated multi-interferometric SAR technique utilized in ground deformation studies and may measure ground displacement with in millimeter accuracy (Andrea Ciampalini ∗, 2016). Persistent Scatterer (PS) InSAR is an extension to the standard InSAR techniques expressed above, which addresses the issues of decorrelation and atmospheric delay. The PSInSAR method relies on the analysis of a backscattered signal from co-registered, multi temporal synthetic aperture radar (SAR) images (at least 15) to spot highly reflective ground elements, which are stable from an electromagnetic point of view, called Permanent Scatterers. This method extract information carried within the radar phase of at least two SLC SAR images acquired in separated times over the identical place, which are used to form an interferometric pair.

CHAPTER THREE

METHODOLOGY

After thoroughly investigating literatures as discussed in the previous sections, the AHP and PS are selected to map susceptibility and to process the time series data, in order to accomplish the goal set at the onset of this research activity. The AHP and PS workflow are commonly used to map susceptibility and to process pre-movement time series data of specific landslides, which took place in the past to test if it was possible to detect the landslides ahead of time to assist monitoring.

3.1 Software used and their Interfaces

3.1.1 Landslide hazard zonation

For landslide hazard zonation mapping different data sets were analyzed and then categorized by utilizing Erdas imagine 2015, ArcGIS 10.7 and Geomatica 2018 software. Using these software, different thematic layers such as slope, drainage density, lineament density, elevation NDVI, LULC, aspect and geology/lithology maps of the study area are generated.

3.1.2 Persistent Scatterer InSAR

For the PS analysis two major software are applied. These are the SNAP (Sentinel Application Platform) (ESA, 2018b) and the StaMPS/MTI (Stanford Method for Persistent Scatterers Multi-Temporal InSAR) (Hooper A., 2012). SNAP is used to import, preprocess and export S-1 data, because it is provided in its native file format and it was necessary to convert it to *.dim format, so that it can be processed SNAP software. The output will be interferograms, suitable for PSInSAR applications. StaMPS/MTI, as the second major software package, uses the exported interferograms to process the DInSAR algorithms PS analysis. SNAP and StaMPS/MTI build the backbone of the whole workflow (Höser, 2018).

Applying appropriate operating system (OS) was a critical issue for some software packages, as the processing was taking large space and they were primarily meant for specific OS. Some packages were especially developed for UNIX based OS, and because of this it was preferred to use the Ubuntu Linux OS. The first step in the data processing was data capturing and the ArcGIS software was used for this purpose to delignate the area of interest, which is an irregular shaped polygon, and convert it to *.KML format. The next step was about the preprocessing of the InSAR

data, where SNAP is chosen as the main application for processing. SNAP is a freely available software, developed for European Space Agency (ESA). There are different ways to work with SNAP, which highly influence processing capability, parameter selection and automated processing Hoser (2018). Bash scripting employed in data processing using freely available source code. Within Matlab, StaMPS/MTI uses two additional software packages so called Triangle and snaphu. Triangle is used for generating exact delaunay triangulations and snaphu is a widely-used phase unwrapping software, which also can be used as a stand-alone (Höser, 2018). For both packages, StaMPS/MTI provides the interface management itself.

Finally, the Matlab results of plots and matrices are further summarized and exported to a .csv file using Matlab to pass it to R open software package in order to visualize the result.

With the shiny package (Chang, 2017), a shiny application uses the .csv table in R to visualize the results. In addition, the deformation time series within the .csv table can now be analyzed statistically using R as an open source software package, allowing a wide group of users to access and analyses the processed time series.

3.2 Data and Sources

3.2.1 Landslide Hazard Zonation

3.2.1.1 Satellite image Archieve

Freely available Landsat imagery of 2018 (OLI) with Path 168 and row 56 and 30m and SRTM DEM were acquired USGS. The Landsat images were used to extract different thematic data layers such as LULC, lineaments and NDVI while the DEM was used to generate drainage networks, slope, aspect, and elevation maps of the study area.

Table 3. 1: Satellite data descriptions

Date of acquisition	Sensor	Spatial Resolution	Data Type	Format	Source
2018	Landsat 8(OLI)	30m	LULC Lineament NDVI	Raster	USGS
2014	SRTM(DEM)	30m	Drainage Density Slope Aspect Elevation	Raster	USGS

3.2.1.2 Ancillary data source

To accomplish the task in addition to a satellite data sources other secondary data sources were employed. This data was collected from internet sources which was prepared by JAPAN INTERNATIONAL COOPERATION AGENCY (JICA) and Arbaminch municipality. The Geological map prepared by JICA helps to extract lithological characteristics of the study area and topographic map from Arbaminch municipality enables the extraction of linear and point features such as river, tributary, roads and different point places with in the study area

Table 3. 2: Ancillary data description

Data Type	Format	Source
Lithology	.pdf	JICA
Topographic Map	.pdf	Arbaminch Municipality

Table 3. 3: The software used to process the data

Software Name	Version	Application in the Process
ArcGIS	10.7	Data analysis and map preparation
Erdas imagine	2015	Image processing
Geomatica	2018	Lineament extraction

3.2.2 PS InSAR

Data acquisition and data processing are very important parts when working with longer time series. As the large amounts of data in InSAR data processing requires careful handling and strategic approach from the very beginning (Höser, 2018) care was taken to enable a high degree of automated processing, from the data selection through the processing to result interpretation stages.

SAR satellites orbit the Earth at an altitude of about 700 km and revisit every location on Earth after a specific time. The time period between two successive visits is called Temporal Baseline. In reality, the satellite may not be on and the same position during acquisition of the next radar image due to limitation in orbit control. The interval between two acquisition spots perpendicular to the satellite viewing direction is referred to as perpendicular baseline (Hooper A. J., 2006). As presented on Table 3.4 the dataset along with perpendicular baseline length with respect to single reference or primary image.

S-1A satellite tracks SAR images in different mode such as strip-map, interferometric wide swath, and extra wide swath and wave swath modes. The interferometric wide (IW) swath mode is the main acquisition mode over the land and satisfy most services requirements. It acquires data with a 250 km swath at 5 m by 20 m spatial resolution (single look) (ESA, 2018a).

S-1A data with different types of products were available in the ESA home page and specific data were downloaded for the InSAR processing. In this thesis the images, were single look complex (SLC) products, polarization VV and sensor operational mode interferometric wide swath (IW) used. Each image pixel is represented by a complex (I and Q) magnitude value and therefore contains both amplitude and phase information (ESA, 2018a).

Table 3. 4: S-1A data acquisition

Data	Mst/Slv	Acquisition	Track	Orbit	Bperp(m)	Btemp (days)	Modeled Coherence	Height Ambg (m)	Delta fDC (Hz)
S1-A	Master	29Nov2017	152	19474	0.00	0.00	1.00	∞	0.00
S1-A	Slave	29Oct2016	152	13699	43.86	396.00	0.61	-289.97	4.87
S1-A	Slave	22Nov2016	152	14049	55.19	372.00	0.63	-237.90	-2.73
S1-A	Slave	16Dec2016	152	14399	53.44	348.00	0.65	-230.35	0.52
S1-A	Slave	24Oct2017	152	18949	59.31	36.00	0.92	-214.3	0.63
S1-A	Slave	23Dec2017	152	19824	-57.43	-24.00	0.93	221.37	2.85
S1-A	Slave	31Oct2018	152	24374	57.13	-336.0	0.66	-222.52	2.52
S1-A	Slave	24Nov2018	152	24724	-11.32	-360.0	0.66	1123.39	2.65
S1-A	Slave	30Dec2018	152	25249	34.51	-396.0	0.62	-368.36	3.12
S1-A	Slave	26Oct2019	152	29624	-73.83	-696.0	0.34	172.21	4.98
S1-A	Slave	07Nov2019	152	29799	36.62	-708.0	0.34	-347.20	0.35
S1-A	Slave	25Dec2019	152	30499	34.24	-756.0	0.30	-371.35	0.18
S1-A	Slave	16Oct2014	152	2849	27.21	1140.0	0.01	-467.27	3.40
S1-A	Slave	09Nov2014	152	3199	67.63	1116.0	0.01	-187.98	-3.53
S1-A	Slave	03Dec2014	152	3549	27.59	1092.0	0.00	-460.87	-1.64
S1-A	Slave	04Nov2015	152	8449	32.87	756.00	0.30	-386.82	3.07

3.3 General PS Methodological workflow

The conceptual workflow for persistent scatterer InSAR deformation analysis employ the implementation of SNAP for pre-processing and StaMPS/MTI for PS processing.

The workflow in Figure (3.1) shows the steps followed to process the InSAR data. 16 radar images with different time stamp that wholly cover the study area are selected to fulfill the goal in the planned InSAR data processing. The first step was to split the images into the needed subswath with selected bursts. Then by applying an orbit file operator it was possible to acquire accurate satellite position and velocity information. Then an optimal master image was selected. The reference master image was selected such that the dispersion of the perpendicular baseline is as low as possible. Moreover, it was chosen in such a way that it maximizes the expected coherence

of the interferometric stack. The choice of "optimal" reference also enhances the visual interpretation of the interferograms and assist the delivery of quality results. With the chosen reference image, a single-reference-stack is formed, where all secondary images are co-registered to the reference image. From this stack, complex interferograms are formed using ($4\ \boldsymbol{\Phi} = \boldsymbol{A_{mst}A_{slv}e^{-j\frac{4\pi}{\lambda}\Delta\rho} = A_{mst}A_{slv}e^{j\Delta\varphi}}$), which results in *n* - 1 interferograms. In order to get interferogram suitable for PSInSAR, topographic phase ($\boldsymbol{\phi^{topo}}$) was estimated and subtracted.

Because StaMPS/MTI was employed for the PS data processing, it was not necessary to carry out multilooking approach, which was usually used to preserves spatial resolution and smoothen interferograms. Multilooking approach was commonly applied in an earlier version of PS-algorithms (Höser, 2018). Using StaMPS/MTI. PS candidates are selected by first calculating the amplitude dispersion index and using a threshold to drop pixels with extremely high dispersion. The remaining pixels enter an extensive phase analysis procedure, as stated in detail by Hooper et al. (2007). The resulting phase signal, which enters the PS processing after the removal of $\emptyset^{topo}$, was then interpreted using the relation

$$\boldsymbol{\phi^{PSc} = \phi^{disp} + \phi^{atm} + \phi^{orbit} + \phi^{LAE} + \phi^{noise}} \ldots\ldots (6)$$

Where $\boldsymbol{\phi^{PSc}}$ is the phase of a PS candidate, $\boldsymbol{\phi^{disp}}$ the phase value due to displacement, $\boldsymbol{\phi^{atm}}$ the atmospheric effect, $\boldsymbol{\phi^{orbit}}$ the residual phase due to orbit inaccuracies, $\boldsymbol{\phi^{LAE}}$ the residual phase from look angle errors resulting due to the applied digital elevation model (DEM) and $\boldsymbol{\phi^{noise}}$ contains noise due to sensor specifications like thermal noise, processing errors occurring in co-registration and the variability of scatterers.

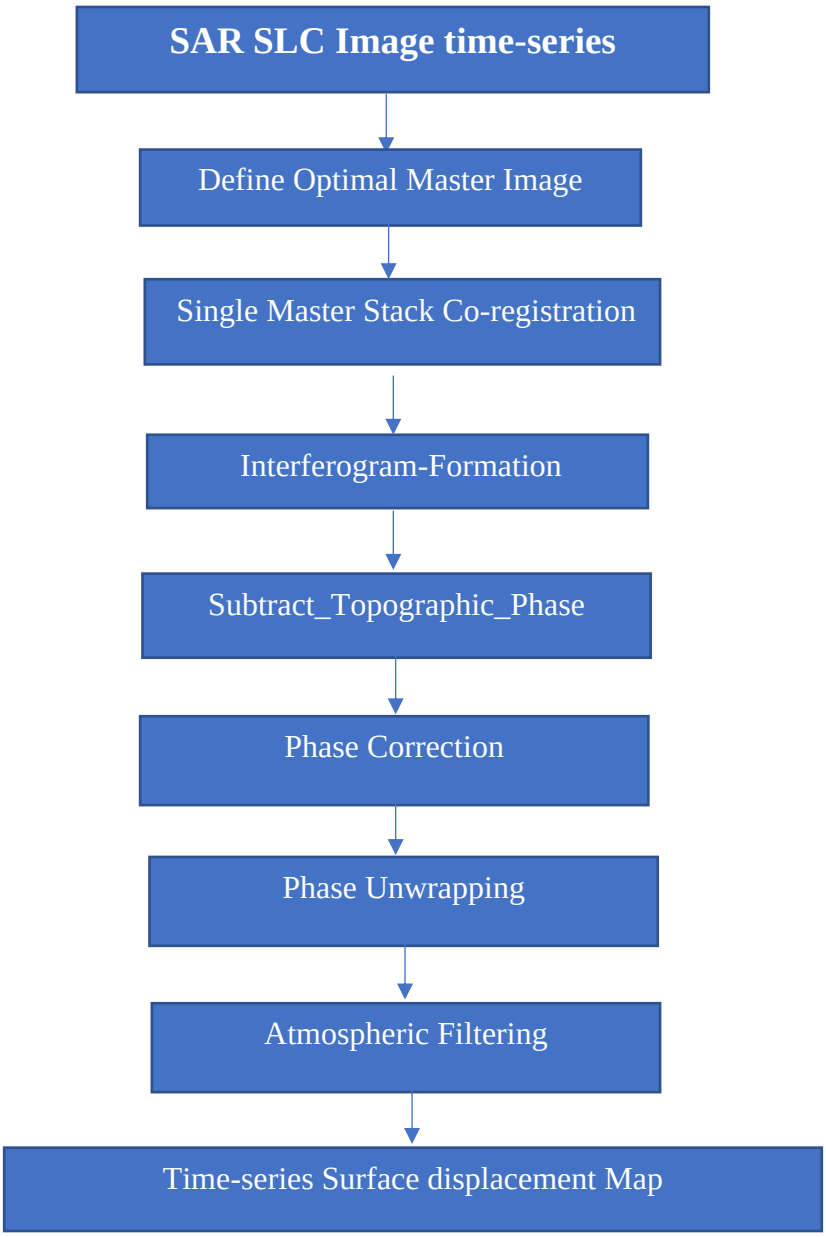

Figure 3. 1: Theoretical workflow for persistent scatterer pre-processing and processing

3.4 Landslide Hazard Zonation Workflow

In previous section an introduction to the theoretical background for general susceptibility zonation mapping and first insight to AHP was given. The implementation of the method to this specific work is summarized and explained in a workflow.

3.4.1 Conceptual Workflow for Landslide hazard zone using AHP Model

Preparation of different thematic data layers was the main activity to build spatial modelling of Geo-hazard susceptibility (Melkamu, 2019). All data layers were implemented as an input for the model. These layers were Lithology, LULC, Lineament density, Drainage density, NDVI, Slope, Elevation and Aspect map. General methodological workflow for landslide Hazard zones is given below.

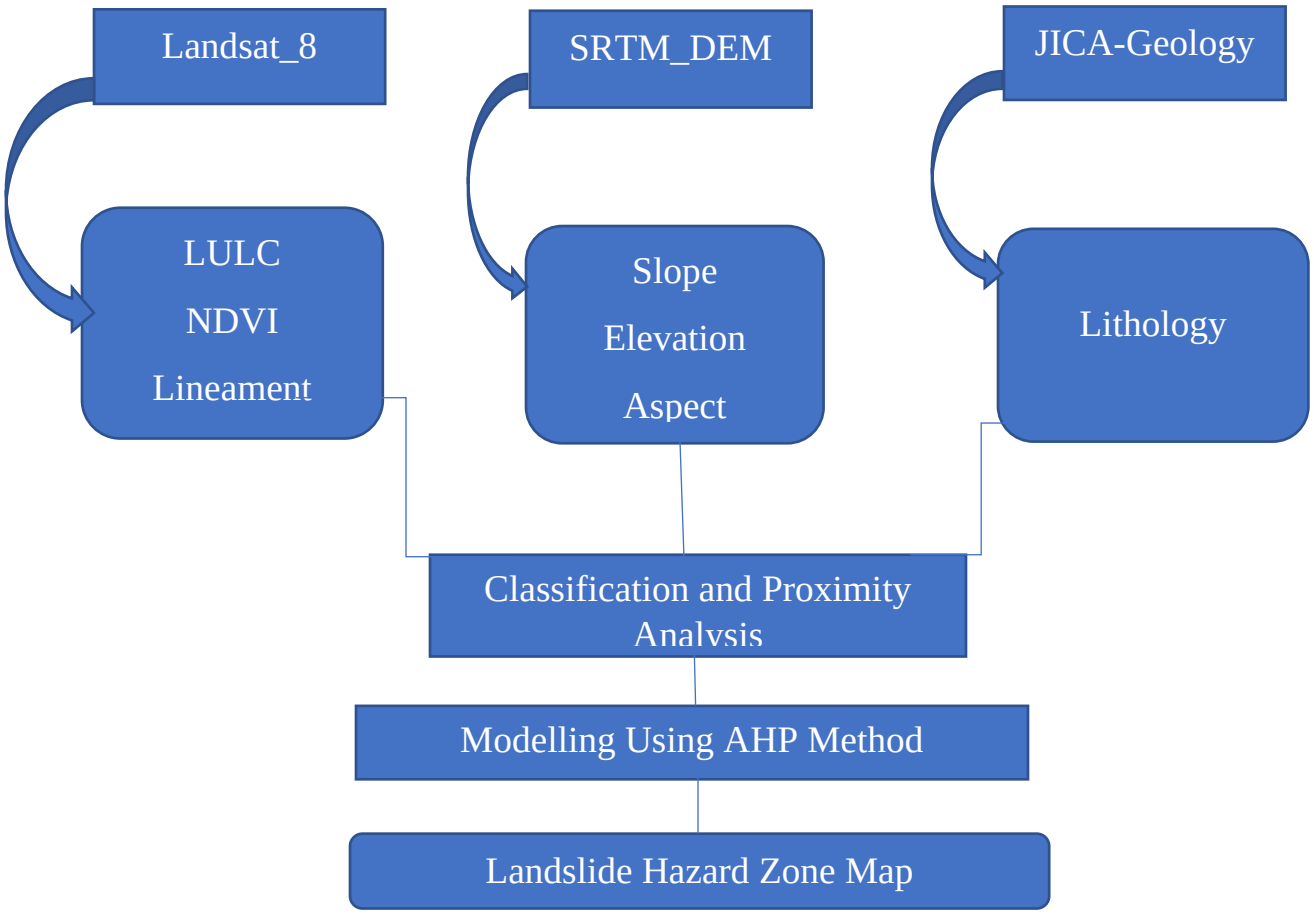

Figure 3. 2: Landslide Hazard zone mapping workflow

CHAPTER FOUR

DATA PROCESSING AND ANALYSIS

4.1 Landslide Hazard Zonation

According to Varnes (1984) landslide hazard zonation is the process of dividing the land surface into areas and ranking of these areas according to the degree of actual or potential hazard from landslides. It is an important step in landslide investigation and landslide risk management. Landslide hazard mapping consist of predicting where a potentially damaging landslide may occur without any reference to the time, or the amount of associated damage (Westen, 2006). Mostly, landslide hazard zonation mappings assume that future landslides will occur in similar areas and under the same conditions as past and present failures (Cararra et al., 2003; Guzzetti et al., 2005). In this study landslide hazard zonation was carried out using AHP based on a given causative factor maps.

4.1.2 Causative Factor Maps

The compilation of landslide hazard zone map involves the extraction of spatial database, from which causative factors are derived. The landslide causative factors that are analyzed to map the landslide hazard zone in the study area, are Slope, Elevation, Aspect, Drainage density, LULC, NDVI, Lineament density and Lithology units.

A. Slope

Slope is one of significant factor which influence slope stability, water content, erosion potential and soil formation. The slope in the study area are divided into five categories (Figure 4.1) based on natural break.

B. Elevation

Elevation is one of the landslide conditioning factors as it is controlled by different geological and geomorphological processes (Ayalew et al., 2005). Most of the time elevation becomes significant causative factor for landslide hazard zone mapping. The Elevation in the study area (Figure 4.2) is extracted from SRTM DEM with a resolution of 30m. As shown in figure 18, the elevation of the study area ranges from 1580 m to 3030 m above mean sea level.

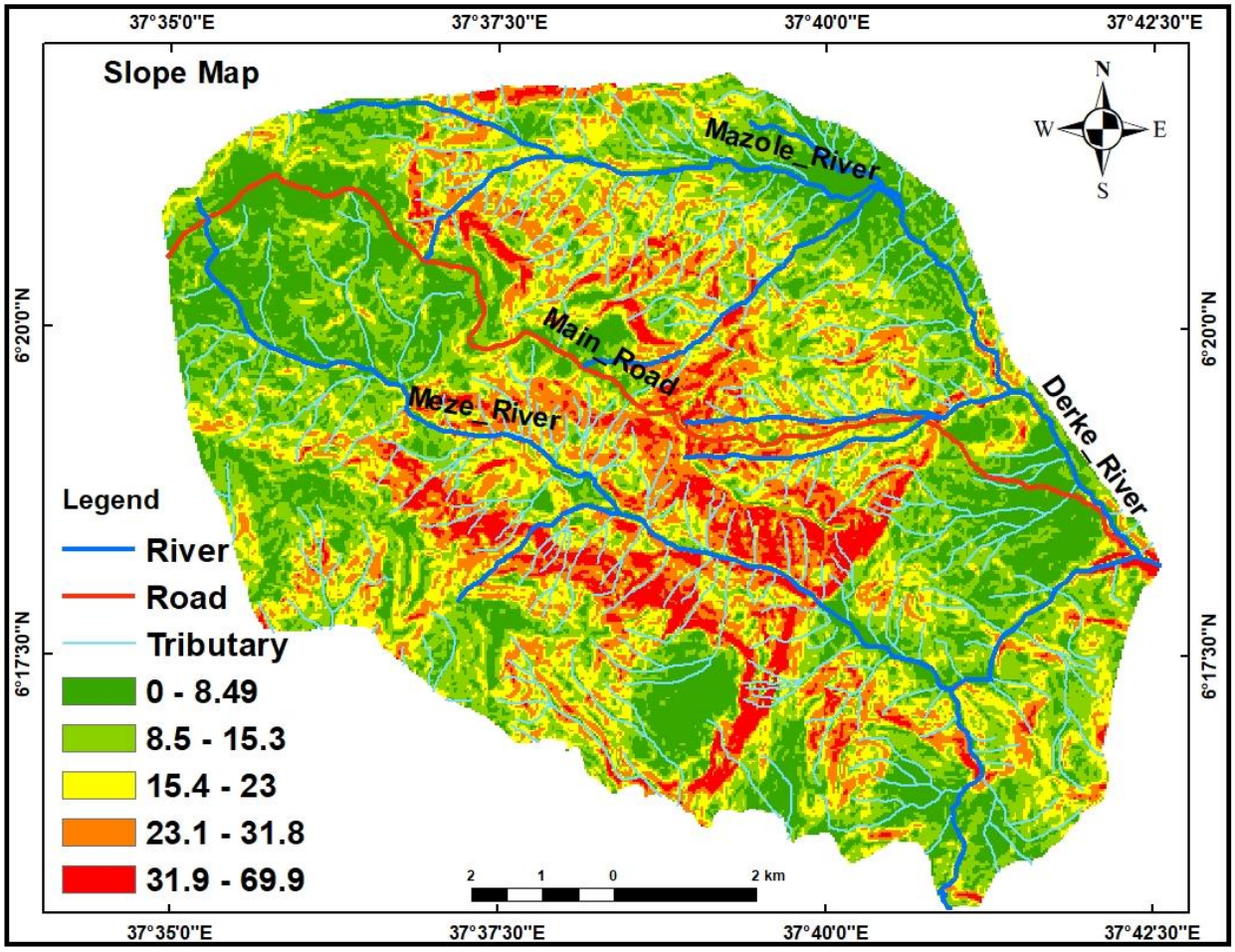

Figure 4. 1: Slope Maps of Study Area

C. Aspect

Slope aspect implies the direction of the terrain surface. Aspect is one of important variable for landslide hazard analysis as it can cause slope instability in the area of study. , Aspect has a direct relation with geochemical processes which operates on the slope and sometimes it becomes the causes for the slope instability (Kumar, 2018). Figure (4.3), which is derived from the SRTM data shows the aspect map of the study area.

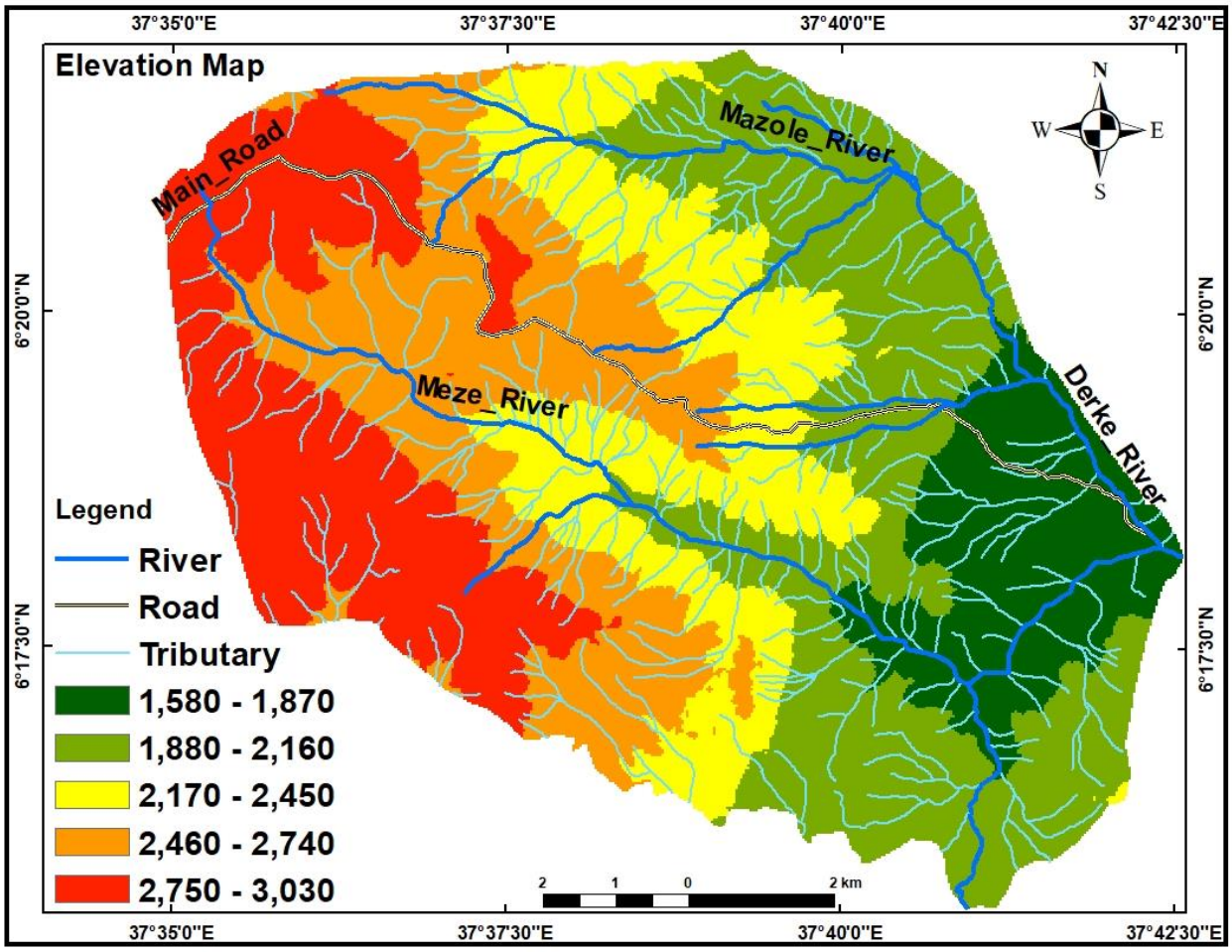

Figure 4. 2: Elevation Maps of Study Area

D. Drainage density

As of different factors, drainage density is one of influencing factor that contribute to landslide. The increasing of drainage density contributes to the process of erosion and water transportation, which makes the area vulnerable to landslide. The higher the drainage density implies the higher the probability of landslide hazard. With this point in mind the drainage density map (Figure 4.4) of the area is prepared from the SRTM data.

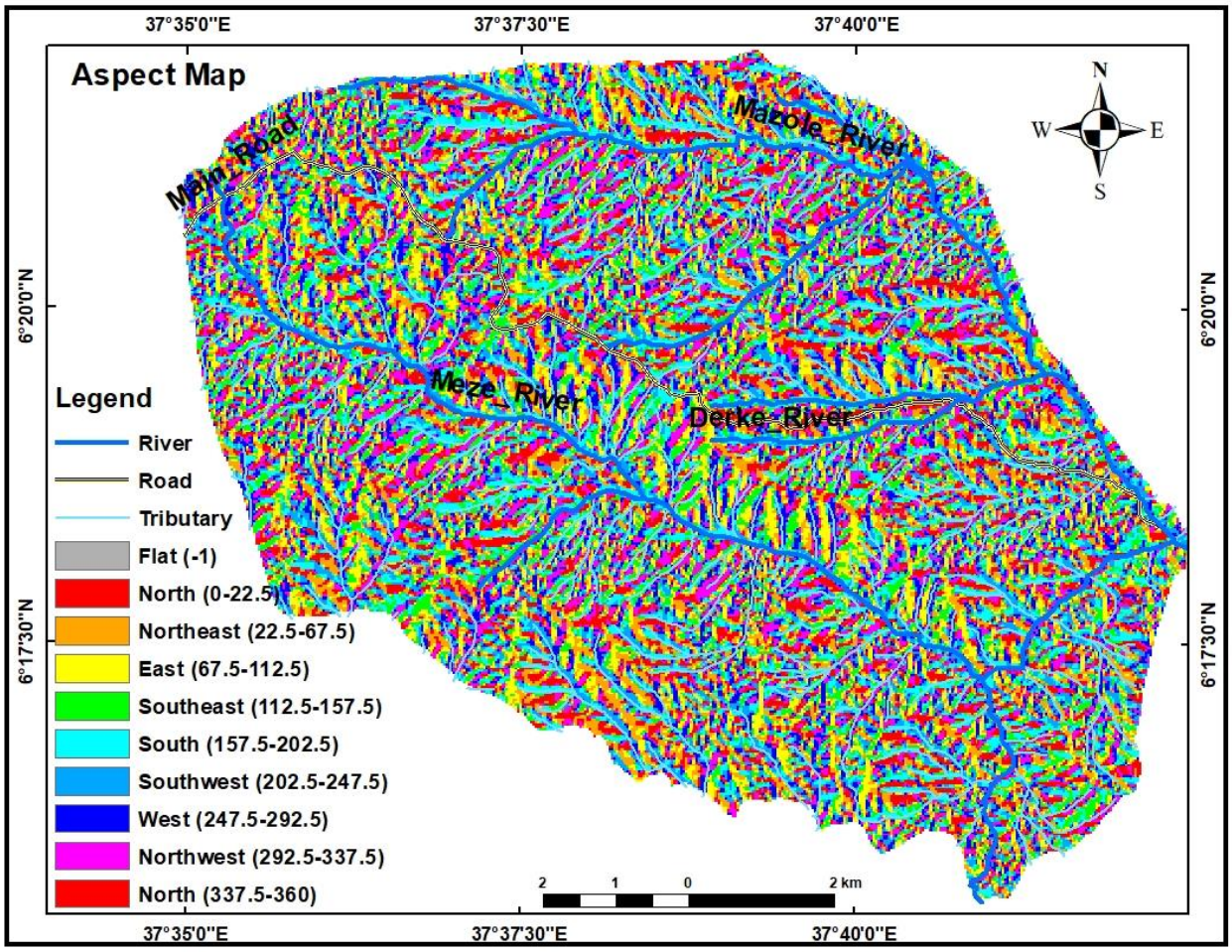

Figure 4. 3: Aspect Maps of Study Area

E. Landuse Landcover

The effects of LULC on the slope instability is dependent on certain local situations, like soil depth, slope, types of plant, rocks and weather condition in the area (Ali Mohammadi,2014).

LULC plays a significant role in aggravating slope instability, since less vegetated areas are prone to erosion relative to densely vegetated areas. Roots of vegetation strengthen soil capabilities to resist erosion and stabilize slopes. They also control the wetness of slopes through evapotranspiration (Wu and Sidle 1995; Lee 2007). The Landsat 8 data was used to study the LULC of the study area, which is given in Figure (4.5)

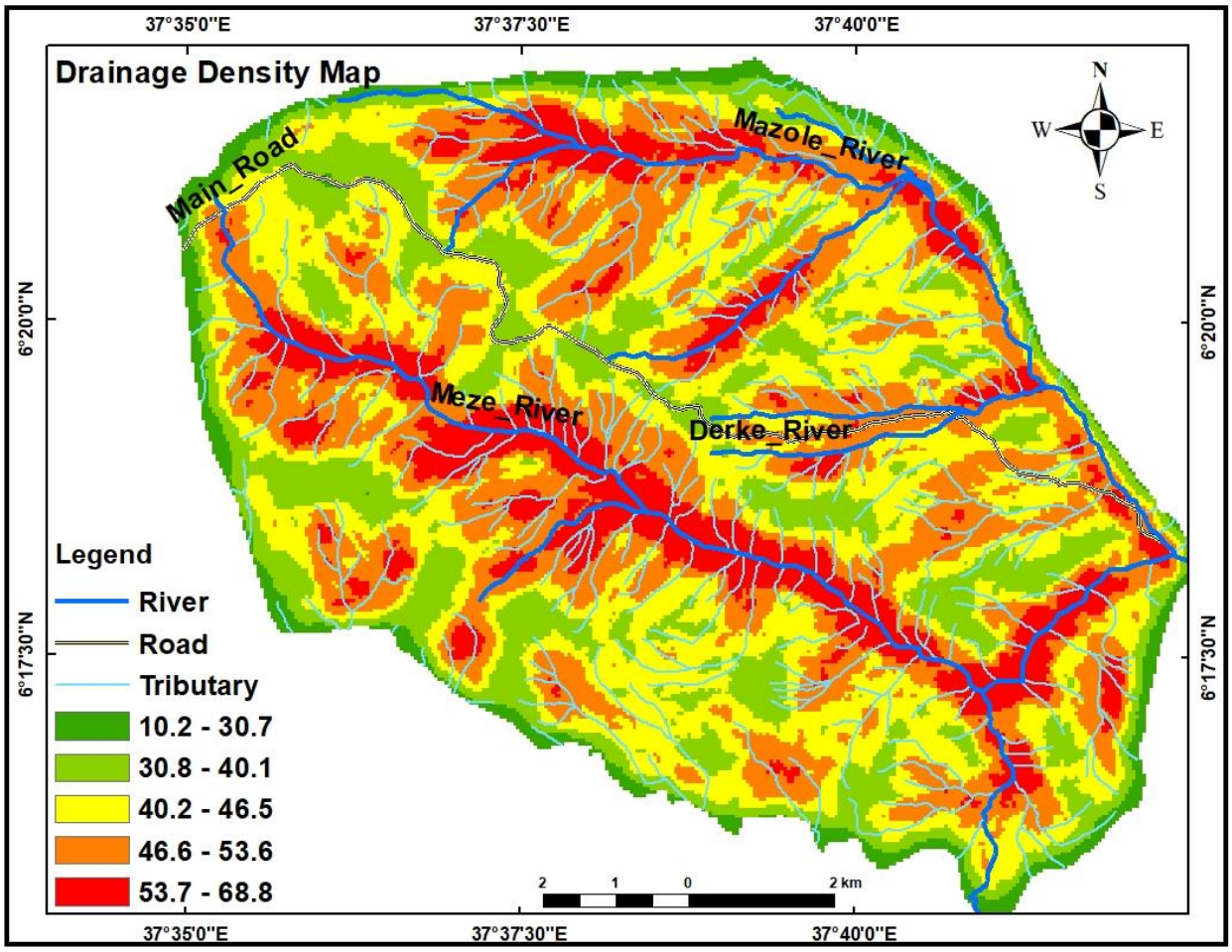

Figure 4. 4: Drainage density Maps of Study area

G. Lineament density

Lineament refers to the surface expression of underlying linear geological structures such as faults, fault-aligned valley, a series fault or fold-aligned hills, a street, coastline or a combination these features (Mandal and Mondal, 2019) High lineament density implies a high probability of landslide occurrence. Figure (4.6) shows the lineament density map of the study area.

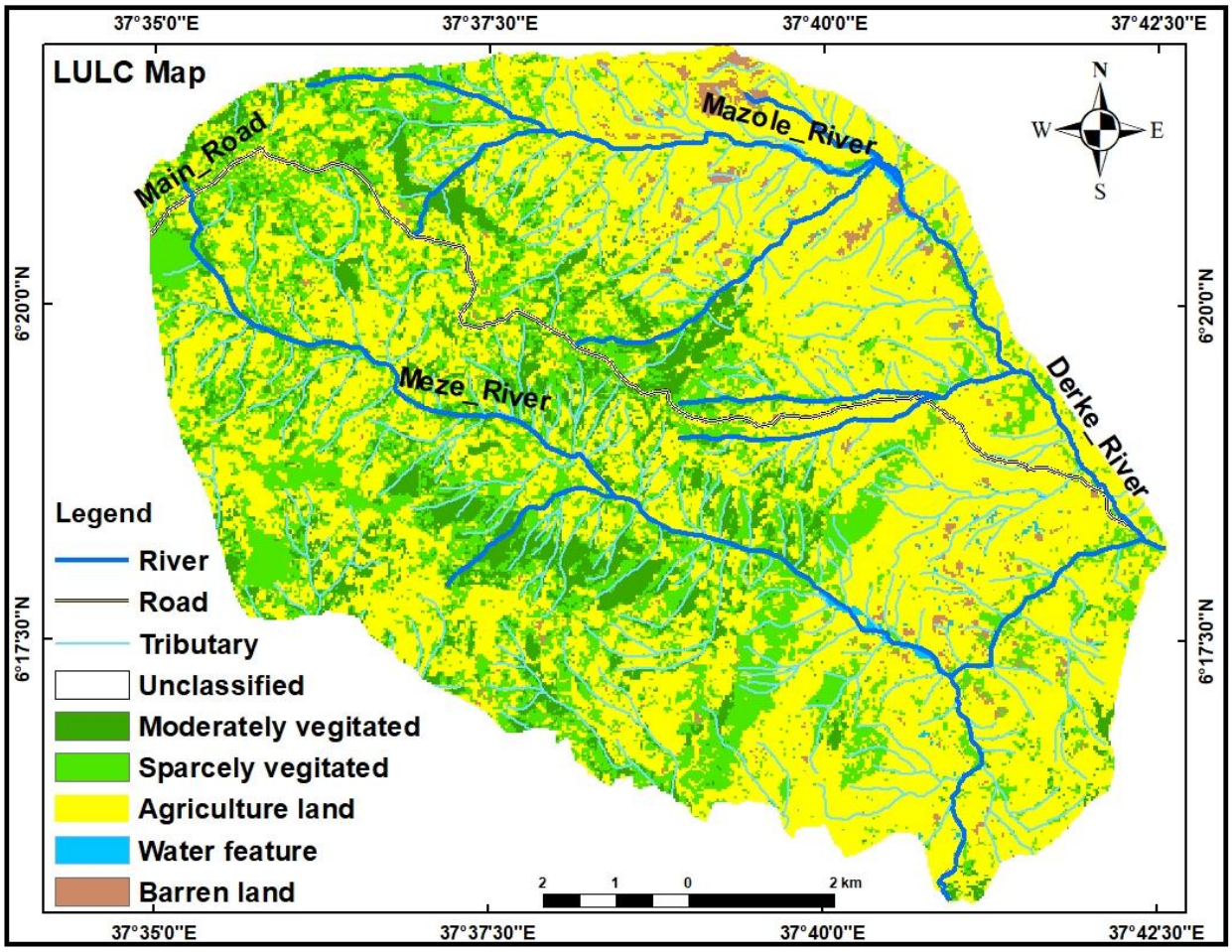

Figure 4. 5: Landuse and Landcover Maps of Study Area

H. Lithology

The lithological maps of the study area (Figure 4.7) is adopted from existing geological map published by Japan International Cooperation Agency (JICA, 2012). Four lithological units are identified in the study area. Lower porphyritic basalt has largest area coverage with a coverage of more than half of the study area and majority of landslides have occurred in this formation.

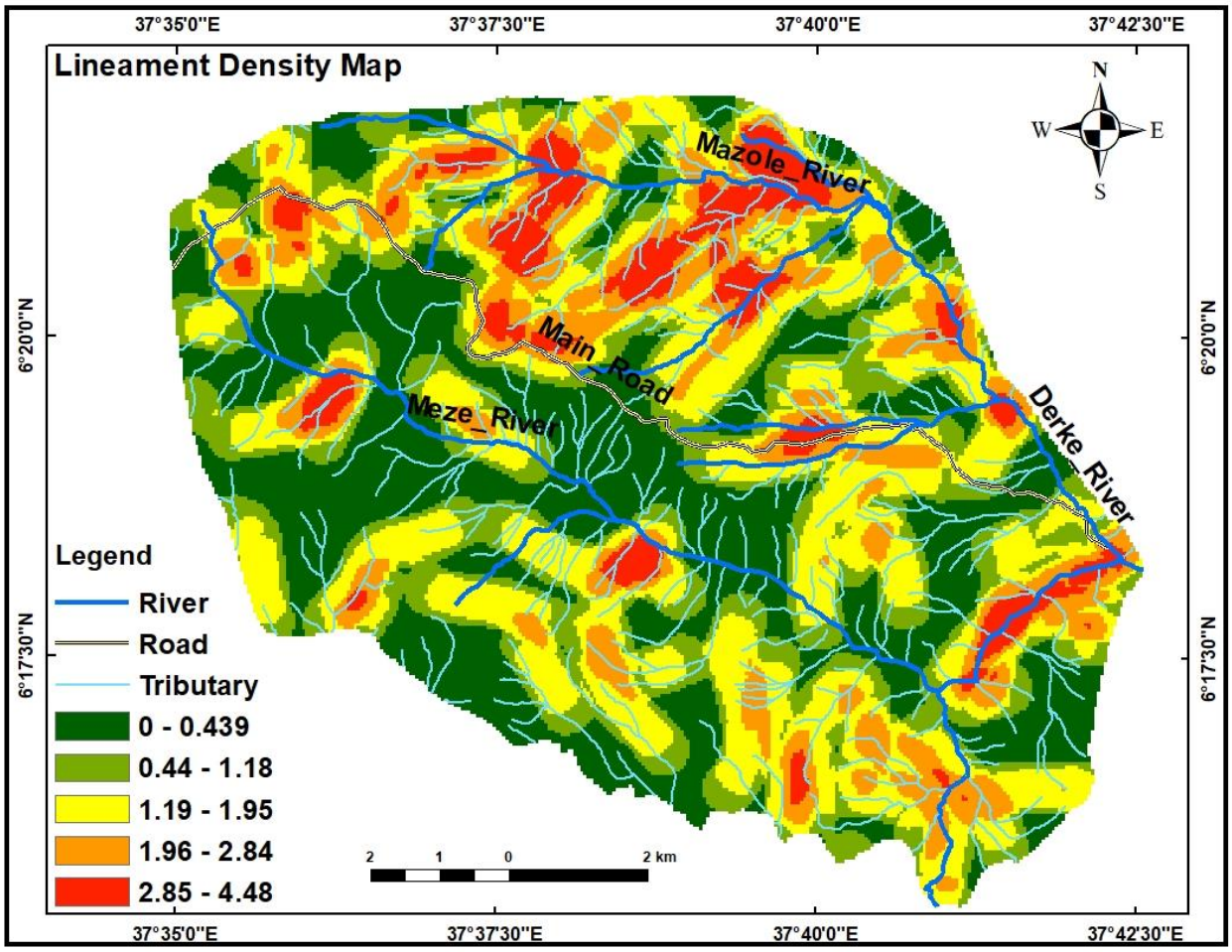

Figure 4. 6: Lineament density Maps of Study Area

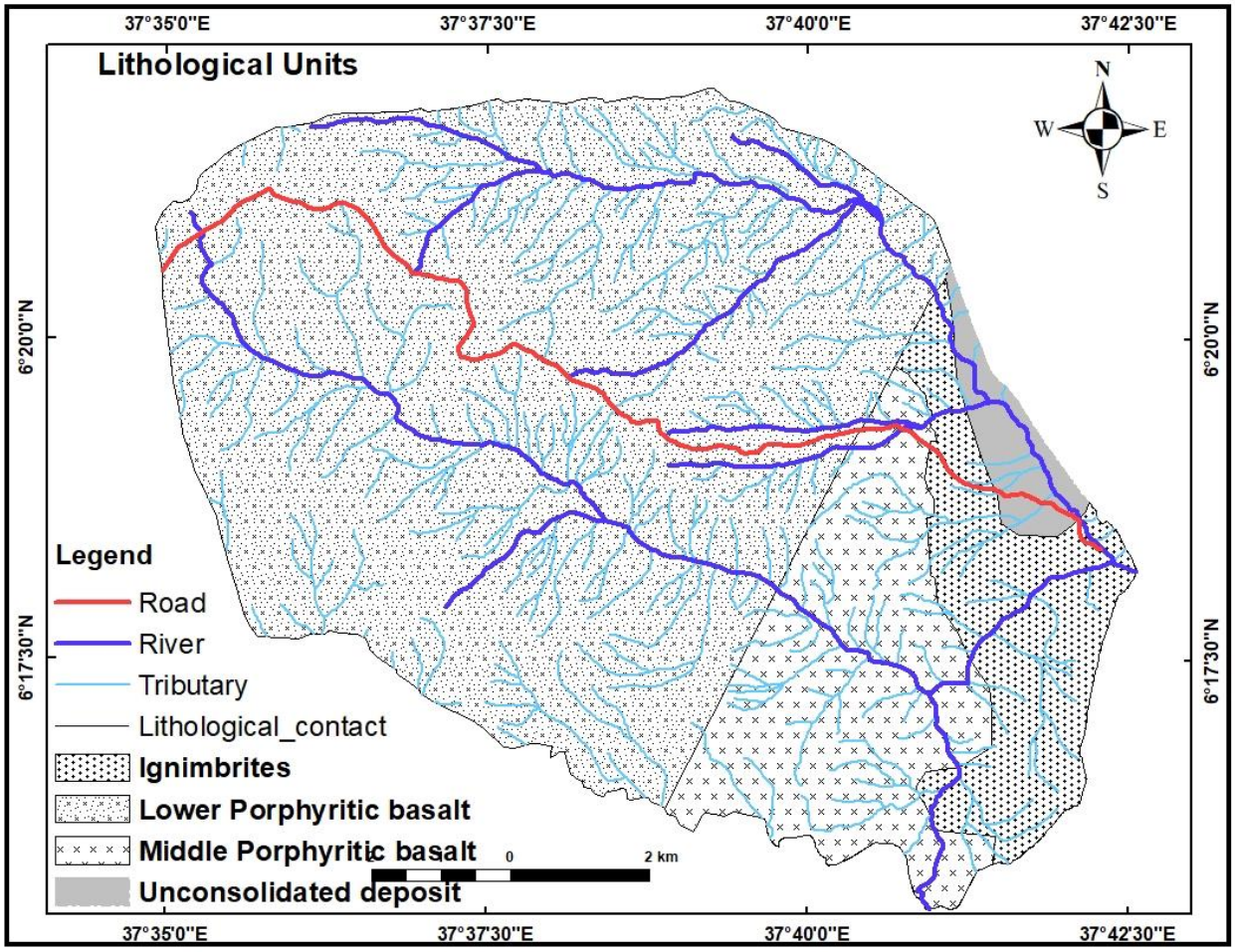

Figure 4. 7: Lithological Maps of Study Area (Adopted from JICA, 2012)

I. Normalized Difference Vegetation Index (NDVI)

Areas with dense vegetation are discernable from their high or positive value of NDVI, due to high concentration of chlorophyll resulting in low reflectance in the red band. In other word sparse vegetation has lower values of NDVI and these areas are more prone to landslide, than areas where the NDVI value are high. The NDVI value map given in Figure (4.8) is extracted from landsat-8 OLI image, which is acquired in 2017.

The values of NDVI ranges from -1 to +1 and values closer to +1 indicate that the area is covered by dense vegetation and the values closer to 0 or less implies that there is less or no vegetation in the area.

$$NDVI = \frac{NIR-RED}{NIR+RED} \ldots\ldots\ldots\ldots (7)$$

Where

NIR = reflection in the near-infrared spectrum

RED= reflection in the red range of the spectrum

As shown in Figure (4.8) the value of NDVI ranges from -.002 to +0.44 in the study area.

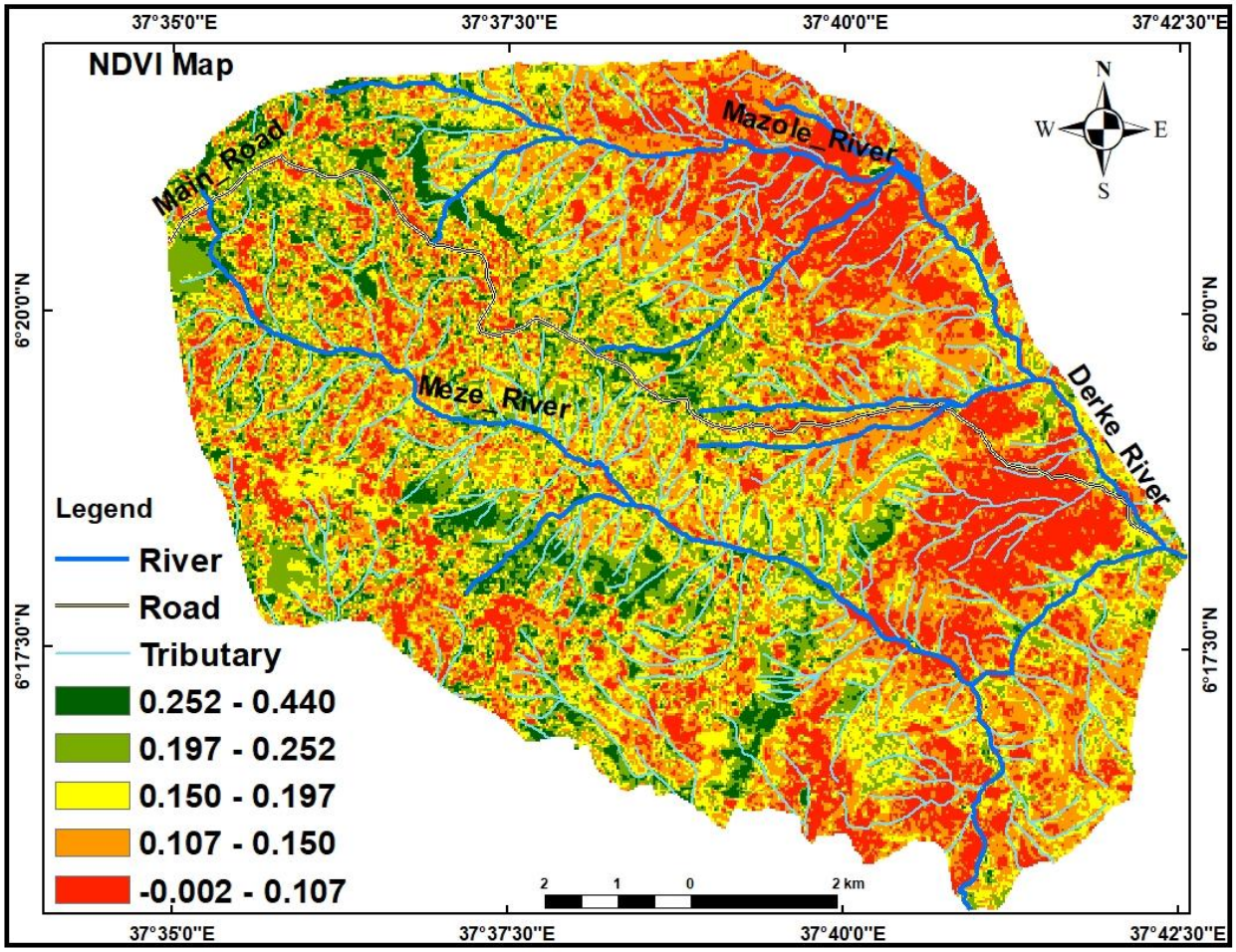

Figure 4. 8: NDVI Maps of Study Area

4.2 Landslide hazard zonation and Evaluation

To map landslides and conduct the hazard zonation the different causative factor were first derived and mapped as discussed in the previous section. The weight of each layers or the causative factor

was determined using the AHP. The first step in the AHP is to subdividing the decision problems into a hierarchy of more easily solvable sub-problems, each of which can be analyzed separately. As the overall aim is to identify vulnerable areas or landslides prone areas, this is achieved by implementing different criteria such as geological, human, environmental, geomorphological and hydrological impacts. Landslide hazard mapping consist of predicting where a potentially damaging landslide may occur without any reference to the time, or the amount of associated damage (Westen, 2006). Mostly, landslide hazard zonation is obtained based on the assumption that future landslides will occur in similar areas and under the same conditions as past and present failures (Cararra et al., 2003; Guzzetti et al., 2005). Intensities of factors for each layer are then subdivided into, very low, low, medium, high and very high as shown in Table (4.1).

Table 4. 1: General Information about classification of spatial data layer

Layer	Class	Priority value	Class importance
Slope(degree)	Very gentle slope	1	Very low
	Gentle slope	2	Low
	Moderately steep slope	3	Medium
	Steep slope	4	High
	Escarpment	5	Very high
Lineament Density	0.0-0.439	1	Very low
	0.44-1.18	2	Low
	1.19-1.95	3	Medium
	1.96-2.84	4	High
	2.85-4.48	5	Very high
LULC	Moderately vegetated	1	Very low
	Sparsely Vegetated	2	Low
	Agricultural land	3	Medium
	Water feature	4	High
	Barren land	5	Very high
Drainage-Density	10.2-30.7	1	Very low
	30.8-40.1	2	Low

	40.2-46.5	3	Medium
	46.6-53.6	4	High
	53.7-68.8	5	Very high
NDVI	0.252-0.440	1	Very low
	0.197-0.252	2	Low
	0.150-0.197	3	Medium
	0.107-0.150	4	High
	-0.002-0.107	5	Very high
Lithology(type)	Ignimbrites	1	Very low
	Lower porphyritic basalt	2	Low
	Middle porphyritic basalt	3	Medium
	Unconsolidated deposits	4	High
Elevation(m)	1580-1870	1	Very low
	1880-2160	2	Low
	2170-2450	3	Medium
	2460-2740	4	High
	2750-3030	5	Very high

4.3 Parameter Weighting

As described above in order to create the suggested hazard susceptibility model, AHP methods of statistical analysis was adopted. Analytic hierarchical process originally proposed by Saaty (1977) to be used in the solution of decision-making problems.

Table 4. 2: Scales pair-wise comparison methods

1/9	1/7	1/5	1/3	1	3	5	7	9
Extremely	Very strongly	Strongly	Moderately	Equally	Moderately	Strongly	Very strongly	Extremely
Less important						Very important		
The rest values								

Intermediates	2,4,6,8	

According to the paired comparison matrices established by saaty (1977), the matrix, aij is that the compared value between i and j, while the diagonal shows the self-comparison of elements that have a worth of 1. The lower left values within the matrix are the comparison results of the expert decision makers; while the upper right values are the reciprocals of the upper right values

$$A=\begin{pmatrix} \mathbf{1} & \boldsymbol{a_{12}} \cdots & \boldsymbol{a_{1n}} \\ \vdots & \ldots & \vdots \\ \boldsymbol{a_{n1}} & \boldsymbol{a_{n2}} \cdots & \mathbf{1} \end{pmatrix} \ldots\ldots\ldots \quad (8)$$

For checking the consistency of the comparison matrix, the consistency ratio (CR) are going to be calculated using (Eq.9) (Saaty, 2008). As the comparison is carried out by subjective judgement some degree of inconsistency may occur, Generally, C.R. ≤ 0.1 is appropriate to proceed.

$$\boldsymbol{C.R} = \frac{\boldsymbol{C.I}}{\boldsymbol{R.I}} \ldots\ldots\ldots (9)$$

Where C.I is consistency index calculated using the formula (Eq.10) and R.I is random index in the comparison matrix.

$$\boldsymbol{C.I} = \frac{\boldsymbol{\lambda max - n}}{\boldsymbol{n-1}} \ldots\ldots\ldots (10)$$

Where n is the order of the matrix and λmax is the major values of the matrix.

Table 4. 3: Values of random index R.I. (Saaty, 1977)

Rank	1	2	3	4	5	6	7		8	9	10
R. I	0.00	0.00	0.58	0.90	1.12	1.24	1.32		1.41	1.45	1.49

4.4 Pair-wise comparisons of Factor Maps

The pair-wise comparison matrix was determined using the same procedure in the last sub-section.

Table 4. 4: Pair-wise comparison of factors used for landslide susceptibility mapping

	Slope	Lithology	Lineament density	LULC	Drainage density	NDVI	Aspect	Elevation
Slope	1	2	3	4	5	6	7	9
Lithology		1	3	4	5	6	7	8
Lineament density			1	3	4	5	6	7
LULC				1	3	4	5	6
Drainage density					1	3	4	5
NDVI						1	3	4
Aspect							1	3
Elevation								1

To identify and map landslide prone areas, the eight data sets described within the previous section have been combined per their significance. The eight major landslide causative factors used in this research are LULC, NDVI, lineament density, Elevation, lithology, soil, aspect and slope. Applying the formulae of AHP the landslide hazard map where computed by summation of each factor's weight multiplied by the class weight of each referred factor using (Eq.11).

$$\boldsymbol{LSI_{AHP}} = \sum_{\boldsymbol{i=1}}^{\boldsymbol{n}} \boldsymbol{Factor\_i} * \boldsymbol{W_{AHP\_i}} \ldots\ldots\ldots (11)$$

Where Factor _*i* represents the landslide conditioning factor such as slope, aspect, lithology, etc.

W-AHP _*i* is the Weight for each causative factor. Pixel (LSI) values derived from above equations are classified into various susceptibility classes (low, moderate, high, and very high) based on natural break.

4.5 Weight and consistency ratio

Finally, after comparison matrix has been developed, consistency ratio of the matrix is checked for its validity. The weight of each individual causative factor is calculated using the ArcGIS built-in software. The procedure by which the weights are produced follows the logic developed by Saaty (1977) under the Analytical Hierarchy Process (AHP). Weight value each factor is shown in Table 4.5.

Table 4.5: Eigenvectors of the pair-wise comparison matrix used for landslide susceptibility mapping

NO.	Factor	Weight	Weight %
1	Slope	0.310	30.991
2	Lithology	0.260	26.036
3	Lineament density	0.167	16.651
4	Drainage density	0.106	10.619
5	LULC	0.068	6.759
6	NDVI	0.043	4.316
7	Aspect	0.028	2.796
8	Elevation	0.018	1.833
Consistency ration = 0.076; consistency is acceptable			

4.6 Persistent Scatterer Interferometry generation

Time-series InSAR techniques are used to depict the temporal characteristics of surface deformation that are generated by merging information from numerous SAR images acquired on different time. To map slope instabilities and associated deformation around Birbir Mariam area, 16 S-1A C-Band SLC images between 2014 and 2019, were acquired from ESA and used for the analysis. S-1A images of 29 Novmber 2017 is selected as the single reference image based on minimized perpendicular baseline.

The data were analyzed using the time-series approach of Persistent Scatterer and the time-series process was conducted to derive a two-dimensional Line-of-Sight (LOS) time-series and displacement map of surface deformation on the slope.

4.6.1 Interfrogram formation

The interferogram in PS InSAR formed by cross multiplying the single reference image with the complex conjugate of secondary images, which is the case for the coherency analysis. In this process the amplitude of the two images is multiplied while their phase is differenced. For this research, the reference image is tracked on 29 Nov 2017, which is done using stack overview in SNAP software. This image is selected in such a way that it minimizes the total decorrelation of all the interferograms. In addition to this, it also maximizes the total correlation of the interferometric stack based on the perpendicular baseline, temporal baseline and the mean Doppler centroid frequency difference (Hooper A. J., 2006). The phase difference between reference image and secondary image are interpreted using equation 6.

4.6.2 Stamps approach in Persistent scatterer analysis

StaMPS (Stanford Method for Persistent Scatterers) is a software package that implements an InSAR persistent scatterer (PS) method, to trace changes even in terrains that are barren of man-made structures and/or undergoing non-steady deformation.

After interferogram generation and removal of the topographic phase the remaining effects are converted to differential interferogram which is suitable for persistent scatterer analysis. Stamps use amplitude dispersion which is that the ratio of the quality deviation and therefore the mean of amplitude value to settle on a subset of pixels that has most of the PS pixels within the dataset. The pixels are selected on the bases of amplitude stability. Those pixels that have a good amplitude dispersion index together with their edge value are selected as initial PS candidates (Hooper A. Z., 2007). This information will then be supplied to the PS-InSAR processing in StaMPS, if necessary, to stack the differential interfrograms that are coregistered to a specific master image. In this study, an edge value of 0.4 was used for amplitude dispersion. The parameter used for StaMPS based PS-InSAR processing is shown in Table (4.6).

Table 4. 6: Parameter employed for PS candidate selection

No	Parameter	value
1	Amplitude Dispersion threshold	0.4
2	Numbers of Patches in range	1
3	Numbers of Patches in azimuth	1
4	Overlapping Pixel between patch in range	50
5	Overlapping pixel between patch in azimuth	200

The primary PS-InSAR examination is the double difference between single reference and secondary for two adjacent PS (Hanssen, 2014). The double difference is taken in both spatial and temporal dimensions. In this study, 3D phase unwrapping was carried out. The two are for spatial and one for temporal. The temporal phase difference, for each PS pixel, were first calculated and later spatially unwrapped, from the reference PS pixels using an iterative least square method. Before unwrapping, the results are filtered using Goldstein phase filter (Figure 4.9).

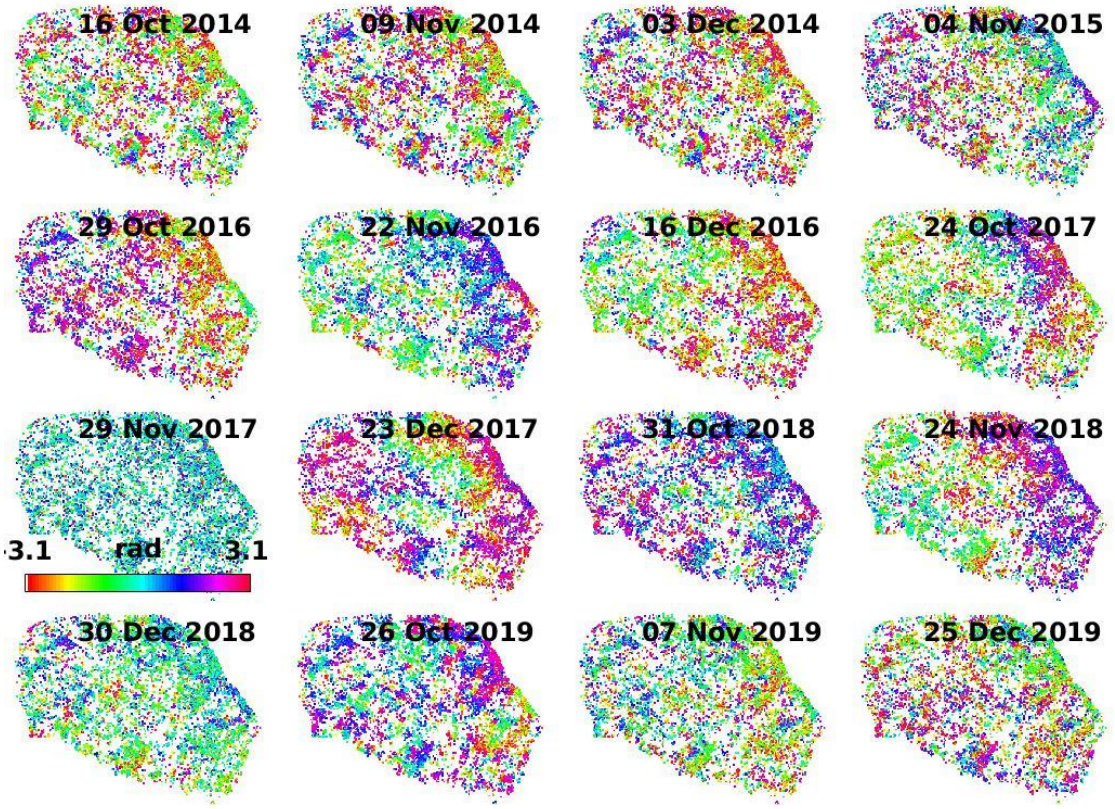

Figure 4. 9: Wrapped interferogram with single reference image 2014-2019

The candidate pixel of wrapped phase is the first output in the Stamps/MTI process and it is noisy. The wrapped interferograms contain phase contributions due to the orbital errors, spatially correlated look angle error, and atmosphere. High-pass filter can be applied to the unwrapped data in order to remove the remaining look angle, atmosphere and orbit errors (SCLA). By subtracting SCLA errors from PS pixels, one ends up with phase data due to deformation only.

The unwrapped interferograms (Figure 4.10) contains the information extracted from the wrapped interferograms.

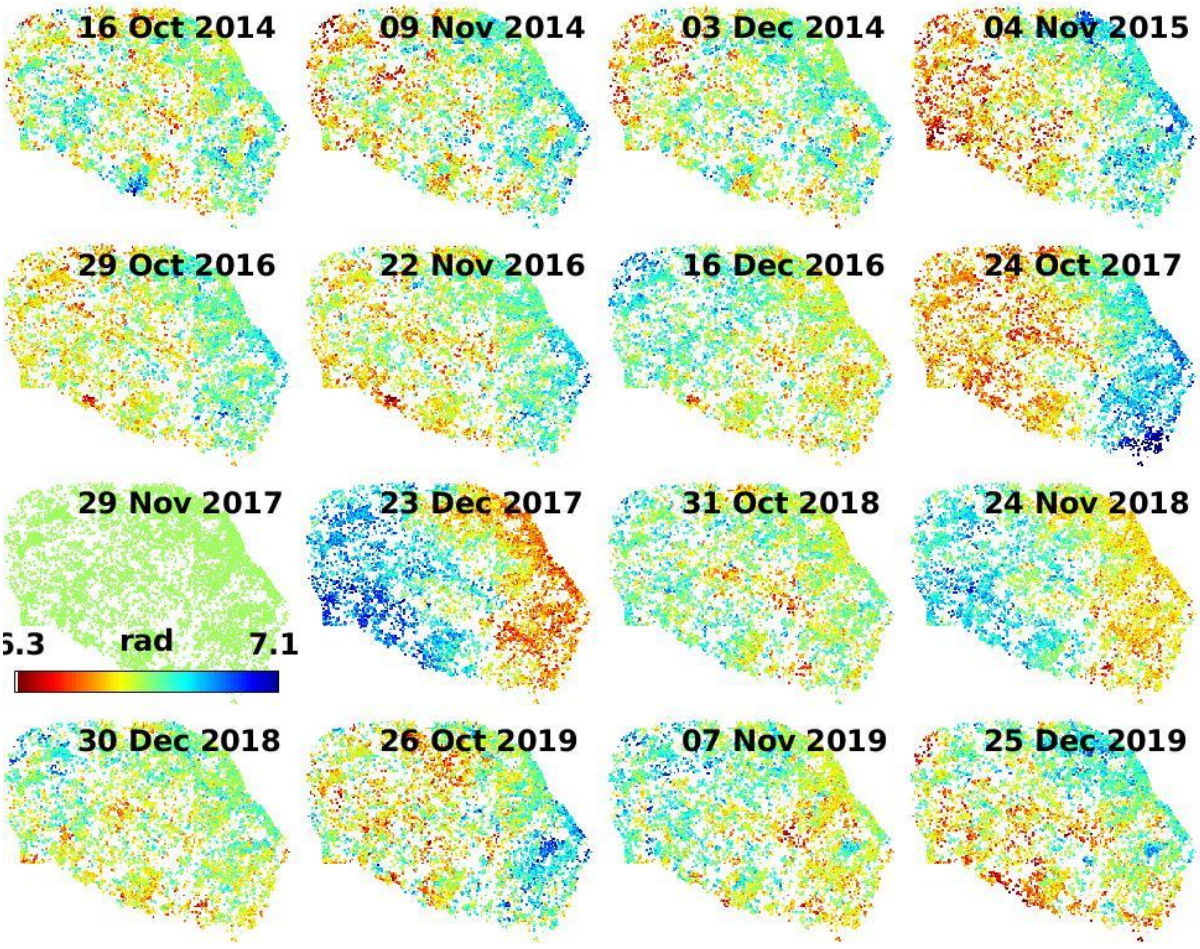

Figure 4. 10: Unwrapped interferogram with single reference image 2014-2019

As the double differencing is used in this work, which is first done with temporal and later with spatial difference, the unwrapped phase implies phase difference in time between neighboring pixels which is used to estimate the noise contribution for each phase arc (phase difference between neighboring pixels).

Figure 4.11 the spatially correlated phase component. It was evaluated using low-pass filtering and high pass filtering of the single reference image and secondary images, respectively. This evaluated phase was then subtracted from the unwrapped phase of all interferograms to obtain the phase only due to surface deformation.

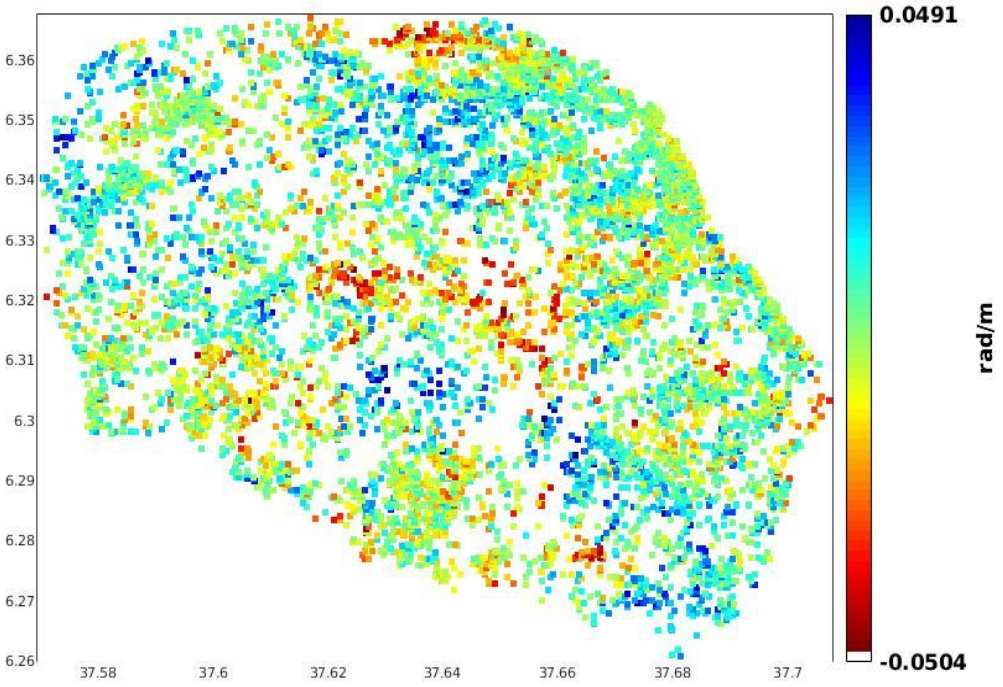

Figure 4. 11 Spatially correlated Topographic Phase

CHAPTER FIVE

RESULT AND DISCUSSION

5.1 Land Inventory Map

In general, a landslide inventory map shows the records location of past landslide occurrence and the types of mass movement that left discernable traces in an area (Guzzetti et al., 2012). Landslide inventory mapping is the base for landslide hazard zonation mapping Dia and lee (2002). It shows the location and characteristics of landslide that have occurred in the past, but do not indicate the mechanism that triggered them and it helps to evaluate the landslide hazard in an area.

Figure (5.1) shows the landslide inventory map that has been prepared based on information gathered in the study area. A complete inventory of the landslides that occurred in the past was not possible, due to accessibility problem. In Appendix (B), images that show some of the previous landslides that occurred in the area are attached.

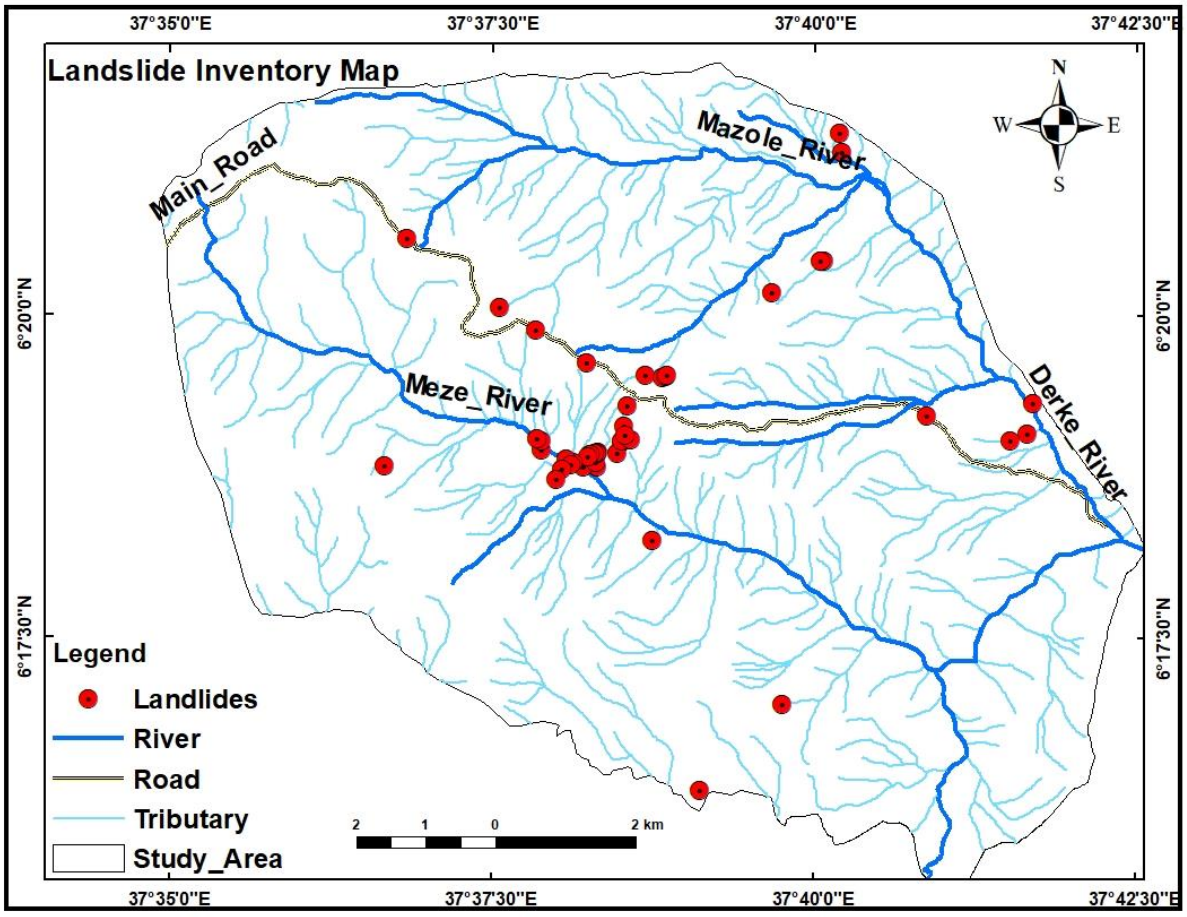

Figure 5. 1 Landslide Inventory Map

5.1.1 Landslide hazard mapping

Applying the Analytic hierarchy process method, the Landslide hazard zone map values were computed by using weighted overlay analysis in Arc GIS 10.7 and AHP plugin. The Landslide hazard zones values were then divided into five classes based on the class of weighted overlay analysis obtained from the computation. These are very low, low, medium, high and very high hazard susceptibility, qualitative class.

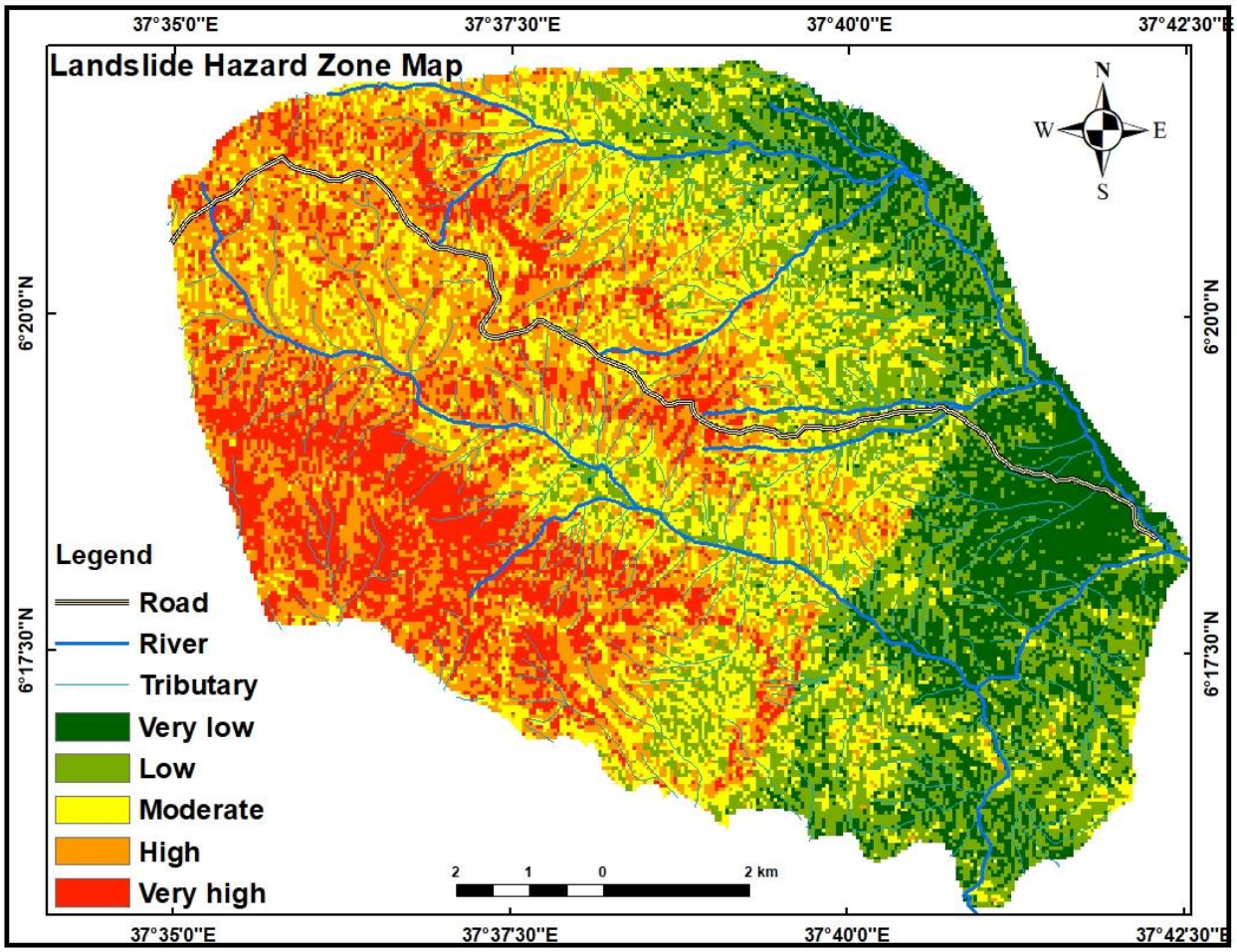

Figure 5. 2: Landslide hazard zone map

The resulting map (Figure 5.2) shows that 15% (16.466km^2) of the area falls on very low hazard zone, 21.45%(23.547km^2) falls under low hazard zone, 23%(25.25km^2) lies within moderate

hazard zone, 25.7%(28.221km^2) of the study area falls within high hazard zone and 14.85%(16.306km^2) falls within very high hazard zones (Table 5.1).

The result of landslide hazard zone map shows that the spatial distribution of landslide prone areas covers almost the whole area in the west, even though the percentages of probable hazard is variable. The susceptibility to landslide highly concentrates in the south west with lesser spatial distribution in the western and northwestern part of the study area.

Table 5. 1: The ranking of Landslide hazard zones and area coverage

ID	Susceptibility Rank	Area (km^2)	Area (%)
1	Very low	16.466	15
2	Low	23.547	21.45
3	Moderate	25.25	23
4	High	28.221	25.7
5	Very high	16.306	14.85
		109.79 km^2	100%

5.1.2 Slope instability (Displacement map and Time series analysis)

As mentioned in section (4.6) persistent scatter interferometry is the advanced multi-interferometric SAR method used in ground deformation analysis and can measure ground displacement with millimeter level accuracy. The deformation in the area was monitored for the time span between October 2014 and December 2019 in the Birbir-Mariam area.

Time series analysis were performed applying PS InSAR technique using 15 interferograms generated with single reference. The resulting image indicates that there is a total of 200,000 PS candidates that are selected based on the Amplitude Dispersion index value. The landslide deformation in the study area is analyzed by employing the mean deformation velocity of PS-InSAR, which assist to monitor displacement in the study area, and observe if places that are mapped as high and very high hazard zones are truly deforming. The result in general shows that there is displacement rate that ranges between +5 mm per year to -5.4 mm per year, as shown in Figure (5.2).

The displacement phase extracted from the interferogram is a measure for the surface displacement in the satellites LOS. Negative displacement indicates that the land surface is moving away from the satellite LOS and the positive sign indicate that the area is moving towards the LOS.

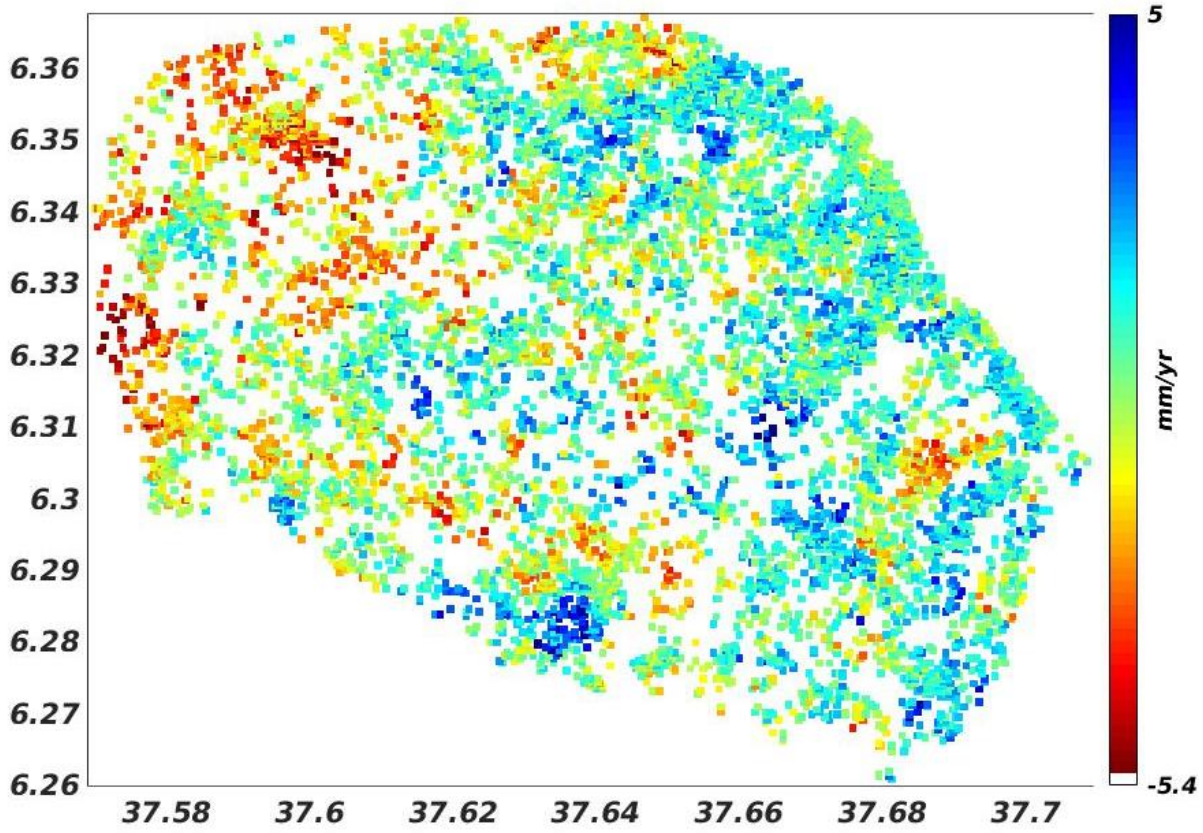

Figure 5. 3: Mean line of sight (LOS) displacement

The result of the analysis shows that the landslide process, which is depicted from the surface displacement was still active in 2019. And the deforming areas area are mostly matching well with the landslide hazard zonation map, except in some few places such as that in the south eastern tip of the area.

A further time series analysis is made, by picking selected areas (Figure 5.4) as shown in Figure (5.5). This analysis shows the observed movement of the selected points in time.

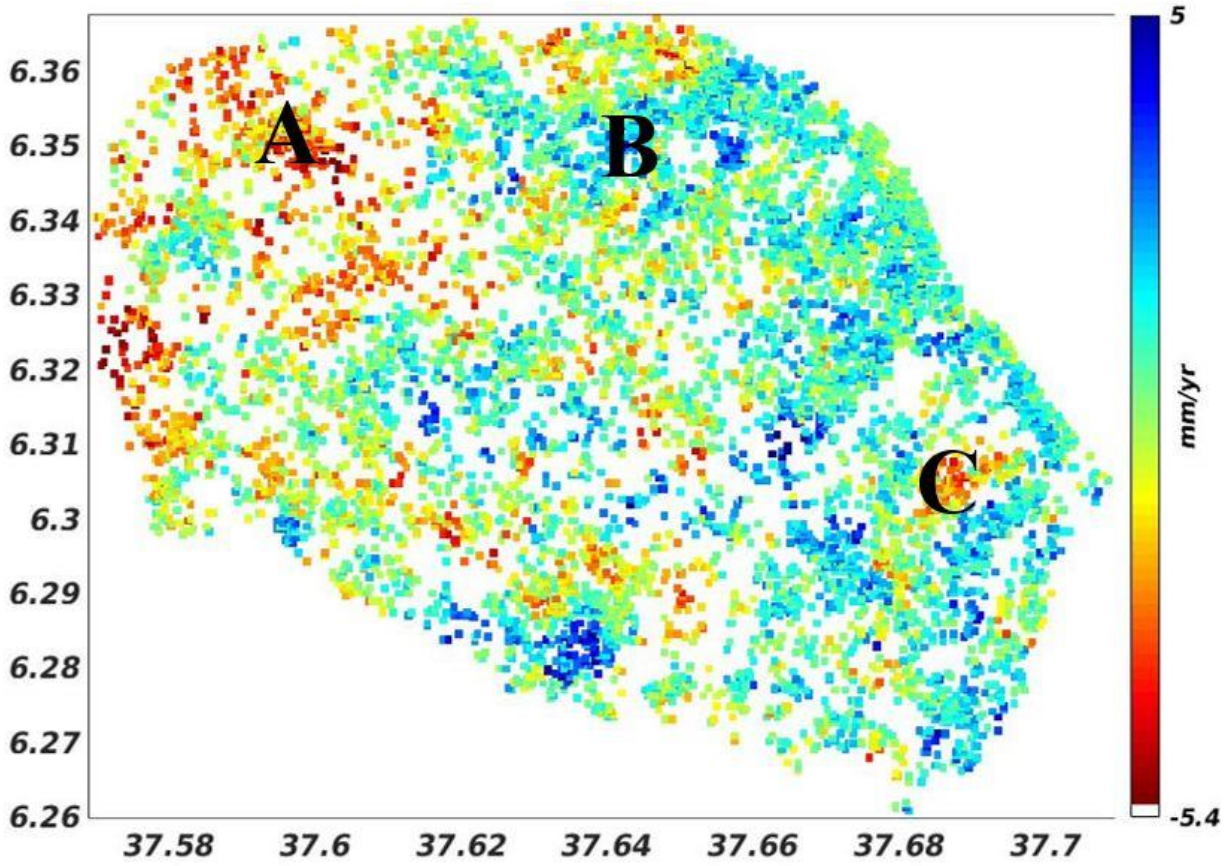

Figure 5. 4: Distribution of PS points selecting area A-C

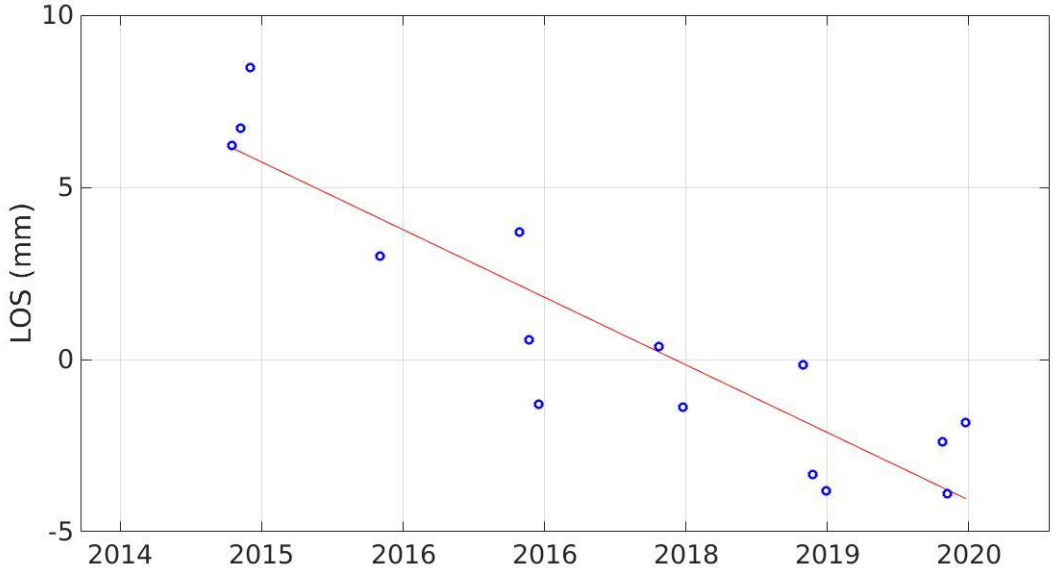

Point B

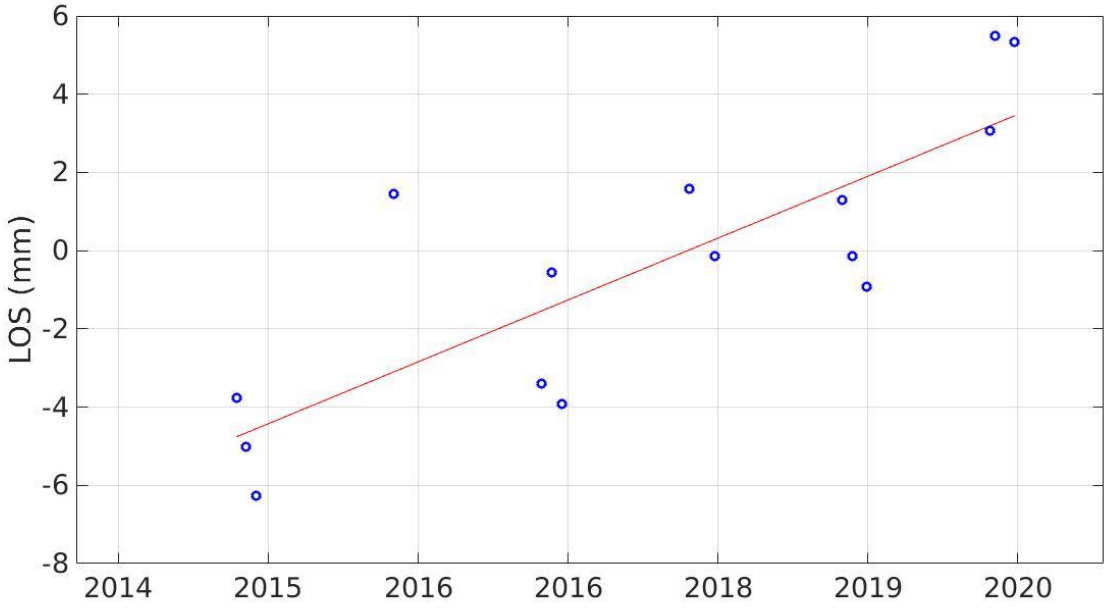

Point B

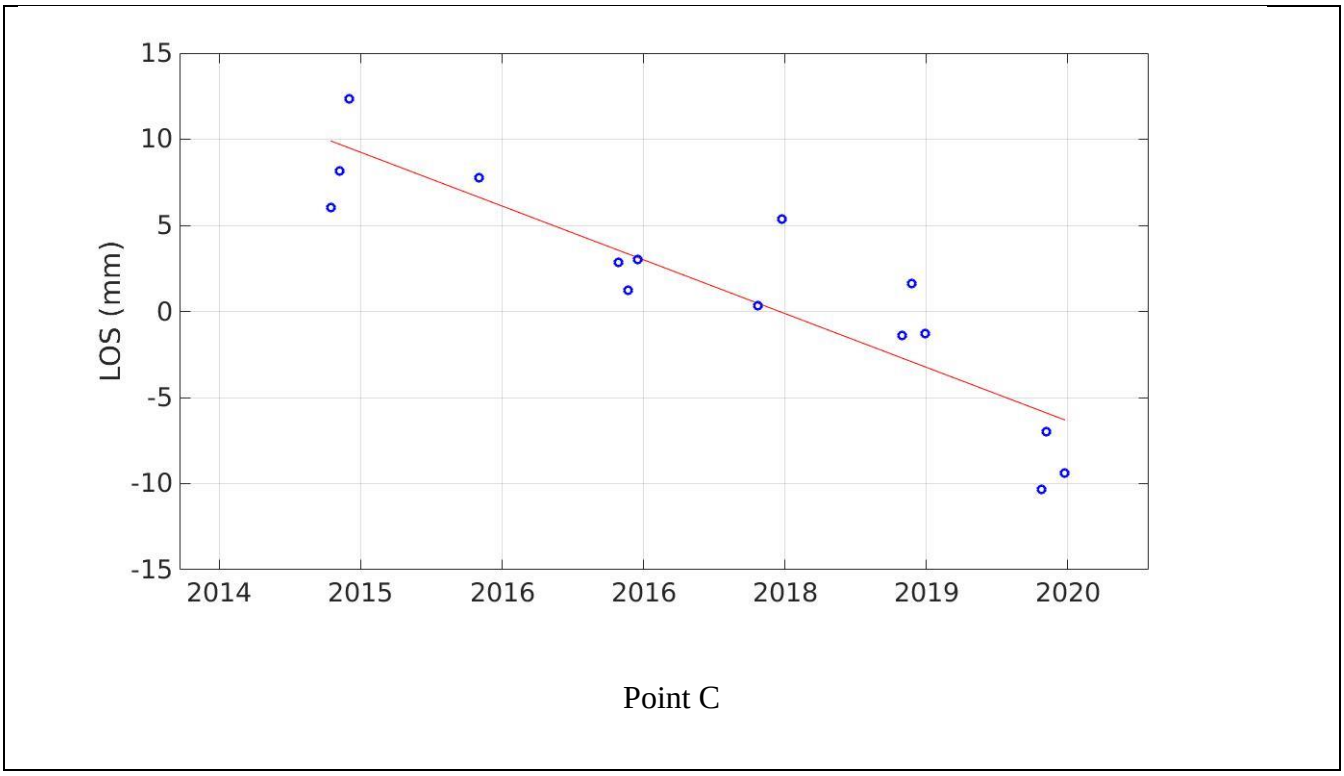

Figure 5. 5: Distribution of PS points in LOS with observed years

5.1.3 Stamps visualizer: A new application for data exploration and presentation

In processing persistent scatterer, the result extracted in MATLAB is difficult to analyze in such that specific time series can hardly be assigned to a PS pixel. To overcome this problem a program called Stamps-Visualizer is implemented. The program is used for a better exploration and presentation of results in such that the user can intuitively browse and compare PS pixels and time series. Towards this, the objects created in MATLAB during StaMPS/MTI processing are first tabulated. The different columns of the table contain information such as the coordinates, deformation and mean velocity of each PS pixel. These are later exported as a .csv file and used in the StaMPS-Visualizer shiny app (Höser, 2018). The result is shown in Figure (5.6)

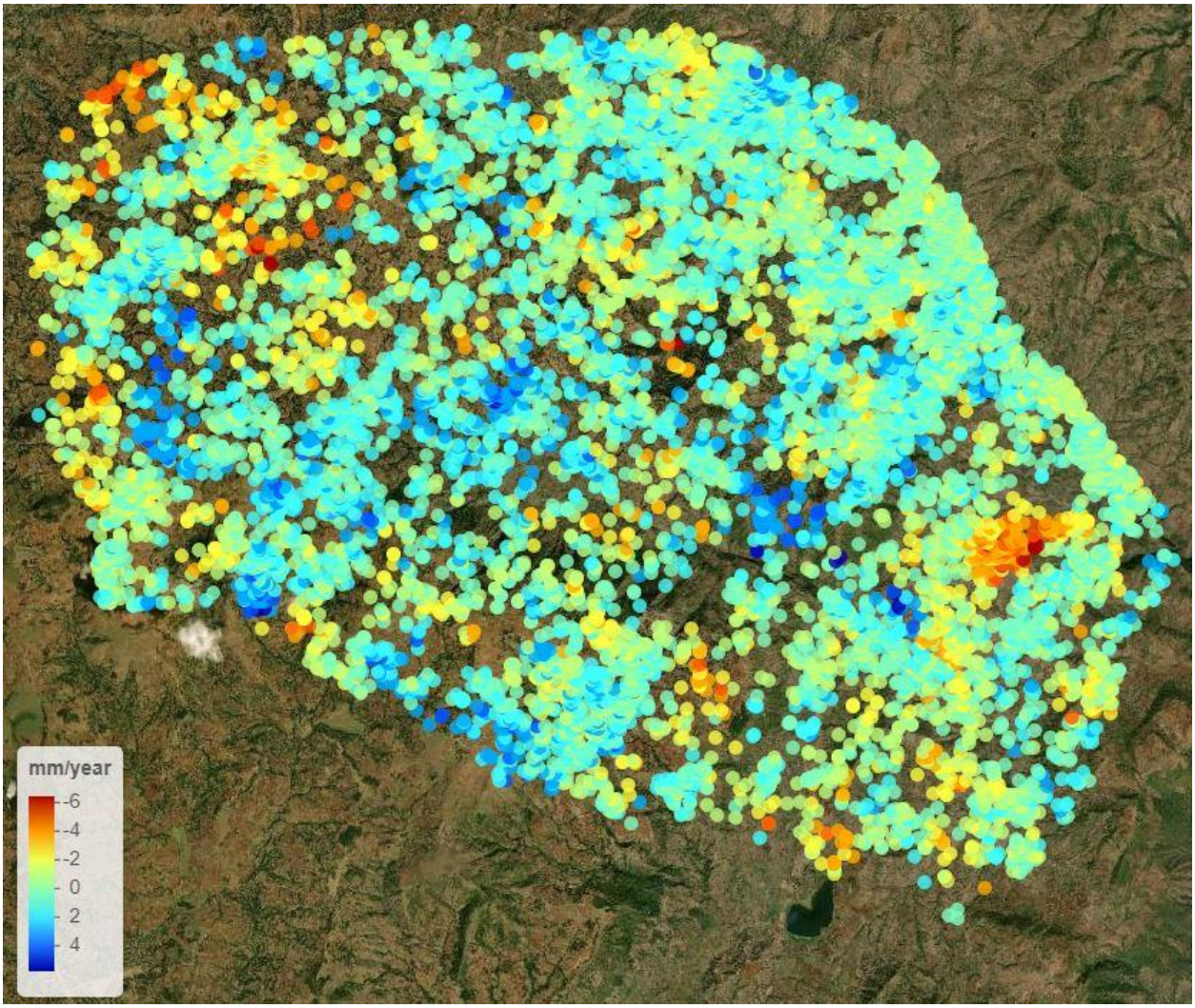

Figure 5. 6: Stamps visualizer showing landslide distribution

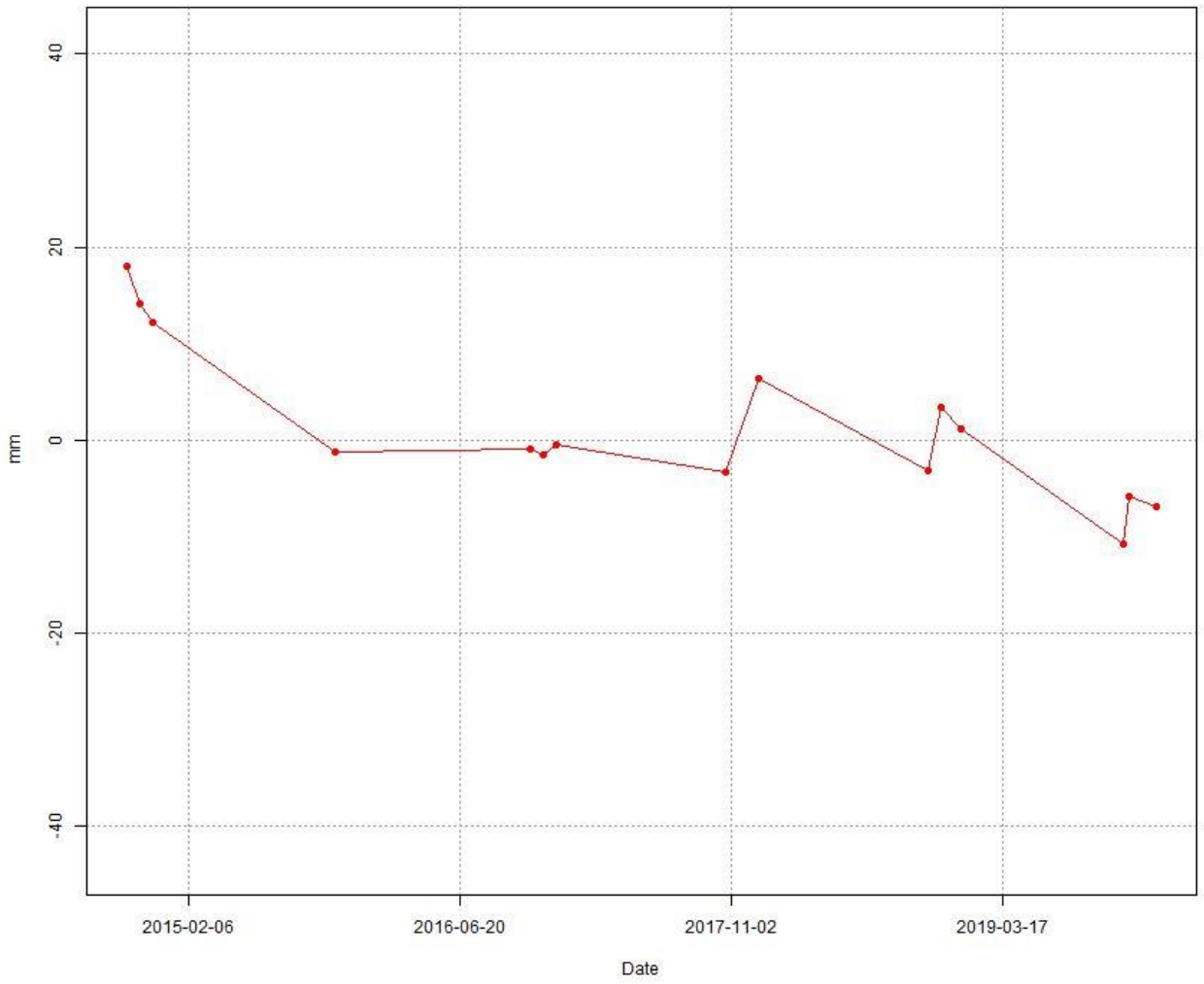

Figure 5. 7: A single PS point showing how it deforms with reference to time at point A

Information such as the one in Figure (5.7) and can be extracted to follow the deformation pattern of a single point. On the other hand, Figure (5. 8) shows the standard deviation of mean LOS displacement. The low standard deviation was due to the low or near-similar displacement rate in different interferograms. The other areas had a high standard deviation that amounts to 2mm/yr. due to the difference in the displacement rate in different interferograms.

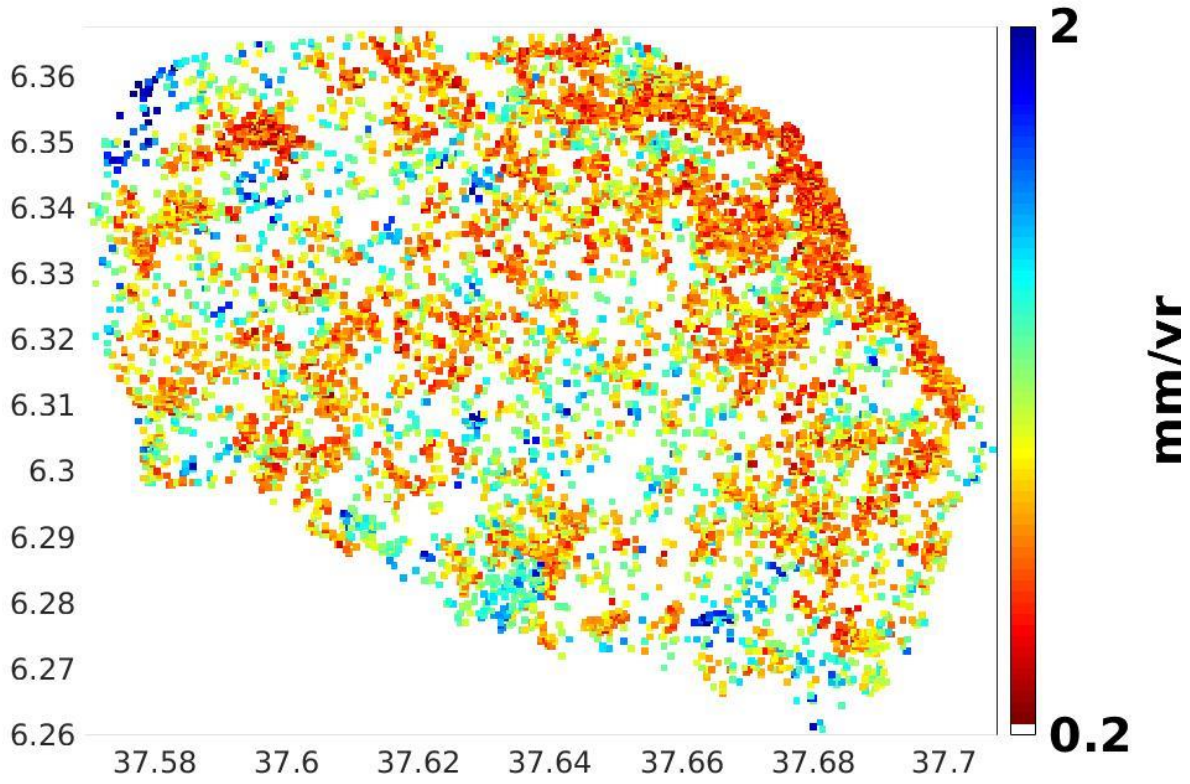

Figure 5. 8: Standard Deviation of Mean LOS Displacement

5.2 Discussion

Landslides are natural hazards that are usually caused by several triggering factors, which differ from place to place (Emmanouil et al., 2020). They are one of the major environmental problem that challenge infrastructure development and urbanization in Ethiopia. This is particularly true for those areas in the Ethiopian rift margins and rift valleys (Melkamu,2019; Bekele Abebe et al.,2010). In order to assess landslide susceptibility of an area, it is important to know these triggering factors and their possible influences on slope instability in the area. The primary assumption which is accompanied in most land slide studies, particularly for those that involve quantitative techniques, is the analysis of the combination of causative factors that have led to the past landslides and analyze the possibility of them appearing again in the area of interest (shano et

al., 2020). In this work, the landslide inventory map of the study area and the analysis of landslide hazard zone as well as deformation time series map ae presented.

There is various approach to map the landslide hazard zone and to analyze the deformation pattern. In this study landslide hazard zonation map and time series deformation map for the entire study area were generated using the techniques of AHP and PS InSAR, respectively.

The landslide hazard zone map was produced by analyzing eight causative factor maps. These are Slope, Elevation, LULC, Lineament density, and Drainage density, NDVI, Lithology and Aspect. The outcome of the data processing by making use of the AHP technique shows that 40.5 % of the study areas belongs to high and very high hazard zone and are situated mainly in the western, southern, central and northwestern parts of the study area. This is associated with the highest elevation and the steepness of the topography. However around 60% of the study area falls under low and moderate hazard zone.

A similar study, which was conducted in the Gidole area (Filagot Mengistu et al., 2018) used information value method to asses landslide hazard zonation map. The paper presented six causative factor maps such as Slope, Elevation, Aspect, NDVI, Lithology and LULC. In their study, 23 % of the study area was under high and very high hazard zone. Raghuvanshi et al., (2015) also used GIS based Grid overlay method versus modeling approach in Meta Robi District of West Showa Zone in Ethiopia for landslide analysis. The paper used six causative factors for landslide hazard zonation; namely slope material, slope, aspect, elevation, land use, and land cover and groundwater-surface traces. The result showed that GIS modeling produced better compared to Grid overlay.

In most cases elevation is found to be the most dominant factor and the major reason for slope instability, this was in good agreement with the conclusion of Filagotu Mengistu et al. (2018). Occurrences of previous landslides in the area were also dominantly concentrated in elevations between 2170 m and 3030 m. Even though they are associated with elevation LULC condition might also play a very crucial role as most part of the slope in this elevation range are used for agriculture practices.

The result of PS-InSAR analysis shows the presence of displacement ranging from +5 mm/yr. to -5.4 mm/yr. The result showed that there exists slope instability in the study area and additional

landslides are probable in the future. Similar study which was carried out in the Gidole area (Filagot Mengistu et al., 2018) assed slope instability using seven sentinel images and applying PS InSAR technique. Their analysis revealed that there is a deformation ranging from +15 mm/yr. to -19 mm/yr. Which is in the order of the current findings.

The current slope instability in the Birbir-Mariam area is associated with relative higher relief, steep slope, and adverse flow of ground water conditions, structural discontinuity, sparsely vegetated land and toe erosion. The result achieved in this study showed the importance of using the well-established GIS based landslide hazard zonation mapping techniques together with the PS InSAR methodology for slope instability assessment and to analyze the deformation of selected areas in time.

In general PS InSAR analysis depicted actively deforming areas in the area and the analysis using optical images based on different factors showed land slide prone areas. In most places, such as in the western, south western and central part of the study area, one can clearly see that, the result from PS-InSAR, where there are red and blue dots (Figure 5. 6) are matching very well with places demarcated as highly landslide prone areas in Figure (5.2). The landslide inventory map (Figure 5.1) also showed that the central part was experiencing landslides. As there are no information about previous landslides, in the western and south western areas, due to accessibility problem, current results of active deformation cannot be compared to the prevalence of previous landslide in these areas. Some discrepancies in results from the PS-InSAR and optical imaging, for example around the south eastern part of the area might arise from the reason that the PS-InSAR was covering data from 2014 to 2019 and the optical image was taken in 2018 only. Moreover, the presence of dense vegetation (for example in the south-central part of the area) has at places hampered the capability PS-InSAR (Figure 4.8) to map possible presence of deformation.

CHAPTER SIX

CONCLUSION AND RECOMMENDATION

6.1 Conclusion

A landslide hazard zonation was carried out using the AHP method to produce a land slide hazard map, while a deformation time series is extracted from PS InSAR technique. The main purpose of the landslide hazard zone mapping was to delignate the spatial distribution of landslide prone areas and the PS-InSAR method is used to monitor which areas are actively deforming. The result of this study illustrated the application of geographic information system and remote sensing techniques for landslide hazard zone mapping and the uses of the software such as SNAP and StaMPS to study the spatial and temporal variability of deformation in the area.

By processing freely available satellite data's such as SRTM-DEM, Landsat, radar data like S-1A and geological information, landslide hazard zone are mapped and time series deformation pattern of the study area are generated. For this purpose, the AHP and PS InSAR methods were used respectively. In this study a landslide hazard zone map were prepared, by making use of eight causative factors and deformation time series map were extracted using 15 interferograms for entire study area.

The causative factors that were used for analysis during the preparation of the land slide hazard map were slope, lineament density, drainage density, LULC, elevation, NDVI, lithology and aspect. These data sets were weighted based on their significance and mathematically combined to map the landslide hazard zone. Finally, the overlay analysis is carried out using the weighted value of each causative factor produced applying AHP technique.

The landslide hazard zone map was then produced using five hazard categories and their spatial distribution are mapped. The map showed that 15% (16.466km^2) of the study area falls on very low hazard zone, 21.45 %(23.547km^2) falls under low hazard zone, 23 %(25.25km^2) lies within moderate hazard zone, 25.7 %(28.221km^2) was within high hazard zone and 14.85 %(16.306km^2) was found to be within very high hazard zones.

The Landslide hazard map of the Birbir-Mariam area has delivered basic information about the landslide susceptible zones. This map can be used as a basis for further studies and to prepare strategies in case of landslide hazard and properly plan future development endeavors.

The mapping of actively deforming zones was made using the PS InSAR technique. The result showed that there are areas that are actively deforming at a rate, of -5.4 mm/yr. to 5 mm/yr., between 2014 and 2019. The negative sign shows that the area is moving away from the Stellate in the LOS direction and the positive towards the satellite. The work showed the capability of the newly evolved processing technologies that allow examination of massive numbers of landslide as well as deformations.

In general, selected sites in the central, northwestern, western and southern parts of the study area showed active deformation. These sites are also mapped as landslide prone areas in the landslide zonation map. The location of previous landslides, from the available landslide inventory map are also mostly located at the central part of the survey area.

6.2 Recommendation

As population increases, the demand for new land will also increase to accommodate settlements, infrastructure development and farmland. Towards this, the current study has properly delignated earthquake prone zones and those that are actively deforming within. However, the results achieved needs to be studied further, by closely monitoring developments, remotely and through field visit and inventory. It is also necessary to make further study towards vulnerability and take enough mitigation measures, if possible, to mitigate and if not to reduce risk. As a result of this study the following recommendations are given.

- Those areas that fall in very high, high, and moderate hazard zones, where active deformations are observed, may probably face landslide occurrence and related slope instability problem in the future. Hence, it is recommended to properly utilize the output of this research work and reserve the landslide prone areas for forestry.
- The land use and manmade developmental activities are the most significant causative parameter of landslide in the study area. Hence, the local government can reduce landslide effects through land use and land cover management policies and regulations. Including

planting of trees, avoiding construction on unstable slopes and cultivation at the foot of the steep slope to decrease landslide induced damage on human life and infrastructure.

- This study highlighted that the poor drainage condition on most of the critical slope played role in inducing instability of slopes, therefore improvement in drainage by using proper sub horizontal drainage to reducing pore-pressure
- As human life and resources are more and more wasted due to landslides, decision makers, land use planners and engineers need to make use of such results and request for it where ever it is not available, to make a wise decision in their planning.
- Further work needs to be done to monitor the development of deforming areas using methods that are demonstrated in this research, other geodetic approaches such as GNSS, geophysical investigation and through field inventor.

REFERENCES

AC Peidou*, G Fotopoulos 2015, an overview of landslide detection and monitoring using geodetic satellite observations

Anbalagan, R., (1992). Landslide hazard evaluation and zonation mapping in mountainous terrain. Eng. Geol. 32:269–277

Bekele Abebe, Francesco, D., Fubelli, G., Mohamed Umer and Asfawossen Asrat (2010), Landslides in the Ethiopian highlands and the Rift margins. Journal of African Earth 56,135-138

Bell, F.G. (2007). Engineering Geology, 7th ed., Elsevier Butterworth-Heinemann Linacre House, London, 61-76.

Blyth, F.J.H and de Freitas, M.H. (2005). Geology for Engineers, 7th ed., Elsevier Butterworth-Heinemann Linacre House, London, 227-239.

Britannica Encyclopedia of Earth science https://www.britannica.com/science/landslide

Cruden DM. 1991.A simple definition of a landslide. Bulletin of the International Association for Engineering Geology 43:27-29

Cruden, D.M., and Varnes, D.J. (1996). Landslide types and processes. In: Turner, A.K., R.L. landslides investigation and mitigation, special report 247. Transportation Research Board, National. Acadamy Press, Washington D.C, 36-75pp

Dahal, R. K., Hasegawa, S., Masuda, T. and Yamanaka, M., 2006. Roadside Slope Failures in Nepal during Torrential Rainfall and their Mitigation. Disaster Mitigation of Debris Flows, Slope Failures and Landslides. Pp. 503–514.

Dai, F. C. and Lee, C. F., 2001. Terrain-based mapping of landslide susceptibility using a geographical information system: a case study. Canadian Geotechnical Journal 38:911 – 923.

Davidson, A Alemu Shiferaw, Eyob G.Luel, Davies, J.C., Moore, J.M, Abera Degefu, Alemayehu W.Rafael and Muluneh Geleta (1983).Preliminary Report on the Geology and Geochemistry of parts of Sidamo, Gamo Gofa and Kefa Provinces. Omo River Report No.1.Imperial Ethiopian Government, Ministry of Mines

Emmanouil P., Andreas P., Konstantinos X. Soulis D. and Ioannis C., 2020. Landslide Mapping and Susceptibility Assessment Using Geospatial Analysis and Earth Observation Data

ESA, 2018a. Earth online. Missions. Sentinel-1 https://earth.esa.int/

ESA, 2018b. Earth online. Missions. Sentinel-1 https://earth.esa.int/

Espizua, L.E and Bengochea, J. D. (2002). Landslide Hazard and Risk Zonation Mapping in the Río Grande Basin, Central Andes of Mendoza, Argentina. Mountain Research and Development. 22:177-185.

Fausto G., Alessandro C., Mauro C., Federica F., Michele S., Kang-T.,2012 Landslide inventory maps: New tools for an old problem

Fisseha, S. and Mewa, G., (2016), Road Failure caused by Landslide in north Ethiopia: a case study from Dedebit - Adi-Remets Road Segment. Journal of African Earth Sciences, 118, 65 – 74

Fubelli G., Dramis F. (2015) Geo-hazard in Ethiopia. In: Billi P. (eds) Landscapes and Landforms of Ethiopia. World Geomorphological Landscapes

Hamza, T. and Raghuvanshi, T. K., 2017. GIS based landslide hazard evaluation and zonation- A case from Jeldu District, Central Ethiopia. Journal of King Saud University–Science, 29(2), 151-165

Highland, L.M. and Bobrowsky, P. (2008). The Landslide Handbook- A Guide to Understanding Landslides. U.S. Geological Survey, Reston, Virginia, 147 pp

Hoek, E. and Bray, J.W. (1981). Rock Slope Engineering (revised third Ed.). Ins. of Mining and Metallurgy, London, 358pp.

Hooper, A., Bekaert, D., Spaans, K., Arıkan, M., 2012. Recent advances in SAR interferometry time series analysis for measuring crustal deformation. Tectonophysics 514-517, 1–13

Höser, Thorsten. 2018. “Analysing Capabilities and Limitations of InSAR Using Sentinel-1 Data for Landslide Detection and Monitoring.” Master’s thesis, Bonn: Department of Geography, Bonn University.

G Berhane, M Kebede, N Alfarah, E Hagos, 2020. Landslide susceptibility zonation mapping using GIS-based frequency ratio model with multi-class spatial data-sets in the Adwa-Adigrat mountain chains, northern. Journal of African Earth …, 2020 - Elsevier.

Keefer, D. K., 2000. Statistical analysis of an earthquake-induced landslide distribution the 1989 Loma Prieta, California event. Eng. Geol. 58:231–249

Kifle Woldearegay. (2013). Review of the occurrences and influencing factors of landslides in the highlands of Ethiopia: With implications for infrastructural development. Mekelle University, Mekelle, Ethiopia. Journal Name Volume. 5:3 31

Levitte D., Dakin F., and Mohr PA, 1972, Geological Report on the Amaro Mountains and the Southern Ethiopia

Mengistu F., Raguvanshi K., Suryabhagavan V., Lewi E., 2019, landslide hazard zonation and slope instability assessment by using optical and InSAR Remote sensing: Journal of Researchgate

Mousavi, S. Z., Kavian, A., Soleimani, K., Mousavi, S. R., & Shirzadi, A. (2011). GIS-based spatial prediction of landslide susceptibility using logistic regression model. Geomatics Natural Hazards and Risk, 2, 33–50

Natural Hazard, what is a landslide and what causes one? https://www.usgs.gov.com/Natural

Raghuvanshi K., Ibrahim J., Ayalew D., 2014: Slope Stability Susceptibility evaluation parameter (SSEP) rating scheme: An approach for landslide hazard zonation. Journal of African Earth Sciences. 99:595 612.

S. Mandal and S. Mondal, 2019 Geomorphic, Geo-tectonic and Hydrologic Attributes and Landslide Susceptibility

Shano L., Raghuvanshi K., Meten M, 2020: Landslide susceptibility evaluation and hazard zonation techniques–a review

TK Mebrahtu, M Alber, S Wohnlich, 2020. Tectonic conditioning revealed by seismic refraction facilitates deep-seated landslides in the western escarpment of the Main Ethiopian Rift. Geomorphology, 2020 – Elsevier. https://doi.org/10.1016/j.geomorph.2020.107382

Turrini, C. T and Visintainer, P., 1998 Proposal of a method to define areas of landslide hazard and application to an area of the Dolomites, Italy. Eng. Geol. 50: 255–265.

Varnes, D.J. (1984) Landslide Hazard Zonation: A Review of Principles and Practice, Natural Hazards. UNESCO, Paris, 63 pp

Wachal, D.J. and Hudak, P.F. (2000). Mapping landslide susceptibility in Travis County, Texas, USA. Geo Journal. 51:245-253

Waltham, T. (2009). Foundations of engineering geology. CRC Press. 3rded. Madison Avenue, New York, 72-74 pp.

Appendix A

Individual wrapped phase result sampled

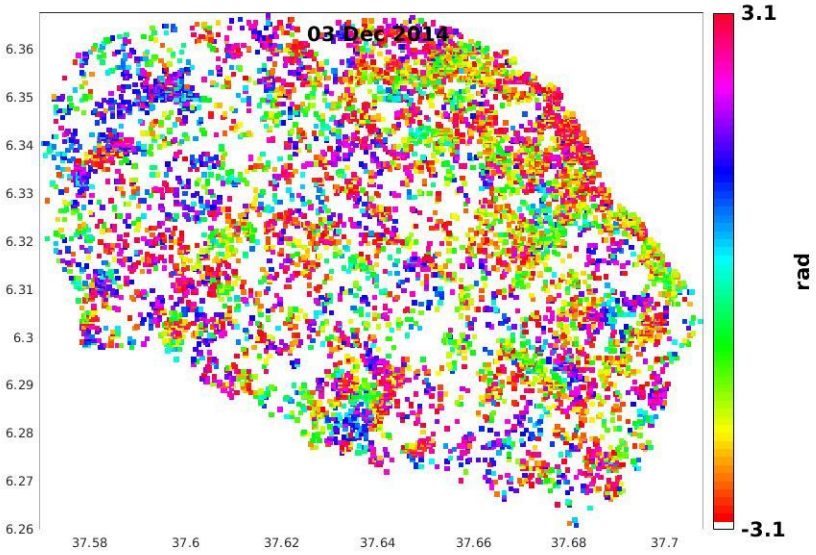

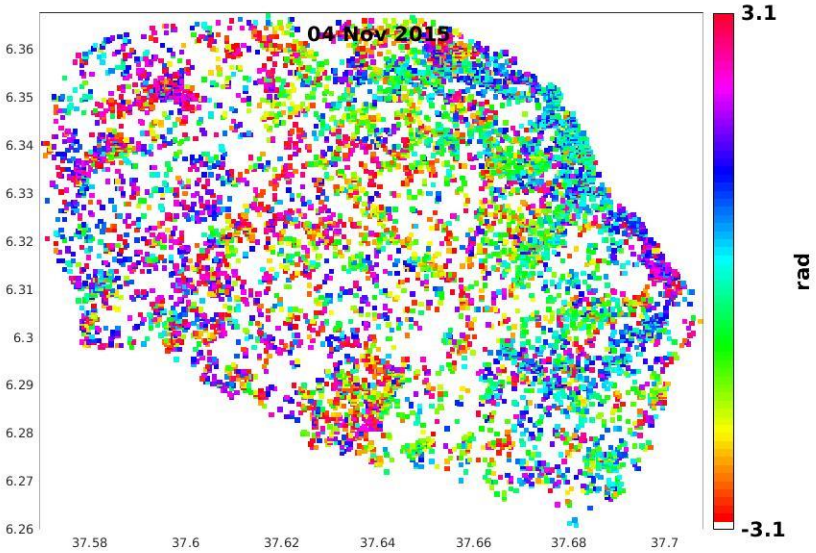

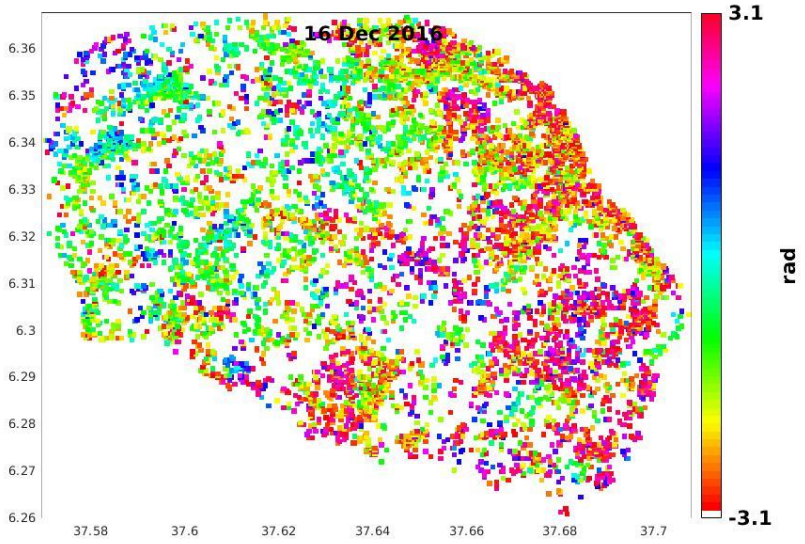
16 Dec 2016
3.1
-3.1
rad
6.36
6.35
6.34
6.33
6.32
6.31
6.3
6.29
6.28
6.27
6.26
37.58
37.6
37.62
37.64
37.66
37.68
37.7

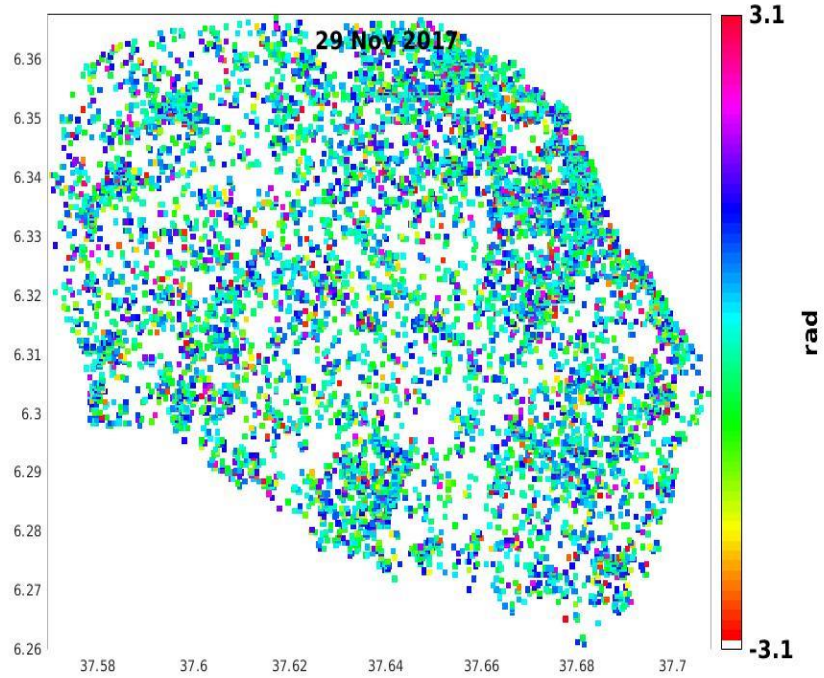
29 Nov 2017
3.1
-3.1
rad
6.36
6.35
6.34
6.33
6.32
6.31
6.3
6.29
6.28
6.27
6.26
37.58
37.6
37.62
37.64
37.66
37.68
37.7

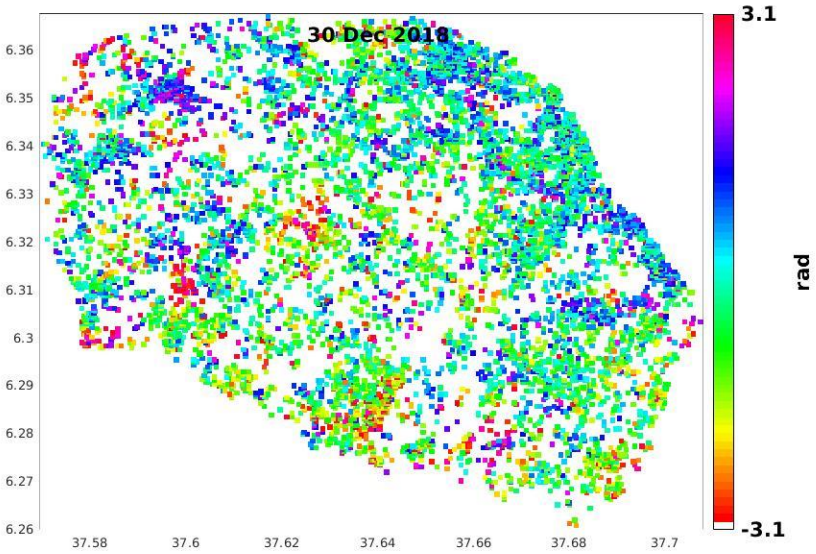
30 Dec 2018
6.36
6.35
6.34
6.33
6.32
6.31
6.3
6.29
6.28
6.27
6.26
37.58
37.6
37.62
37.64
37.66
37.68
37.7
3.1
rad
-3.1

Individual phase Unwrapping results

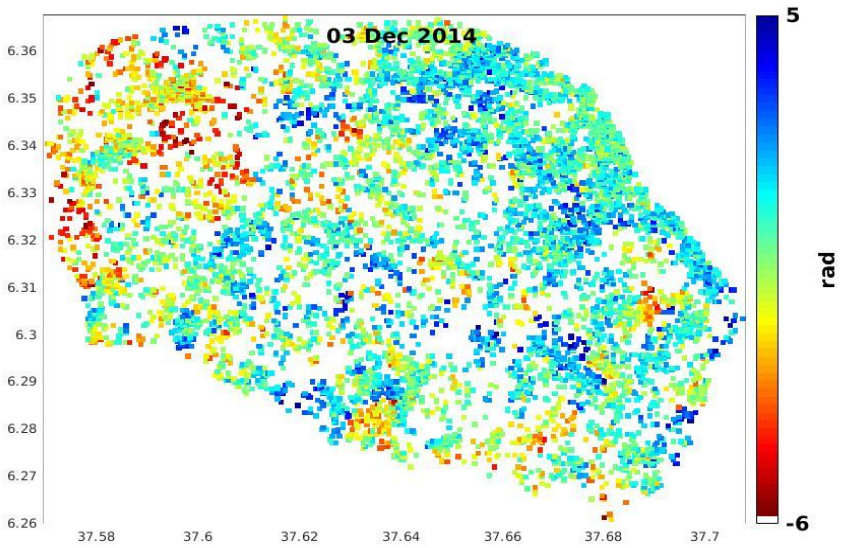

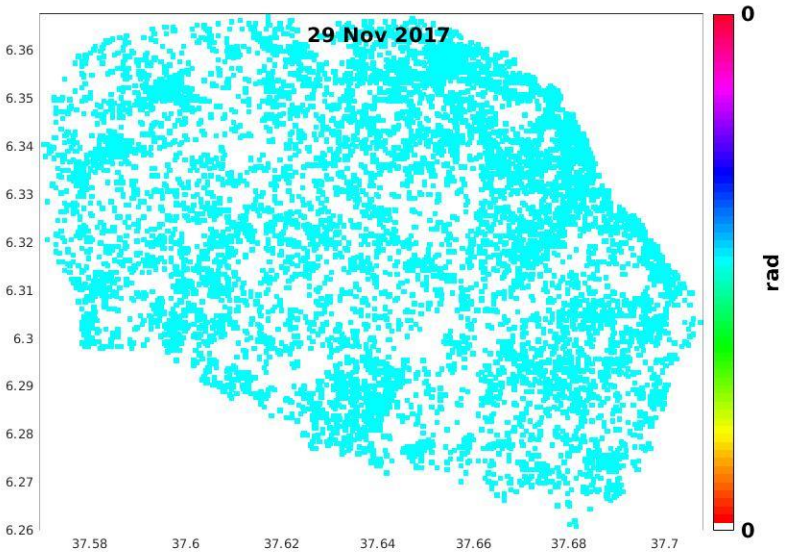

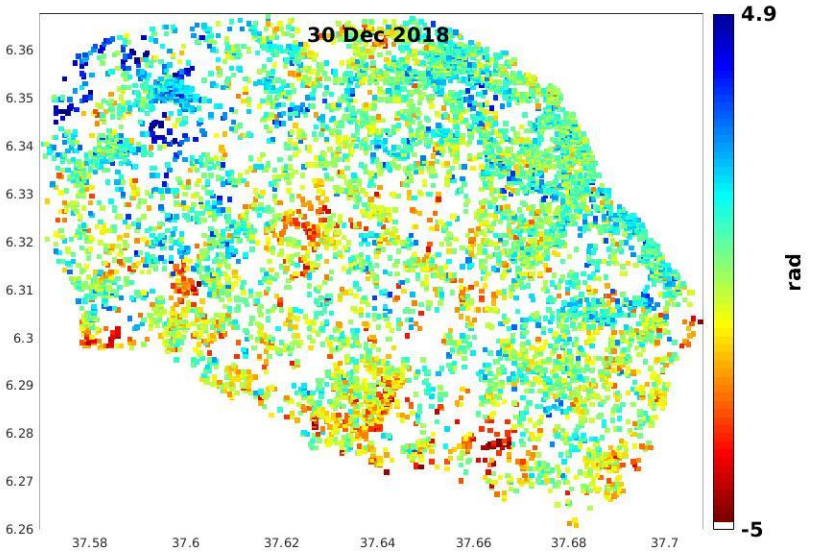
30 Dec 2018
6.36
6.35
6.34
6.33
6.32
6.31
6.3
6.29
6.28
6.27
6.26
37.58
37.6
37.62
37.64
37.66
37.68
37.7
4.9
rad
-5

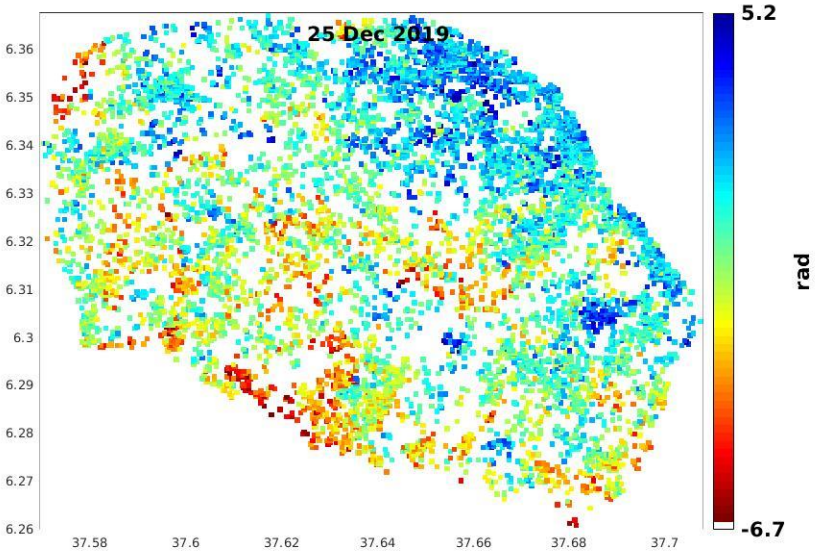
25 Dec 2019
6.36
6.35
6.34
6.33
6.32
6.31
6.3
6.29
6.28
6.27
6.26
37.58
37.6
37.62
37.64
37.66
37.68
37.7
5.2
rad
-6.7

Appendix B

Image showing landslide in the study area